The Effectiveness of Persulfate and Hydrogen Peroxide on the Oxidation of Hydrocarbon Contaminants at 30^0C: A Study with Focus on the Performance of Compound Specific Isotope Analysis

by

Waleed Gusti

A thesis
presented to the University of Waterloo
in fulfillment of the
thesis requirement for the degree of
Master of Science
in
Earth Sciences

Waterloo, Ontario, Canada, 2018

Author's Declaration

This thesis consists of material all of which I authored or co-authored: see Statement of Contributions included in the thesis. This is a true copy of the thesis, including any required final revisions, as accepted by my examiners.

I understand that my thesis may be made electronically available to the public.

Statement of Contributions

This thesis is an extended version that has full interpretation of the data collected from the studied sites by Kashir et al. (2017). The paper by Kashir et al. (2017) titled "Chemical oxidation using stabilized hydrogen peroxide in high temperature, saline groundwater impacted with hydrocarbons and MTBE" has Waleed Gusti and Orfan Shouakar-Stash as co-authors. This thesis and the paper by Kashir et al. (2017) have the results of BTEX and MTBE degradation from the hydrogen peroxide experiments along with C isotope analyses. This thesis has the results of BTEX and MTBE degradation from the persulfate experiments along with C and H isotope analyses which were not reported or interpreted in Kashir et al. (2017). Mr. Gusti has done all the calculations required to determine the extent of hydrocarbon contaminant degradation during the persulfate and hydrogen peroxide experiments and the carbon and hydrogen isotopic enrichments for the residual contaminants.

Abstract

Two oxidants, persulfate and hydrogen peroxide, were used to investigate the effectiveness of in-situ chemical oxidation (ISCO) on target contaminants (sourced from industrial wastewater) in saline and high-temperature groundwater. Benzene, toluene, ethylbenzene, xylene (BTEX), trimethylbenzenes (TMBs), methyl tert-butyl ether (MTBE), and naphthalene were the target contaminants investigated.

Different aspects were examined during this study: 1) the effectiveness of two different ratios of the activator Fe^{2+} to a stabilizer (citrate) relative to an activator-free control using persulfate as an oxidant; 2) the performance of three stabilizers - citrate, phytate, and silica - for hydrogen peroxide in three separate experiments; and 3) two dimensional compound specific isotope analysis (2D-CSIA) was performed using carbon and hydrogen isotopes to evaluate the extent of the transformation of BTEX, MTBE and TMBs between persulfate and hydrogen peroxide experiments, and to determine the degradation mechanism more precisely by the resulting enrichment factors using the Rayleigh equation which calculated the changes in stable isotope ratios of C and H isotopes with changes in the concentration of the contaminant compounds.

As expected, the results showed that the activated persulfate caused a faster rate of contaminant oxidation than non-activated persulfate, and most of the hydrocarbons reached undetectable concentrations by the end of the experiments, with the exception of benzene, toluene, and MTBE. Of these compounds, MTBE was found to have the lowest rate of removal (~5%), as a result of the low persulfate concentration (5 g/L) used in the experiments. Compared to the persulfate, hydrogen peroxide was more efficient at oxidizing BTEX, TMBs, naphthalene, and MTBE, especially when citrate was used as a stabilizer ($\geq$ 93% of destruction).

Isotopically, CSIA was successful at distinguishing the isotopic changes for carbon and hydrogen isotopes, and provided insights on the best method for hydrocarbon degradation that resulted in the largest isotope enrichments. The experiments involving activated persulfate with a high ratio of citrate/iron caused the largest carbon isotopic fractionation compared to the other activated and unactivated persulfate experiments for MTBE (2.1‰ to 3.7‰) and toluene (8.0‰ to 9.3‰), as well as the largest hydrogen isotope fractionation for MTBE

(5.0‰ to 34‰). However, the duplicate experiments at site #1 and site #2 involving hydrogen peroxide stabilized by citrate were more pronounced than the activated and unactivated persulfate experiments in terms of carbon isotope fractionation and exceeded the carbon isotope analytical uncertainty (± 0.5‰) with a range of (2.3 ± 0.5‰ to 4.0 ± 0.5‰), and (1.6 ± 0.5‰ to 2.8 ± 0.5‰) for MTBE and benzene, respectively. Unfortunately, hydrogen isotopes were not analyzed for the hydrogen peroxide experiment due to the lack of sufficient volume of samples. The utilized 2D-CSIA has helped the interpretation of the isotopic changes, especially when the extent of isotopic fractionation for one isotope does not exceed analytical uncertainties, like that observed for benzene in the unactivated persulfate experiment where the changes in carbon isotopic composition were within the analytical uncertainty.

Acknowledgments

First and foremost, I thank God for his guidance and support.

I would like to sincerely thank my current supervisors, Dr. Orfan Shouakar-Stash and Dr. Brian Kendall, and my former supervisors, Dr. Neil Thomson and Dr. Ramon Aravena, for their guidance, support and constructive critical insights throughout this thesis. I would like to express my appreciation to Orfan for giving me the opportunity to work on and analyze the samples at Isotope Tracer Technologies (IT^2).

A special appreciation to Brian who guided me on my thesis and supported me with valuable advices through the last two years of my study.

I would also like to thank my committee members, Neil Thomson, Fereidoun Rezanezhad and Jim Barker for their feedback, advice, constructive comments and guidance throughout this study.

Special thanks are also due to Shirley Chatten for analyzing the groundwater samples and for the fast responses to my emails.

I would also like to acknowledge Mirna Stas**,** Nart Bakir, Amjad Yahia, Kamal Baik, Irem Albak, Adam Mihailov, Richard Drimmie**,** Shamila Khurshid, and Jacqueline Whiteside for their support, assistance, and help during the work at IT^2.

I wish to extend my thanks to my supervisors at King Abdulaziz University, Dr. Ali Subyani, and Dr. Saleh Bajabaa, and Mr. Waleed Hawsawi, thank you very much for trusting me and for supporting and guiding me with advices that helped me on my study, and for their friendship and support over the years. Thank you for your valuable time and your critical and constructive comments that enriched my thesis.

A special Thanks to my friends inside Canada, Rakan Al-Otaibi, Saleh Al-Harthi, Moayyad Bitar, Abdulhameed Al-Sairafi, Eyyad al-Ghamdi, and Wael Al-Jahani.

Above all else, I am indebted to my family for their support, endless patience and unconditional love. They inspired me to work hard and they taught me the value of education. Special thanks to my mother Nora and my sisters; Nesreen, Neveen and Gufran, who always encouraged me, trusted me and inspired me. I would like also to extend my grateful to my brother, Nomay, and my cousins, Mazen, Muhammed, and Abdullah for their continuous support and undying encouragement to pursue my dreams.

My gratitude to my wife, Samaher, who supported me and had countless encouragement through my study and during my stay in Canada. Samaher, the completion of this work would not have been possible without your support, encouragement, belief in me and understanding.

Finally, Special thanks to the Saudi Arabian Cultural Bureau (SACB) for giving me the opportunity to have a scholarship to support my MSc. Furthermore, this study had benefited from research funds given to Dr. Shouakar-Stash from various sources including NSERC and industrial partners.

Dedication

To the memory of my father, Abdulaziz who taught me to chase my dream of becoming a great professor in the future.

I want to dedicate my thesis to my mother, Nora, for believing in me to have the master degree, and to my wife, Samaher, for the countless support during my study and for my little prince, Elyas, who turned our lives to a colored live with love and passion.

Table of Contents

List of Figures

List of Tables

Chapter 1

Introduction

1.1 Motivation and thesis objectives

The oil-gas industry requires a large amount of water for production purposes such as cooling, washing, and cleaning. This water may contain chemicals (e.g., hydrocarbons) that affect the environment or humans by, for example, accidental leaking to the surface or subsurface and thus can cause serious problems (Luca et al., 2011). Hydrocarbons (HCs) are one of the commonly found contaminants in groundwater and are often present as light nonaqueous phase liquids (LNAPLs) (e.g., benzene) (Liang et al., 2011) or as dense nonaqueous phase liquids (DNAPLs) (e.g., trichloroethene) (Stroo et al., 2012). Therefore, concerns regarding groundwater contamination associated with oil-gas extraction and refining have been raised and has become a global issue (Boyd et al., 2006; Yen et al., 2011).

A hydrocarbon compound is a combination of two major elements: hydrogen and carbon. Petroleum hydrocarbons are a large group of different compounds, and can be divided into four categories: the saturates, the aromatics, the asphaltenes, and the resins (Das & Chandran, 2011). Volatile organic compounds (VOCs) are organic chemicals that have high vapor pressures and low boiling points. These chemicals, such as benzene, toluene, ethylbenzene, and xylene (BTEX) are categorized as *aromatic hydrocarbons* (Dorer et al., 2014). These contaminants are widespread and difficult to remediate especially at the contaminant source zones (Stroo et al., 2012). Hence, many studies have been conducted to investigate the behavior of these contaminants to better understand their effect on the environment in general, and on groundwater in particular, with the goal of decreasing their influence on groundwater quality (Karpenco et al., 2009; Roy & Bickerton, 2012; Stroo et al., 2012).

In the last few decades, many *in-situ* treatment strategies have been applied with the aim of eliminating the contaminants or to reduce the risk of contamination to an acceptable level (Smith, 1985). The remediation of contaminants can be done using a wide variety of applications that depends on the nature of the contaminants as well as the nature of

groundwater (e.g. pH, alkalinity, temperature, total dissolved solids). One of these applications is called in-situ chemical oxidation (ISCO), which involves the delivery of specific chemicals that help to diminish the contaminants (Bennedsen, 2014; Siegrist et al., 2014).

ISCO has proved to be an attractive method for the treatment of organic contaminants (Liang et al., 2003; Lemaire et al., 2011; Usman et al., 2012; Ferreira et al., 2017). Chemical oxidants such as persulfate, permanganate, ozone, and hydrogen peroxide act as oxidizing agents that can boost the remediation processes (Yen et al., 2011; Ranc et al., 2016; Ferreira et al., 2017). The percent of contaminants removed via remediation can be calculated by using the following equation (Manoli & Samara, 2008; Ranc et al., 2016):

$$PAH\ removal\ \% = \left(1 - \frac{C_{final}}{C_{initial}} \text{ x } 100 \right) \qquad \text{(Eq.1)}$$

where C_{final} is the concentration of the treated compound (i.e., after remediation) and $C_{initial}$ is the initial concentration (i.e., before remediation) of the same compound.

CSIA is a useful tool to interpret the degradation process of hydrocarbons, such as BTEX, chlorinated hydrocarbons, and methyl tert-butyl ether (MTBE) (Braeckevelt et al., 2012). The mechanism of CSIA application is to determine the isotopic composition of specific molecules (Schmidt et al., 2004; Chikaraishi et al., 2008), and to track the attenuation of contaminants through changes in the isotopic ratios (Braeckevelt et al., 2012; Cincinelli et al., 2012; Dorer et al., 2014) of different elements (e.g., C, H, Cl) that make up the contaminant. Combining different technologies, such as GC-IRMS with CSIA, has been well developed for tracing the fate of contaminants in the environment (Wu et al., 2017), and to assess the interpretation of remediation processes (Boyd et al., 2006; Cassidy et al., 2015). In other words, CSIA is a tool that can improve the interpretation of the fate of contaminants by understanding the distribution of molecules of a specific compound along with changes of its isotopic compositions.

The purpose of this study is to evaluate the effectiveness of the chemical oxidants persulfate and hydrogen peroxide on contaminant hydrocarbons in saline and high-

temperature groundwater. In this study, samples were taken from two contaminated sites: site #1 and site #2. The location of the two sites are not disclosed for confidentiality reasons. The main objectives of this study are: 1) evaluate the effectiveness of ISCO using sodium persulfate (iron-activated and unactivated) on the targeted contaminants (BTEX, naphthalene, MTBE, and TMBs); 2) examine the effect of three stabilizers (citrate, phytate, and silica) to maintain hydrogen peroxide activity for MTBE oxidation on samples from site #1; and 3) examine the effectiveness of hydrogen peroxide stabilized by citrate and silica on the oxidation of the targeted hydrocarbons (BTEX, naphthalene, MTBE, TMBs). As part of these objectives, CSIA using C and H isotopes was used to evaluate the extent of degradation of contaminants during the chemical oxidation over time.

1.2.0 Oxidants

1.2.1 Persulfate

When a persulfate salt such as sodium persulfate ($Na_2S_2O_8$) is added to water, it dissociates to form the persulfate anion ($S_2O_8^{2-}$) (Eq.2) (Tsitonaki et al., 2010). Generally, the persulfate decomposition depends on the solution chemistry (i.e., alkaline, neutral, weakly acidic, strongly acidic; Kolthoff & Miller, 1951). In alkaline, neutral and weakly acidic solutions, O_2 is formed as a byproduct (Eq. 3). In strongly acidic solutions, the decomposition of persulfate will yield Caro's acid (H_2SO_5) (Eq. 4), which will break down to hydrogen peroxide (H_2O_2) via hydrolysis (Eq. 5) (Kolthoff & Miller, 1951).

$$Na_2S_2O_8 \rightarrow 2Na^+ + S_2O_8^{2-} \quad \text{(Eq.2)}$$

$$S_2O_8^{2-} + H_2O \rightarrow 2HSO_4^- + \tfrac{1}{2}\, O_2 \quad \text{(Eq.3)}$$

$$H_2S_2O_8 + H_2O \rightarrow H_2SO_5 + H_2SO_4 \quad \text{(Eq.4)}$$

$$H_2SO_5 + H_2O \rightarrow H_2O_2 + H_2SO_4 \quad \text{(Eq.5)}$$

Persulfate is one of the most common oxidants (Peluffo et al., 2016) that have been used in the remediation of groundwater contaminants. Persulfate ($S_2O_8^{2-}$) is a powerful oxidant with a high oxidation potential (E°= 2.01 V) (Eq.6), and has the capability to produce strong sulfate free radicals ($SO_4^{\bullet-}$) that have an even higher oxidation potential (E°= 2.6 V) (Eq.7) (House, 1962; Tsitonaki et al., 2010; Yan et al., 2013).

$$S_2O_8^{2-} + 2\ e^- \rightarrow 2SO_4^{2-} \qquad E°= 2.01\ V \qquad \text{(Eq.6)}$$

$$S_2O_8^{2-} \xrightarrow{\text{Heat/ Metal}} SO_4^{\bullet-} \qquad E°= 2.6\ V \qquad \text{(Eq.7)}$$

Persulfate is a widely-accepted oxidant because it has many advantages such as high water solubility, low cost, and benign by-products (Tsitonaki et al., 2010). It is chemically stable and requires higher activation energy than other hydrocarbon oxidants such as permanganate (Liang et al., 2008; Peluffo et al., 2016). According to Liang et al. (2003), the activation energy required for persulfate oxidation of trichloroethylene (TCE) is 93 kJ/mol, while the required activation energy of permanganate is 35 kJ/mole (Liang et al., 2008). Due to its reaction kinetic limitations, persulfate reacts more slowly than other oxidants if it is used without an activator (Deng et al., 2014; Wu et al., 2014). Hence, introducing the persulfate to an activator helps advance hydrocarbon oxidation at a favorable rate (House, 1962).

Persulfate can be activated by heat or by a transition metal such as Fe^{2+} to produce free sulfate radicals that are stronger than the persulfate anion (Liang et al., 2003; Usman et al., 2012). However, rapid oxidation of persulfate activated by Fe^{2+} may cause precipitation of metals, which then react with the sulfate radicals, thus reducing the efficiency of this method for contaminant remediation (Tsitonaki et al., 2010; Yan et al., 2013). In order to maintain the availability of Fe^{2+} in the solution, chelating agents such as citrate have been used (Liang et al., 2008; Usman et al., 2012).

1.2.2 Hydrogen peroxide

Hydrogen peroxide (H_2O_2) is a well-known oxidant that has been used extensively in groundwater remediation (Karpenco et al., 2009). It can be used without an activator, but is kinetically slow to degrade contaminants (Interstate Technology & Regulatory Council [ITRC], 2005). The most common activator of H_2O_2 is Fe (II). The mix of H_2O_2 and Fe^{2+} (Fenton's reagent) is a well-established treatment for organic contaminant remediation (Bergendahl & Thies, 2004) since Fe is an abundant and non-toxic element and hydrogen peroxide is environmentally safe (Levchuk et al., 2014). The result from the mix of H_2O_2 and Fe^{2+} is the formation of hydroxyl radicals (Eq.8) (Watts et al., 2007; Lemaire et al., 2013;

Viisimaa & Goi, 2014) that attack contaminants (Usman et al., 2012). The hydroxyl radicals generated from Eq.8 are non-specific oxidants that have high oxidation potential (E° = 2.8 V) and thus can react with a wide range of contaminants (Zingaretti et al., 2016; Bendouz et al., 2017).

H_2O_2 is an effective oxidant in acidic and alkaline conditions (Devi et al., 2016). However, it has been demonstrated that the decomposition of H_2O_2 in the presence of Fe (II) is rapid (occurs within hours) (Karpenco et al., 2009), limiting its efficiency to react with contaminants (Schmidt et al., 2011). To avoid this issue, introducing H_2O_2 to a stabilizer (e.g., chelating agent) may maintain the longevity of its reaction in the presence of Fe (II) (Ferrarese et al., 2008; Watts et al., 2000; Zengaretti et al., 2016).

$$H_2O_2 + Fe^{2+} \rightarrow OH^{\cdot} + OH^{-} + Fe^{3+} \qquad (E° = 2.8\ V) \qquad \text{(Eq.8)}$$

1.3 Chelating agents

Chelating agents (like citric acid, cyclodextrins, and catechol) are complex compounds that are used to enhance the oxidation process, for example, by maintaining the availability of an activator (e.g., Fe^{2+}) in the solution and to avoid scavenging reactions that downgrade the efficiency of the oxidation (Ferrarese et al., 2008). In the case of persulfate, a chelating agent can be used to control the concentration of iron in the solution for the activation of persulfate by preventing iron precipitation as iron hydroxide/iron oxide and therefore improve the oxidation effectiveness (Han et al., 2015; Ma et al., 2018). Moreover, using chelating agents with hydrogen peroxide has been shown to slow down the rapid decomposition of H_2O_2, thus enhancing the production of hydroxyl radicals that destroy different contaminants (Ferrarese et al., 2008). A study by Kashir et al. (2017) found that using citric acid to stabilize hydrogen peroxide for MTBE oxidation yielded significant results by a mean of 94 percent of MTBE removal over the 7-day experiment. Several studies agreed that the use of a chelating agent and stabilizer with hydrogen peroxide is a favorable solution for the treatment of a wide variety of contaminants such as PAHs (Venny et al., 2012), chlorinated hydrocarbons (Cai et al., 2012), and BTEX (Zhao et al., 2011).

1.4 The role of pH

pH plays an important role when chemical oxidation processes are dependent on pH. For example, in the oxidation of hydrocarbon by persulfate, the rate of persulfate decomposition increases as much as 200% when the pH increases from 8 to 12 and therefore enhanced the rate of degradation (Li et al., 2017). However, further increase of pH from 12 to 13 resulted in $CO_3^{\bullet-}$ which was generated from scavenging reactions involving HCO_3^- and $SO_4^{\bullet-}$ or $HO^\bullet$ (Eq. 10 & 11). Because of the low reactivity of $CO_3^{\bullet-}$, the degradation rate slowed down and therefore reduced the efficiency of persulfate oxidation to remediate contaminants (Li et al., 2017). Additional scavenging reactions may occur at higher pH, for example, halide ions (e.g., Cl^- and Br^-) may react with the free radicals, causing slow or even negligible oxidation (Grebel et al., 2010). On the other hand, decreasing the pH might enhance the oxidation reaction, for instance, using a chelating agent like citric acid (Ferrarese et al., 2008). In an unactivated persulfate experiment performed by Sra et al. (2013), the pH decreased to < 3 and resulted in acid-catalyzation of persulfate, thus enhancing the oxidation reactions (Eq.9).

$$S_2O_8^{2-} + H_2O \xrightarrow{H^+} H_2SO_5 + SO_4^{2-} \quad \text{(Eq.9)}$$

$$SO_4^{\bullet-} + HCO_3^- \rightarrow CO_3^{\bullet-} + SO_4^{2-} + H^+ \quad \text{(Eq.10)}$$

$$HO^\bullet + HCO_3^- + CO_3^{\bullet-} + H_2O \quad \text{(Eq.11)}$$

1.5 The effect of temperature and salinity

The reaction rate depends on the temperature. Increasing the temperature will make molecules move faster and hence increase the chances for more collisions and reactions between molecules, thus producing chemical changes (Tyagi, 2009). The free radicals can be generated by activating the oxidant (e.g., persulfate or H_2O_2), for example, thermally or by using a transition metal (Eq. 7, 8). This study has a relatively higher system temperature (30°C), and thus a higher rate of sulfate and hydroxyl radical generation would be expected. This would result in a higher rate of oxidation for the contaminants. Saeed (2011) reported that high temperature (30°C) enhanced the mineralization efficiency of the organic compounds compared to the temperature of 10°C. Thus, the temperature is an important parameter to consider when trying to gain the most efficient production of radicals to oxidize contaminants.

It has been demonstrated that chloride and bromide will react rapidly with sulfate and hydroxyl radicals to form halogen atoms (Peyton, 1993). Cl^- and Br^- are radical scavengers as shown in Eq. 12 - 13 (Peyton, 1993) and Eq. 14 - 15 (Grebel et al., 2010). Traces of Br^- in a NaCl solution were found to have a greater effect than Cl^- itself showing the significant reactivity of Br^- (Grebel et al., 2010). Still, both ions have the capability to react rapidly with the free radicals which as a result may slow or inhibit the oxidation of the target organic compounds (Grebel et al., 2010).

$$SO_4^{\bullet-} + Cl^- \rightarrow SO_4^{2-} + Cl^{\bullet} \qquad (k_{12} = 2 \times 10^8\ M^{-1}\ s^{-1}) \qquad \text{(Eq.12)}$$

$$SO_4^{\bullet-} + Br^- \rightarrow SO_4^{2-} + Br^{\bullet} \qquad (k_{13} = 3.5 \times 10^9\ M^{-1}\ s^{-1}) \qquad \text{(Eq.13)}$$

$$OH^{\bullet} + Cl^- \leftrightarrow ClOH^{\bullet-} \qquad (k_{14} = 4.3 \times 10^9\ M^{-1}\ s^{-1}) \qquad \text{(Eq.14)}$$

$$OH^{\bullet} + Br^- \leftrightarrow BrOH^{\bullet-} \qquad (k_{15} = 1.1 \times 10^{10}\ M^{-1}\ s^{-1}) \qquad \text{(Eq.15)}$$

1.6 Isotopes

Elements differ from each other by the number of protons, and therefore elements have different atomic weights (Braeckevelt et al., 2012). Isotopes have the same number of protons but different numbers of neutrons; for example, the carbon isotopes ^{12}C and ^{13}C have the same number of protons (6) and have 6 and 7 neutrons, respectively. Isotopic fractionation during progressive oxidation of a contaminant hydrocarbon compound results in a change in the carbon isotopic composition (ratio of heavy ^{13}C to light ^{12}C isotopes) of the residual contaminant. Due to mass-dependent differences in the activation energy between ^{12}C and ^{13}C, ^{12}C is lighter than ^{13}C, and ^{12}C will react faster than ^{13}C because of the rapid diffusion of molecules having only ^{12}C compared to the ones with ^{13}C, therefore, the residual contaminant would likely be enriched in ^{13}C (Bouchard et al., 2008; Braeckevelt et al., 2012; Marchesi et al., 2013). The isotopic ratio (R) between heavy and light isotopes, for example, carbon isotopes ($^{13}C/^{12}C$) is expressed in units of per mil (‰) relative to the Vienna Pee Dee Belemnite (VPDB) standard. The isotopic composition of a sample is expressed in δ notation and is given by the following equation

$$\delta^{13}C\ (‰) = \left(\frac{(^{13}C/^{12}C_{\ sample}) - (^{13}C/^{12}C_{\ standard})}{(^{13}C/^{12}C_{\ standard})} \right) \text{ x } 1000 \qquad \text{(Eq.9)}$$

The same formula is used to report other stable isotope ratios, for example, hydrogen isotope ratios, δ^2H, are reported relative to V-SMOW, and nitrogen isotope ratios are reported relative to atmospheric nitrogen.

The isotopic fractionation factor α is an important parameter in isotope geochemistry, and describes the partitioning of isotopes caused by a reaction and its equation is defined as

$$\alpha = \frac{R_{reactant}}{R_{product}} \qquad \text{(Eq.10)}$$

where R is the ratio of the heavy to light isotopes of an element, e.g., $^{13}C/^{12}C$ in two phases (Chan et al., 2012).

CSIA is a promising tool in which isotope ratios are measured for each chemical component/contaminant of concern. In recent years, CSIA has been applied to hydrocarbons in a number of different ways, for example, the biodegradation of a wide range of contaminants such as aromatic and chlorinated hydrocarbons (Bouchard et al., 2008; Elsayed et al., 2014). CSIA has proved to be a useful tool for *in situ* applications, and can be used to identify the source of contaminants and their distribution and migration patterns (Lutz & Bruekelen, 2014; Solano et al., 2017). The application of CSIA includes the investigation of the reaction mechanism of contaminants and their degradation pathways (Audí-Miró et al., 2015) because the extent of isotope fractionation during a compound transformation is highly reaction-specific (Palau et al., 2014). Bouchard et al. (2008) observed isotopic changes during the degradation of VOCs, and concluded that the depletion of ^{13}C was likely due to faster diffusion of molecules containing lighter isotopes, rather than the biodegradation process. In some cases, physical processes such as dispersion, dilution, and sorption may cause a decrease in contaminant concentration, but not an actual decrease in the total contaminant

mass. Hence, isotope fingerprints can be used to differentiate between different degradation processes (Braeckevelt et al., 2012). Furthermore, the extent of degradation can be identified by measuring the isotopic fractionation of carbon or hydrogen in a specific compound (Palau et al., 2014), in which a change in the contaminant's concentration is associated with a change in its isotopic composition. For example, a study conducted by Shin & Lee (2010) found that carbon isotope composition of the residual fractions of benzene and toluene increased with higher extents of degradation and yielded significant fractionation factors.

The outcome of the traditional CSIA approach is not always beneficial, depending on the site conditions. For instance, according to Fischer et al. (2008), analyzing the isotopic composition of a single element is not always sufficient to identify the reaction mechanism. As a result, a powerful tool called two-dimensional compound specific isotope analysis (2D-CSIA) has been developed to overcome the limitations of using a single isotope method. For 2D-CSIA involving hydrocarbon contaminants, carbon and hydrogen isotopes (the most abundant elements in hydrocarbons) are used to recognize the reaction mechanism and the extent of degradation (Zwank et al., 2005), and to characterize the degradation pathways (Herrmann et al., 2009) of pollutants. According to Dorer et al. (2014), about 90% of ethylbenzene degraded by biodegradation and resulted in different enrichment values of heavy carbon and hydrogen isotopes, which helped to differentiate between the aerobic and anaerobic pathways of ethylbenzene degradation.

The enrichment factor (ε) corresponds to the changes in stable isotope ratios (R_t/R_0) with changes in the concentration of a compound (C_t/C_0) by using a simplified version of the Rayleigh equation, which is expressed as (Fischer et al., 2009):

$$\frac{(\delta_t+1000)}{(\delta_0+1000)} = \left(\frac{C_t}{C_0}\right)^{\frac{\varepsilon}{1000}} \quad \text{(Eq.11)}$$

where δ_t and δ_0 represent the isotope ratio at a given time and at the beginning of the reaction, respectively.

The enrichment factor can be calculated from the logarithmic form of the Rayleigh equation by plotting $\ln(C_t / C_0)$ versus $\ln[(\delta_t + 1000) / (\delta_0 + 1000)]$:

$$ln\left(\frac{(\delta_t+1000)}{(\delta_0+1000)}\right) = \frac{\varepsilon}{1000}\ ln\left(\frac{C_t}{C_0}\right) \quad \text{(Eq.12)}$$

The enrichment factor is related to the slope (m) by:

$$m = \frac{\varepsilon}{1000} \quad \text{(Eq.13)}$$

Furthermore, using the ratio of the enrichment factors (ε) of the two isotopes as shown in the lambda (Λ) equation below (Eq.14) provides more information about the reaction mechanism, and whether it involves one pathway or multiple pathways (e.g., aerobic and anaerobic) (Fischer et al., 2008).

$$(\Lambda = \Delta\delta^{2}H / \Delta\delta^{13}C \approx \varepsilon H / \varepsilon C) \quad \text{(Eq.14)}$$

1.7 The importance of this research

Groundwater contamination by industrial waste such as petroleum products leads to scarcity of potable groundwater. Typically, groundwater bodies in arid areas are characterized by high temperature and elevated salinity. There are few studies have been completed on elevated salinity groundwater like those existing in arid areas (Kashir et al., 2017). Furthermore, several studies have reported that the use of chemical oxidants such as persulfate, hydrogen peroxide, and permanganate may have the capability to increase the contaminant degradation process by transforming the toxic chemicals into less harmful compounds. Table 1 shows some previous studies that used different oxidants. Overall, these studies agreed that using chemical oxidants to treat a wide variety of pollutants is a favorable solution for contaminant remediation. Along with the chemical oxidants, factors such as temperature, pH, total dissolved solids (TDS) and aquifer minerals should be considered prior to selecting an oxidant to achieve the most efficient contaminant remediation.

The research work involved laboratory experiments examining the chemical oxidation effectiveness at 30^0C for site #1 and site #2 that have total dissolved solid concentrations of 7,000 mg/L and 18,000 mg/L, respectively. Although there were several previous contaminant remediation studies conducted using these oxidants, there are few experimental studies that have

been done at conditions similar to the saline, high-temperature groundwater of the sites used in this study. For example, a recent study by Kashir & McGregor (2015) conducted experiments in which sodium persulfate ($Na_2S_2O_8$) and sodium percarbonate ($Na_2(CO_3)_2$) were used as oxidants to oxidize target hydrocarbons and MTBE, with carbon isotope analysis used to identify the isotopic changes during the oxidation process. The difference between Kashir & McGregor (2015) and this study is that the current study used sodium persulfate ($Na_2S_2O_8$) and hydrogen peroxide (H_2O_2) as oxidants and utilized CSIA with carbon and hydrogen isotopes to study the contaminant oxidation process. The current study also uses 2D-CSIA to assess hydrocarbon degradation using persulfate oxidation. The expectations from the results of this study were at least to have significant contaminant degradation from reaction with both persulfate and hydrogen peroxide based on the results observed by previous studies (Ray et al., 2002; Bergendahl & Thies, 2005; Sra et al., 2013; Kashir et al., 2015).

Table 1: The use of different treatment applications for the oxidation of targeted hydrocarbons compiled from the literature

Oxidants	Targeted contaminants	Sample Condition	System	Authors
Persulfate (PS)	59 VOC's	• Artificial • EPA SW-846 method 8260B	• Thermal activation • 20^0C, 30^0C, and 40^0C	(Huang et al., 2005)
H_2O_2 Persulfate (PS) Permanganate (KMnO4)	PAH's	• Contaminated freshwater sediments – Italy	• H_2O_2 and PS • Catalyzed by Fe (II) • Catechol as a chelate agent • Potassium permanganate (KMnO4) • Ambient temperature and neutral pH	(Ferrarese et al., 2008)
Persulfate (PS)	BTEX	• Aqueous and soil slurry system - southern Taiwan	• Heat activation • Chelated agents* • 20^0C	(Liang et al., 2008)
H_2O_2	PAH's	• Contaminated soils • Former coking plant sites – N of France	• Fenton-like oxidation	(Usman et al., 2012)

H_2O_2 Persulfate (PS) Permanganate Percarbonate	PAH's	• Sandy loam soil • Former steel manufacturing site - France	• H_2O_2 • Sodium persulfate • Potassium permanganate • Sodium percarbonate • Chelating agent (Citric acid)	(Lemaire et al., 2013)
Persulfate (PS) & Percarbonate	BTEX, MTBE, Naphthalene, and TMB's	• Laboratory experiment and a subsequent field study	• Sodium persulfate $Na_2S_2O_8$ • Percarbonate $Na_2(CO_3)_2$ • + 30^0C • High salinity +31,000 mg/L	(Kashir et al., 2015)
Persulfate	Carbamazepine	• Artificial	• Activated by: heat, UV, iron, and H_2O_2	(Monteagudo et al., 2015)
Persulfate	(BTEX, TMBs, and naphthalene), TPH, and PHC fractions F1 and F2	• Borden and LC34-LSU aquifers • Artificial chemicals	• Unactivated persulfate • Activated by peroxide, chelated ferrous, and alkaline pH	(Sra et al., 2013)

∗ The chelating agents used in this experiment were citric acid and alternative chelating agents such as ethylenediaminetetraacetic acid (EDTA) and hydroxypropyl-b-cyclodextrin (HPCD).

1.8 Scope of work

The scope of work of this research project was as follows:

1) Oxidation of the targeted contaminants (BTEX, naphthalene, MTBE, and TMBs) using iron-activated and unactivated persulfate (control) was evaluated. The persulfate activator was Fe^{2+} chelated with citrate (sodium citrate $Na_3C_6H_5O_7$) at high and low citrate/Fe ratios at or near the groundwater temperature of 30^0C at site #1 by using groundwater and aquifer materials from that site.

2) Three stabilizers (citrate, phytate, and silica) along with the control (no stabilizer) experiment were prepared to evaluate the activity of H_2O_2 for MTBE oxidation on samples collected from site #1. Each stabilizer was prepared at high and low concentration expressed as H and L, respectively.

3) The two stabilizers, citrate and silica, at high concentrations similar to the high concentrations from #2 were used along with the control experiment (no stabilizer) to

examine the effectiveness of oxidizing the targeted hydrocarbons (BTEX, naphthalene, MTBE, TMBs) on samples collected from site #1 and site #2.

To accomplish #1, the concentrations of the various hydrocarbon contaminants as well as their C and H isotopic compositions were measured. The MTBE concentrations were measured for #2. For #3, the concentrations of the various hydrocarbon contaminants and their C and H isotopic compositions were measured.

Chapter 2

Experimental Design and Methods

2.1 Experimental design and materials

Two oxidants, sodium persulfate ($Na_2S_2O_8$) and hydrogen peroxide (H_2O_2), were used for the oxidation experiments. Three stabilizers, citrate (citric acid), phytate (phytic acid), and silica (metasilicate), were used for stabilization of the oxidants. The following reagents are used: glass distilled dichloromethane and methanol, organic-free deionized water, reagent grade benzene, toluene, ethyl benzene, p,m,o-xylenes, trimethylbenzenes, naphthalene and m-fluorotoluene (25 mg/L) as an internal standard. The contaminated groundwater that was used to conduct the experiments was collected from two sites named Site #1 and Site #2. Table 2 shows the main characteristics of the two sites. The chemical characteristics of the samples were analyzed by Maxxam Company for the persulfate and hydrogen peroxide stabilized by citrate, phytate, and silica experiments, and by Civil and Environmental Engineering (CEE) Groundwater & Soil Remediation Laboratory (University of Waterloo, Canada) for the experiments of hydrogen peroxide stabilized by citrate and silica.

The pH was measured using a pH probe and meter, and the calibration was done using solutions of pH 4, 7 and 10. Approximately 10 mL of sample is transferred to a 20 mL vial. The probe was inserted into the sample and a reading was taken from the meter after a stabilization period of about 1 min. The precision is ± 0.2 pH units.

Total inorganic carbon was measured by subtracting the total organic carbon from the total carbon (TIC = TC – TOC) using Shimadzu Total Organic Carbon Analyzer TOC-L with the 680°C combustion catalytic oxidation method, equipped with a ASI-L auto-sampler with a detection limit of 4 µg/L and a good precision of < 5%. The groundwater containers were shipped to the laboratory on ice, then preserved by sodium azide and filled full without aeration to prevent the biodegradation of organic compounds and stored in the fridge at 4^0C until needed.

Table 2: The characteristics of Site #1 and Site #2

	Site #1	Site #2
Aquifer materials	Tertiary deposits Conglomeratic sand, sandstone, and fissured limestone	Tertiary deposits Marine and lacustrine units Carbonate rocks, sandstone, and siltstone
Salinity	7000 mg/L	18000 mg/L
pH	~ 7.7	~ 7.9
TIC	~ 43.4 mg/L	~ 26.0 mg/L

2.2 Gas chromatography and mass spectrometry

For all experiments, gas chromatographic (GC) analysis was used to determine the concentrations of several aromatic hydrocarbons in groundwater samples. These hydrocarbons are: benzene, toluene, ethyl benzene, p, m, o-xylenes, the trimethylbenzenes, naphthalene, and methyl tert-butyl ether (BTEX + TMBs + naphthalene + MTBE).

Samples and standards were extracted in 20 or 40 ml vials with Teflon-faced silicone septa. The determinations were performed on a gas chromatograph (HP 7890) equipped with a splitless injection port, a 0.25 mm X 30M DB5 capillary column with a film thickness of 0.25 μm and a flame ionization detector. The chromatographic conditions were as follows: injection port temperature = 275^0C; initial column temperature = 35^0C; initial time = 0.5 min; heating rate = 15^0C/min; final temperature = 300^0C; final time = 2 min; detector temperature = 325^0C; column flow rate = 1 ml/min helium. The method detection limits range from 2-5 μg/L with a precision of < 5%.

For isotope analyses, a CF-IRMS (Deltaplus XL, Thermo Finnigan, Germany) is used to conduct this type of analysis. The IRMS is interfaced with an Agilent 6890 Gas Chromatograph (GC) (Agilent, USA) that is coupled with GC Combustion III (Thermo Finnigan, Germany). The GC is used to separate the different organic compounds after which

all separated compounds are combusted to CO_2 gas for carbon isotope analysis and pyrolyzed to H_2 gas for the hydrogen isotope analysis and then the gases are directed to the IRMS for the carbon or the hydrogen isotopic ratio measurements.

All hydrocarbon samples were originally in 20 ml vials and were refrigerated with no headspace to minimize the loss of gases. After that, a portion of each sample was extracted and placed in a new 20 ml vial and diluted with distilled water, with ~2 ml headspace for gas extraction. Solid phase micro extraction (SPME) was used to extract gases from samples that were first placed in a magnetic stirrer for approximately 20 min. All carbon and hydrogen isotope measurements were performed using an isotope ratio mass spectrometer (IRMS), with an analytical uncertainty of ± 0.5‰ and ±5.0‰, respectively. Continuous monitoring of the isotope fractionation of BTEX standards provides the first check on the analytical results. Samples are run in batches. Each batch consists of a set of samples and a set of standards. Typically, standards are analyzed before and after analyzing the set of samples. At least one repeat is conducted for every seven samples. Once a batch is analyzed, the data are evaluated, and the isotopic ratios of the samples are corrected to the standards. Average and standard deviations of the standards are calculated. Typically, an acceptable standard deviation is < 0.5 ‰ for carbon and < 5.0 ‰ for hydrogen.

2.3.0 Detailed experimental methods

2.3.1 Oxidation by persulfate of target hydrocarbons and MTBE from site #1

The persulfate experiments were divided into three sets: 1) persulfate control (PSC) without the addition of activator or chelating agent, 2) the addition of iron chelated by sodium citrate ($Na_3C_6H_5O_7$) with a low molar ratio of citrate compared to persulfate and iron where the persulfate/citrate/Fe ratio is 20/2/10 (CFEL), 3) the addition of iron chelated by sodium citrate ($Na_3C_6H_5O_7$) with a high molar ratio of citrate compared to persulfate and iron where the persulfate/citrate/Fe ratio is 20/10/10 (CFEH). Each experiment was conducted in duplicate using a 1L glass bottle (microcosm). Samples were taken for analysis at: day 0 (5 min, 1 hour, 3 hours), day 1, day 3, day 7, day 10, and day 14.

For each persulfate control experiment, 750 ml of groundwater from site #1 was mixed with 2-5 mg/L spiked BTEX, naphthalene, and trimethyl-benzene (TMB), 50-100 mg/L MTBE, and 150 g of aquifer materials from site #1. After mixing the samples and placing in a water bath at 30^0C to simulate the groundwater temperature at site #1, 50 mL of the mixture was taken to determine the initial concentration (INIT1). Then, 7.5 mL of a 5 g/L persulfate solution (prepared from a 100x dilution of a 500 g/L stock solution) was added and then another 20 mL sample from the mixture was taken immediately for the second initial concentration (INIT2).

For each activated persulfate experiment, 750 ml of groundwater from site #1 was mixed with 2-5 mg/L spiked BTEX, naphthalene, trimethyl-benzene (TMB), and 50-100 mg/L MTBE, and 150 g of aquifer materials from site #1. As with the persulfate control experiment, the mixture was mixed at near 30^0C. Then, 50 ml of the mixture was taken for initial concentrations (INIT1). After that, the remaining mixture from site #1 was dispensed into four microcosms (2 for high ratio and 2 for low ratio). Then, a mixture of persulfate, citrate, and Fe was prepared with different (low and high) citrate/Fe ratios and added to each of the four microcosms. A 20 mL sample was taken immediately for the second initial concentration (INIT2). Samples were taken for analysis at: day 0 (5 min, 1 hour, 3 hours), day 1, day 3, day 7, day 10, and day 14.

2.3.2 The oxidation of MTBE from site #1 by hydrogen peroxide using three stabilizers: citrate, phytate, and silica

The experiments for examining the effectiveness of three stabilizers (citrate, phytate, and silica) were prepared in seven sets of duplicates: 1) controls without stabilizer (CON 1); 2) low concentration of citrate stabilizer (CIT L); 3) high concentration of citrate stabilizer (CIT H); 4) low concentration of phytic acid stabilizer (PHY L); 5) high concentration of phytic acid stabilizer (PHY H); 6) low concentration of silica stabilizer (SIL L); and 7) high concentration of silica stabilizer (SIL H). In details, all experiments were prepared in duplicates using 7L of MTBE spiked groundwater from site #1 and then dispensed into seven 1L bottles containing a known amount of a stabilizer: citrate, phytate, or silica (SiO_2) (two bottles for each stabilizer and one bottle without stabilizer named Control). The two bottles of

each stabilizer have different concentrations; 1L for high concentration and 1L for low concentration, expressed as H and L, respectively. Table 3 describes the concentration of each stabilizer along with the control bottles. Each 1L bottle was dispensed in duplicate into 500 ml plastic bottles that have 400 ml of spiked water and 100g of aquifer material. Finally, 45 ml of a 50% solution of H_2O_2 was added to each 500 ml plastic bottle and then capped and placed in a water bath at 30^0C. The percentage of H_2O_2 was analytically measured using a titration method with 0.1N potassium permanganate. Samples were analyzed at: day 0 (1 hour), day 2, day 4, day 9, and day 14.

Table 3: The concentrations of citrate, phytate, and silica stabilizers used for hydrogen peroxide along with a control experiment in which no stabilizer was added

Control	Citrate H	Citrate L	Phytate H	Phytate L	Silica H	Silica L
No stabilizer	0.05 M (9.6 g/l citric acid)	0.01 M (1.9 g/l citric acid)	10 mM (6.6 g/l Phytic acid)	1 mM (0.66 g/l Phytic acid)	2 mM (0.56 g/l sodium metasilicate)	0.2 mM (0.056 g/l sodium metasilicate)

2.3.3 The effectiveness of hydrogen peroxide using citrate and silica as stabilizers on samples from site #1 and site #2

The samples were prepared in duplicate using 2L bottles. In detail, samples were divided into control (without stabilizer), citrate, and silica experiments. In all experiments, 1600 ml of spiked groundwater (BTEXN+MTBE+TMBs) was dispensed into 2L glass bottles (microcosms). Then, 15.4g (0.05 M) citric acid and 0.9g (2 mM) sodium metasilicate were added to each microcosm except for the control experiment (no addition of stabilizers). After the dissolution of stabilizers, 300g of aquifer materials was added to all microcosms. For the initial analysis, before H_2O_2 addition, 160 ml from each bottle was removed and then 160 ml of 50% H_2O_2 was added to all microcosms. After the addition of H_2O_2, samples were taken immediately for initial H_2O_2 analysis, and then the microcosms were capped by septa along with a gas bag to collect O_2 from the decomposition of H_2O_2. For the following samples taken

for analysis, septa were taken out, samples were taken, and then the microcosms were capped with new septa. Finally, all microcosms were placed in a water bath at 30^0C and shaken daily to make sure that the reaction was taking place everywhere in the bottles. Samples were taken for analysis over 7 days at: day 0 (4 hours), day 1, day 3, and day 7.

Chapter 3

Results and Discussion

3.1.0 Hydrocarbon concentrations

3.1.1 Experiments with activated and unactivated persulfate for site #1

The results showed that the activated persulfate experiment (at high and low ratios of citrate stabilizer to chelated Fe) had a higher removal percentage of hydrocarbons than the control experiments. Note that the rate of oxidation was not remarkably different for low versus high citrate/Fe ratios (Figure 1). Only benzene, toluene, and MTBE remained at the end of day 14. The other compounds were fully oxidized by day 14 in all experiments. Therefore, only the results from MTBE, benzene, and toluene will be interpreted (Appendix A shows the concentration of hydrocarbons, pH, TIC, and persulfate). In details, based on (Eq.1), the removal percentages for benzene were 62.1%, 59.4%, and 65.1% for PSC, CFEL, and CFEH, respectively (Figure 1a). Toluene had the best result with 99.4% of destruction in the CFEH experiment followed by PSC with 97.7% and the CFEL experiment with 97.0% (Figure 1b). The result of the PSC experiment was close to the one obtained from the CFEL experiment. MTBE showed a small removal (4.2%) during the PSC experiment, with an initial value of 73.45 µg/L and a final value of 70.35 µg/L by day 14. In the CFEL experiment, MTBE degraded by 6.6% (from 87.05 µg/L to 81.30 µg/L). The CFEH experiment showed a better result for MTBE in comparison with the PSC and CFEL experiments, with close to 13% removal in which the concentration decreased from 83.25 µg/L to 72.65 µg/L (Figure 2a).

The oxidation of MTBE results in tert-butyl alcohol (TBA) formation. The Production of TBA is an evidence of the oxidation of MTBE. It is also important to know the fate of TBA and know whether the TBA is degrading or accumulating since the TBA is considered to be a toxic byproduct of MTBE and its accumulation is not desirable. All experiments showed TBA production. In details, the PSC experiment had the higher TBA production (around 14 µg/L) at the end of day 14, followed by the CFEH experiment (4.65 µg/L). The least production of

TBA occurred with the CFEL experiment (3.75 µg/L) (Figure 2b). Furthermore, the small removal of MTBE oxidation in the PSC allowed the formation of TBA to take place and accumulate until the end of the experiment. Unlike the PSC, the concentration of TBA with the activated persulfate (low & high ratio of citrate/Fe) was small (~ 4). The small amount of TBA accumulated from the activated persulfate was due to the oxidation of MTBA, in which the chelated iron was capable to maintain the oxidation processes for any TBA formed from the MTBE oxidation.

By looking at the results obtained from the three experiments, the CFEH experiment generally had the best results of contaminant destruction followed by CFEL and then PSC.

Changes in the major ion chemistry of the water can be seen in Table 4. The groundwater at site # 1 has a significant salinity with elevated Cl^-, SO_4^{2-}, Na^+, and Ca^{2+} and there was also significant dissolved Si. Moreover, additional SO_4^{2-} was generated from persulfate with the experiment having the lower citrate/Fe ratio (CFEL) generating the most SO_4^{2-}. No significant change in concentration of the other anions was noted (the detection limit for Br^- was very high). The increase in Na^+ reflects the use of sodium persulfate in the experiment, and increased Ca^{2+} and TIC (total inorganic carbon) resulted from calcite dissolution.

Overall, the activated persulfate with an activator (Fe^{2+}) accompanied by a chelating agent (citrate) achieved good results over the unactivated persulfate for contaminant remediation. No remarkable changes in the persulfate concentration were observed. The persulfate concentration dropped (by about 2000-3000 µg/L) in the activated persulfate experiments because of the addition of chelate which maintained the persulfate in the solution to oxidize the contaminants; while with the unactivated persulfate, the concentration did not change significantly until the end of the experiment and decreased to around 4500 µg/L (Figure 1c).

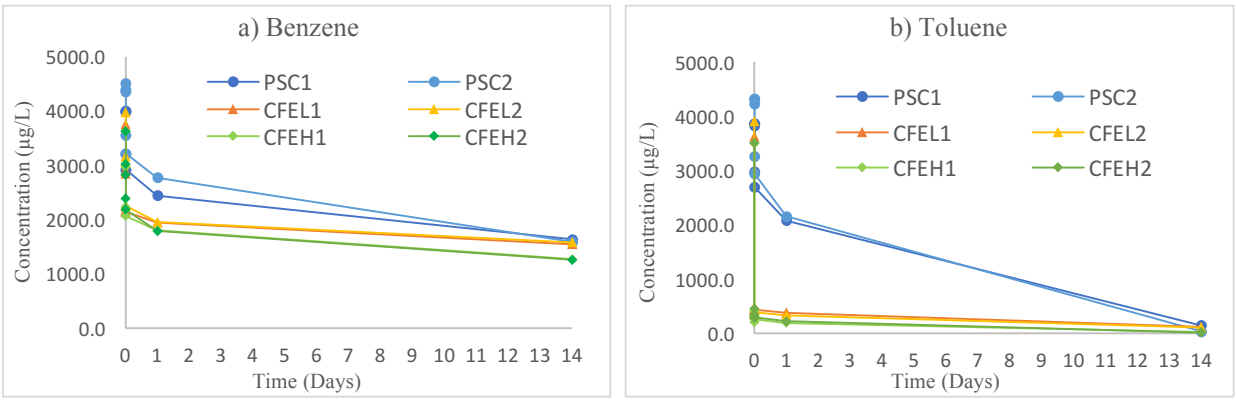

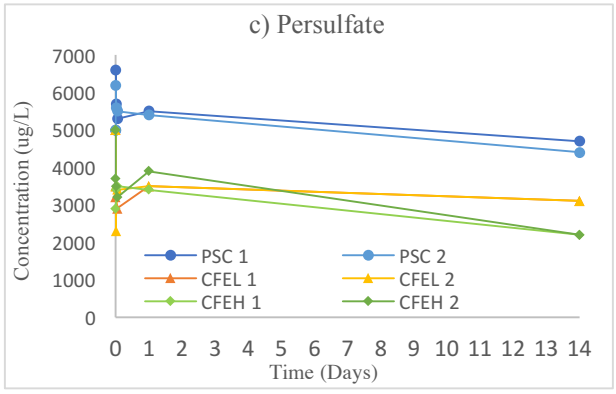

Figure 1: The concentration (µg/L) with time (days) of a) benzene and b) toluene during the persulfate experiments at site #1. c) represents the concentration (µg/L) of persulfate versus time (days). PSC = unactivated persulfate (Control), CFEL = persulfate activated by chelated iron with a lower citrate/Fe ratio, CFEH = persulfate activated by chelated iron with a higher citrate/Fe ratio.

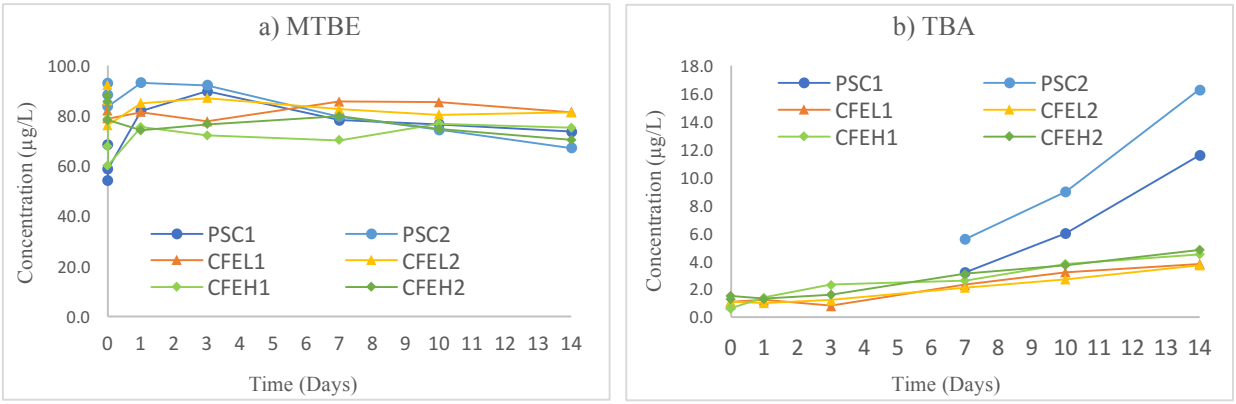

Figure 2: The concentration (µg/L) with time (days) of a) MTBE oxidation and b) TBA production during the persulfate experiments at site #1. PSC = unactivated persulfate (Control), CFEL = persulfate activated by chelated iron with a lower citrate/Fe ratio, CFEH = persulfate activated by chelated iron with a higher citrate/Fe ratio.

Table 4: Initial and final concentration (mg/L) of the major ions (anions and cations) during the persulfate experiments for site #1

	UNITS	Initial Anion	PSC[1] Anion	RDL*	QC Batch*	CFEL[2] Anion	RDL	CFEH[3] Anion	RDL*	QC Batch*
Anions										
Fluoride (F^-)	mg/L	1.2	1.2	0.10	4287119	1.1	0.10	1.6	0.10	4287119
Orthophosphate (PO_4^{3-})	mg/L	0.018	ND	0.010	4287330	ND (5)	0.20	ND (5)	0.20	4288168
Nitrite (NO_2^-)	mg/L	ND (4)	ND (4)	0.050	4286735	ND (4)	0.050	ND (4)	0.10	4286735
Dissolved Chloride (Cl^-)	mg/L	2700	3100	50	4285881	3100	50	3100	50	4285881
Nitrate (NO_3^-)	mg/L	4.56	6.43	0.50	4286735	5.48	0.50	ND	1.0	4286735
Nitrate + Nitrite	mg/L	4.56	6.43	0.50	4286735	5.48	0.50	ND	1.0	4286735
Dissolved Bromide (Br^-)	mg/L	ND	ND	50	4285881	ND	50	ND	50	4285881
Dissolved Sulphate (SO_4^{2-})	mg/L	1800	3000	50	4285881	3700	50	4500	50	4285881
	UNITS	**INITIAL CATION**	**PSC CATION**	**RDL**	**CFEL CATION**	**RDL**	**CFEH CATION**	**RDL**	**QC Batch**	
Cations										
Dissolved Calcium (Ca^{2+})	mg/L	460	780	0.05	980	0.5	930	0.5	4288300	
Dissolved Iron (Fe^{2+})	mg/L	0.28	ND	0.02	52	0.2	550	0.2	4288300	
Dissolved Magnesium (Mg^{2+})	mg/L	190	210	0.05	220	0.5	220	0.5	4288300	
Dissolved Manganese (Mn^{2+})	mg/L	0.07	ND	0.01	0.6	0.1	1.3	0.1	4288300	
Dissolved Potassium (K^+)	mg/L	210	190	1	190	10	180	10	4288300	
Dissolved Silicon (Si^{4+})	mg/L	23	20	0.2	12	2	22	2	4288300	
Dissolved Sodium (Na^+)	mg/L	1600	2700	5	2700	5	2600	5	4288300	

*RDL = Reportable Detection Limit
*QC Batch = Quality Control Batch
ND = Not detected
(1) PSC = unactivated persulfate (Control).
(2) CFEL = persulfate activated by chelated iron with a lower citrate/Fe ratio.
(3) persulfate activated by chelated iron with a higher citrate/Fe ratio
(4) Nitrite: Due to the sample matrix, sample required dilution. Detection limits were adjusted accordingly.
(5) Due to color interferences, sample required dilution. Detection limit was adjusted accordingly.

3.1.2 Experiments with H_2O_2 stabilized by citrate, phytate, and silica for site #1

A set of experiments was performed to evaluate the effectiveness of three stabilizers (citrate, phytate, and silica) that are utilized to maintain the H_2O_2 activity for the oxidation of MTBE. This experiment was accompanied with a control (no addition of stabilizer)

experiment as well. Almost all experiments showed significant results of MTBE degradation. In detail, in the control experiment, the degradation was around 94.0%, and both experiments of H_2O_2 stabilized by citrate (at high and low concentrations) had a range of removal between 93.3% to 95.8% (Figure 3a). Moreover, the silica stabilized H_2O_2 (high and low) experiments showed a high destruction of 91.0%. In addition, the high concentration of phytate yielded a result close to the ones obtained from other experiments. However, the result from the low phytate experiment showed only 75% of MTBE degradation by day 14 (Figure 3b), and this is because phytate was totally consumed via MTBE oxidation. Although there was a small amount of H_2O_2 (~3%) remaining until the end of day 14, this H_2O_2 became destabilized after the complete consumption of phytate during the oxidation process and therefore, the production of hydroxyl radicals was decreased and affected the oxidation of MTBE (Figure 4b). Hydrogen peroxide stabilized by citrate was the most successful for MTBE destruction for both the high and low stabilizer concentration experiments.

In terms of persistence, hydrogen peroxide stabilized by citrate was successful to maintain the hydrogen peroxide oxidation until the complete removal of MTBE. In addition, the citrate stabilizer was also capable of consuming all H_2O_2 via the complete removal of MTBE by day 14 (Figure 4). Moreover, the low phytate experiment seemed to maintain the persistence of hydrogen peroxide more than the high phytate experiment, but again, no significant results of MTBE oxidation were obtained from preserving H_2O_2 until the end of the experiment (Figure 4).

Production of TBA occurred because of MTBE oxidation. The high concentration of citrate and phytate resulted in high production of TBA (Figure 5a), whereas low phytate and high silica concentrations appeared to produce the lowest amount of TBA (Figure 5b). The small amount of TBA for the low phytate concentration experiment was due to the persistence of H_2O_2 (Figure 4b), in which the remaining H_2O_2 was able to maintain the oxidation of both MTBE and TBA. Appendix B shows the concentration of MTBE and TBA with time in the control, silica, citrate, and phytate experiments.

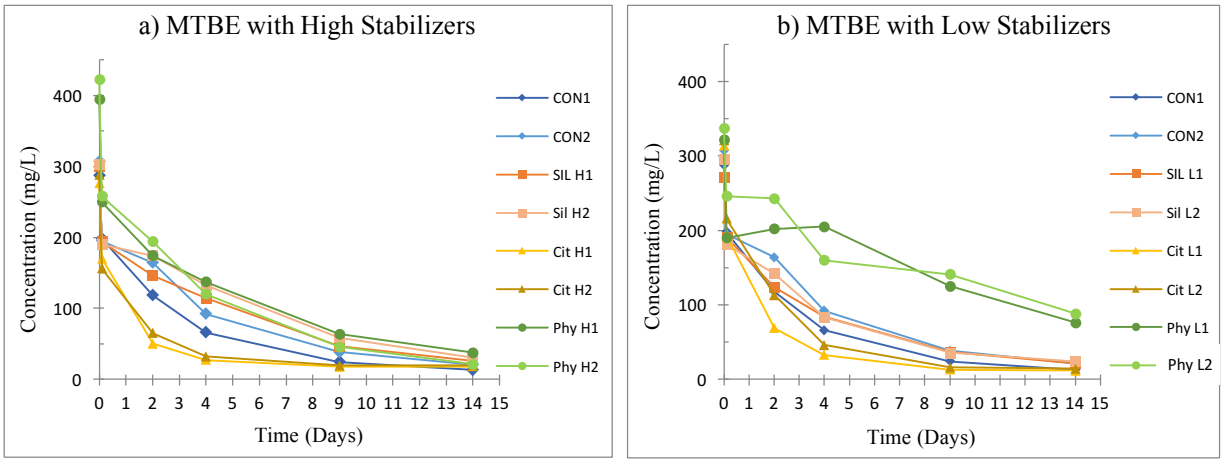

Figure 3: The concentrations (mg/L) of MTBE with time (days) during the use of hydrogen peroxide at a) high and b) low concentrations of silica, citrate, and phytate for site #1. (see Table 3 for stabilizer concentrations). CON = control samples (no stabilizers), Sil = silica experiment, Cit = citrate experiment, Phy = phytate experiment.

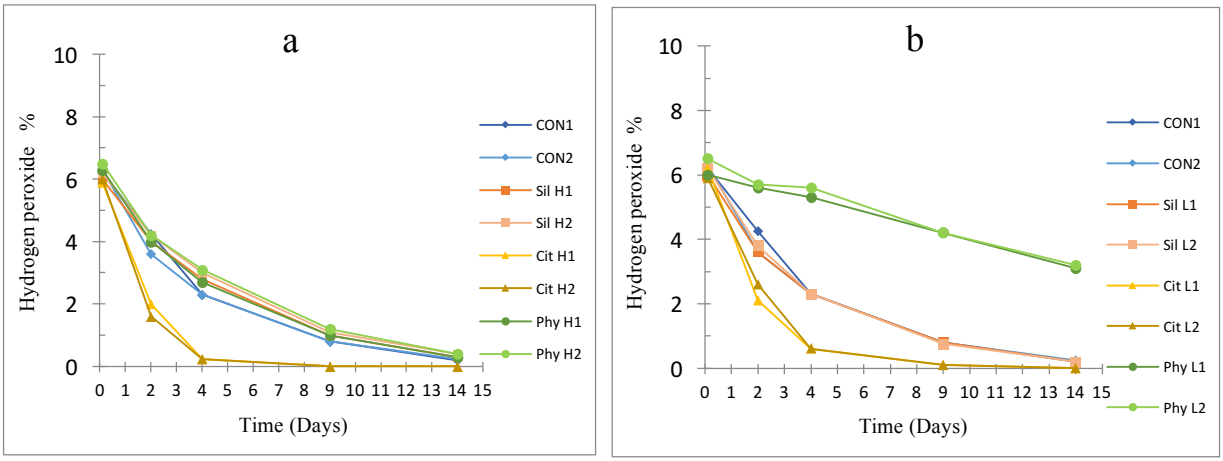

Figure 4: The persistence of H_2O_2 at a) high and b) low concentrations of silica, citrate, and phytate for site #1. CON = control samples (no stabilizers), Sil = silica experiment, Cit = citrate experiment, Phy = phytate experiment.

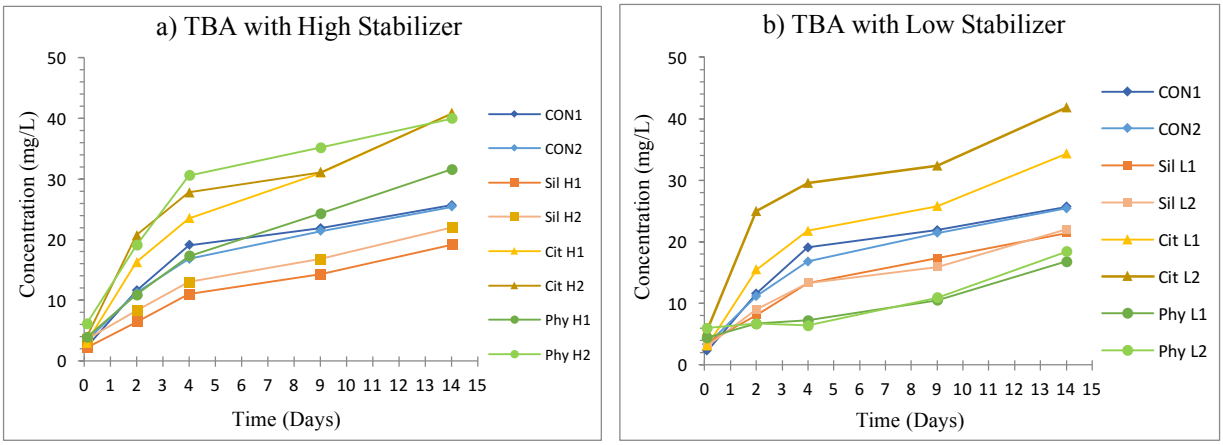

Figure 5: The production of TBA (mg/L) with time (days) at a) high and b) low concentrations of silica, citrate, and phytate for site #1. CON = control samples (no stabilizers), Sil = silica experiment, Cit = citrate experiment, Phy = phytate experiment.

The stabilizers are used to minimize the reaction of hydrogen peroxide with the available Fe^{2+}. However, Fe^{2+} might be leached from the sediments. The analyses of leachable Fe are shown in Appendix C. The leached Fe is low in the initial sediments at site # 1 (Fe^{2+} ~ 0.03 mg/g; Fe total ~ 0.37 mg/g). After fourteen days, minor to negligible changes in the amount of Fe^{2+} occurred after the oxidation by H_2O_2 in which the final concentration of Fe^{2+} was ~ 0.05 mg/g and total Fe was ~ 0.32 mg/g, indicating that additional Fe was not leached from the sediment during oxidation of MTBE.

A large increase in the total inorganic carbon (TIC) concentration to ~166 mg/L, and a decrease in the citrate concentration occurred in the low citrate microcosms at the end of the experiment because much of the citrate was oxidized to dissolved TIC. In contrast, the high citrate microcosms experiments showed an initial increase of the TIC to over 300 mg/L but this increase was followed by a sharp decrease to less than 5 mg/L of TIC at the end of the experiments. The higher increase of TIC in the high citrate microcosm was due to the high concentration of citrate that yielded more acidic conditions. Little change in the major inorganic species was observed, except for the increased Ca^{2+}, especially in the citrate-stabilized system. The increased Ca^{2+} formed in the citrate experiment was due to the addition of citric acid, which reduced the pH (acidic condition), and enhanced the calcite dissolution that yielded Ca^{2+} (Table 5).

Table 5: The initial and final concentration of anions and cations from the site #1 experiments of controlled H_2O_2 (no stabilizer), H_2O_2 stabilized by citrate (high and low ratio), phytate (high and low ratio), and silica (high and low ratio)

	Unit	Control		Silica L		Silica H		Citrate L		Citrate H		Phytate L		Phytate H		
		Initial	Final	Initial	Final	Initial	Final	Initial	Final	Initial	Final	Initial	Final	Initial	Final	RDL *
Anions																
Chloride (Cl^-)	mg/L	2900	2700	2900	2700	3000	2800	2900	2700	3000	2700	3000	2700	2900	2700	20
Sulphate (SO_4^{2-})	mg/L	1800	2300	1800	2400	1800	2500	1700	1900	1600	1700	1800	1900	1800	2300	20
Nitrate (NO_3^-)	mg/L	4.09	7.52	4.21	6.15	4.33	1.45	4.24	1.59	4.09	7.50	2.08	4.63	4.14	7.12	0.10
Nitrite (NO_2^-)	mg/L	0.017	0.083	ND	0.088	ND (1) *	ND (1)	ND (1)	ND (1)	ND	ND (1)	ND (1)	ND (1)	ND (1)	0.065	0.010
Fluoride (F^-)	mg/L	1.3	1.1	1.2	1.1	0.89	0.91	0.95	1.6	1.1	1.6	1.2	0.44	1.2	0.99	0.10
Bromide (Br^-)	mg/L	ND	ND	ND	ND	ND	ND	ND	ND	ND	ND	ND	ND	ND	ND	20
Orthophosphate (PO_4^{3-})	mg/L	0.013	ND	0.011	ND	0.013	ND	ND	3.4	ND	2.3	0.055	ND	0.62	ND	0.010
Cations																
Sodium (Na^+)	mg/L	1800	1700	1800	1800	1900	1900	1800	1800	1800	1800	2700	2500	1800	1600	5
Calcium (Ca^{2+})	mg/L	480	740	450	750	350	730	470	1100	470	2300	470	180	450	670	0.5
Magnesium (Mg^{2+})	mg/L	210	200	210	200	210	190	200	200	210	220	210	110	210	200	0.05
Potassium (K^+)	mg/L	220	200	220	200	220	200	220	200	220	210	220	180	220	200	1
Iron (Fe^{2+})	mg/L	ND	ND	ND	ND	ND	ND	0.07	ND	0.07	0.08	3.1	ND	ND	ND	0.02
Manganese (Mn^{2+})	mg/L	ND	0.73	ND	0.74	ND	0.67	0.14	0.90	0.11	2.0	0.45	0.11	ND	0.82	0.01

*RDL = Reportable Detection Limit
*(1) Nitrite: Due to the sample matrix, sample required dilution. Detection limits were adjusted accordingly.
*ND: not detected

3.1.3.0 Experiments with H_2O_2 stabilized by citrate and silica for site #1 and site #2

3.1.3.1 Site #1:

The experiment of citrate-stabilized hydrogen peroxide showed a significant degradation to nearly 100% of most hydrocarbons and thus reached non-detectable levels by day 3 for most hydrocarbons (see Appendix D). However, ethylbenzene and m-xylene had the lowest removal percentage by citrate-stabilized hydrogen peroxide, with around 25 µg/L remaining by day 7, which represents 99.5% removal of these two compounds (Figure 6c, d). In the control and silica-stabilized experiments, all hydrocarbons showed some degradation to < 100 µg/L except for naphthalene, which had a lower degradation than the other compounds and remained ≥ 100 µg/L after day 7 (Figure 6e). The results from the silica-stabilized H_2O_2 experiments were similar to the results from the controlled H_2O_2 experiments (Figure 6).

In the case of MTBE, the control and silica-stabilized H_2O_2 experiments showed some degree of MTBE destruction in seven days by about 82% and 80% of removal, respectively. By comparison, the citrate-stabilized H_2O_2 experiment showed a greater reduction in MTBE concentration to < 30 mg/L which represents 94% of removal. Moreover, all cases of MTBE oxidation resulted in the production of TBA. In details, for the control H_2O_2 experiment, the production of TBA was between 12 and 24 mg/L, whereas the citrate-stabilized H_2O_2 experiment produced 50 mg/L of TBA due to the more rapid destruction of MTBE. Overall, the removal of MTBE was greater than the observed accumulation of TBA, which means that although TBA is produced, it is also consumed by the oxidation process (Figure 7).

In terms of persistence, H_2O_2 appeared to persist longer in the control and silica-stabilized experiments compared with the citrate experiment. In the citrate-stabilized H_2O_2 experiment, H_2O_2 was consumed by Day 3 via oxidation of hydrocarbons (Figure 8), with a total removal of all hydrocarbons occurring by Day 7 (Figure 6). The remaining MTBE and TBA will depend on biodegradation for their removal. Although there was about 20 mg/L of dissolved oxygen (DO) at the end of the experiment, this amount was not sufficient to mineralize the remaining MTBE and TBA.

The production of more than 280 mg/L TIC (dominantly HCO_3^- at near-neutral pH) in the citrate experiment was apparently quickly buffered. Moreover, the increased Ca^{2+} and Mg^{2+} in the citrate-stabilized microcosms is likely due to the dissolution of carbonate minerals

($CaCO_3$ and $MgCO_3$) rather than from mineralization of the added citrate (Table 6). In the control and silica experiments, Ca^{2+} increased slightly (Table 6) while TIC declined, suggesting little carbonate mineral dissolution occurred in these microcosms.

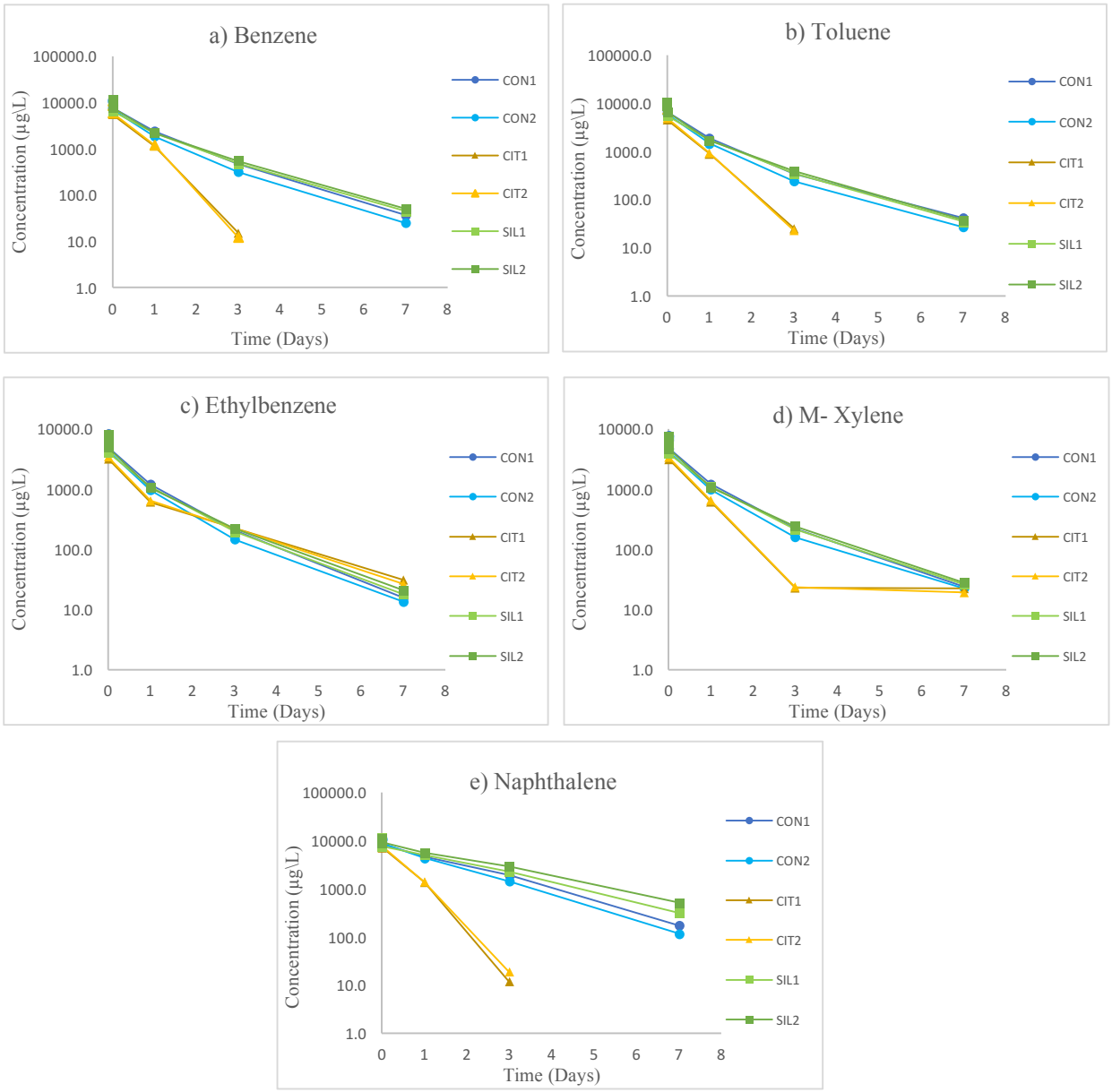

Figure 6: The concentration (µg/L) with time (days) of a) benzene, b) toluene, c) ethylbenzene, d) M-xylene, and e) naphthalene during the experiment of H_2O_2 stabilized by citrate and silica for site #1. CON = control samples (no stabilizers), Cit = citrate experiment, Sil = silica experiment.

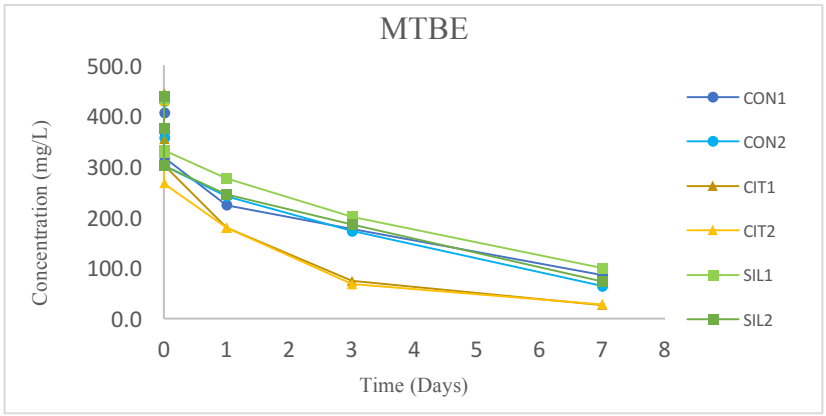

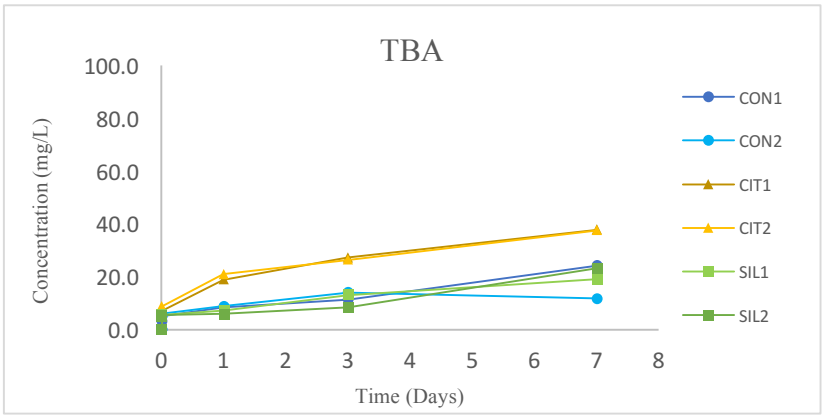

Figure 7: The concentration of MTBE (mg/L) versus TBA production (mg/L) with time (days) in the control, citrate, and silica experiments with H_2O_2 for site #1. CON = control samples (no stabilizers), Cit = citrate experiment, Sil = silica experiment.

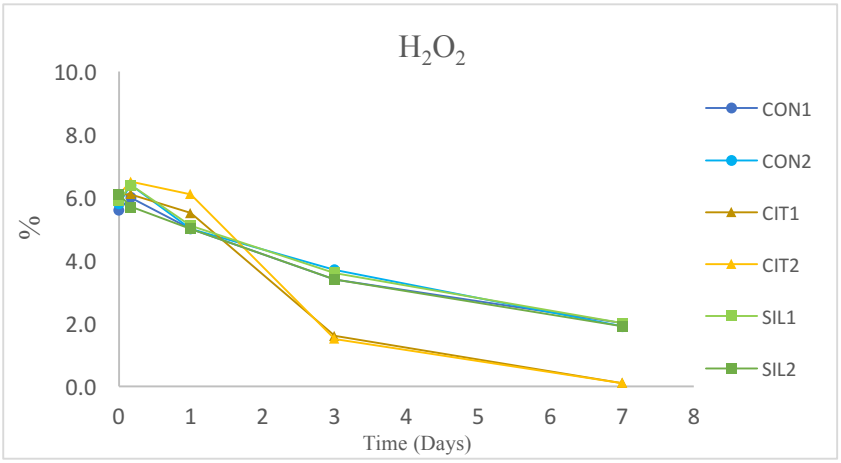

Figure 8: Persistence of H_2O_2 in the control, citrate, and silica experiments for site #1. CON = control samples (no stabilizers), Cit = citrate experiment, Sil = silica experiment.

Table 6: The initial and final concentration (mg/L) of anions and cations in the hydrogen peroxide stabilized by citrate and silica experiments along with the control (no stabilizer) experiment for site #1

Anions	Unit	Initial values	Control final	Citrate final	Silica final	RDL
Chloride (Cl^-)	mg/L	2500	2300	2300	2300	20
Sulfate (SO_4^{2-})	mg/L	1500	2200	2200	2200	20
Nitrate (NO_3^-)	mg/L	3.68	5.91	6.18	5.86	0.10
Nitrite (NO_2^-)	mg/L	0.016	0.080	0.026	0.090	0.010
Fluoride (F^-)	mg/L	1.0	0.74	1.1	0.74	0.10
Bromide (Br^-)	mg/L	ND	ND	ND	ND	20
Orthophosphate (PO_4^{3-})	mg/L	0.010	ND	3.1	ND	0.010
Cations						
Sodium (Na^+)	mg/L	1600	1500	1500	1600	5
Calcium (Ca^{2+})	mg/L	410	710	2200	660	0.5
Magnesium (Mg^{2+})	mg/L	180	170	200	180	0.5
Potassium (K^+)	mg/L	170	150	150	150	10
Iron (Fe^{2+})	mg/L	ND	ND	ND	ND	0.2
Manganese (Mn^{2+})	mg/L	ND	0.9	2.2	0.5	0.1

*ND: not detected

*RDL: reportable detection limit

3.1.3.2 Site #2:

The results showed that all hydrocarbons demonstrated some degradation to < 100 µg/L except for naphthalene in both the control and silica-stabilized experiments in which the remaining concentration was ≥ 100 µg/L by day 7 (Figure 9c). The control and silica-stabilized experiments were similar in terms of the rate of H_2O_2 oxidation. On the other hand, the citrate-stabilized experiment showed a higher removal and reached undetectable concentration levels by day 3 for most hydrocarbon compounds (e.g., benzene & toluene; Figure 9a, b) (see Appendix D).

In the control and silica-stabilized experiments, MTBE concentrations were reduced from 420 mg/L to less than 75 mg/L, respectively, and 10-20 mg/L of TBA was generated. In the citrate experiment, the MTBE concentrations declined from 420 mg/L to 17 mg/L, and a larger amount of TBA was produced (30 mg/L) (see Appendix E). Overall, the experiments showed that the destruction of MTBE was greater than the accumulation of TBA (Figure 10).

In terms of H_2O_2 persistence, H_2O_2 in both the unstabilized (control) and silica-stabilized experiments persisted longer than in the citrate-stabilized experiment. All H_2O_2 was quantitatively destroyed via hydrocarbon oxidation by Day 3 in the citrate-stabilized experiment (Figure 11). Like the results obtained from Site #1, the citrate-stabilized H_2O_2 was more effective for the removal of hydrocarbons within 7 days. Although there was some DO (around 20 mg/L) at the end of the citrate-stabilized experiment, this amount would not be enough to mineralize the remaining MTBE and TBA.

The production of more than 340 mg/L TIC in the citrate microcosms was apparently quickly buffered by the groundwater and aquifer solids from site #2. Furthermore, there was an increase in Ca^{2+} and Mg^{2+} in citrate-stabilized microcosms to about 2900 mg/L and 380 mg/L, respectively, which is likely due to the dissolution of carbonate minerals ($CaCO_3$ and $MgCO_3$) rather than from mineralization of the added citrate (Table 7). Unlike the citrate experiment, the Ca^{2+} and Mg^{2+} in the control and silica experiments had a small decrease to 1100 mg/L and ~355 mg/L, respectively, suggesting that the dissolution of carbonates during this experiment was minimal.

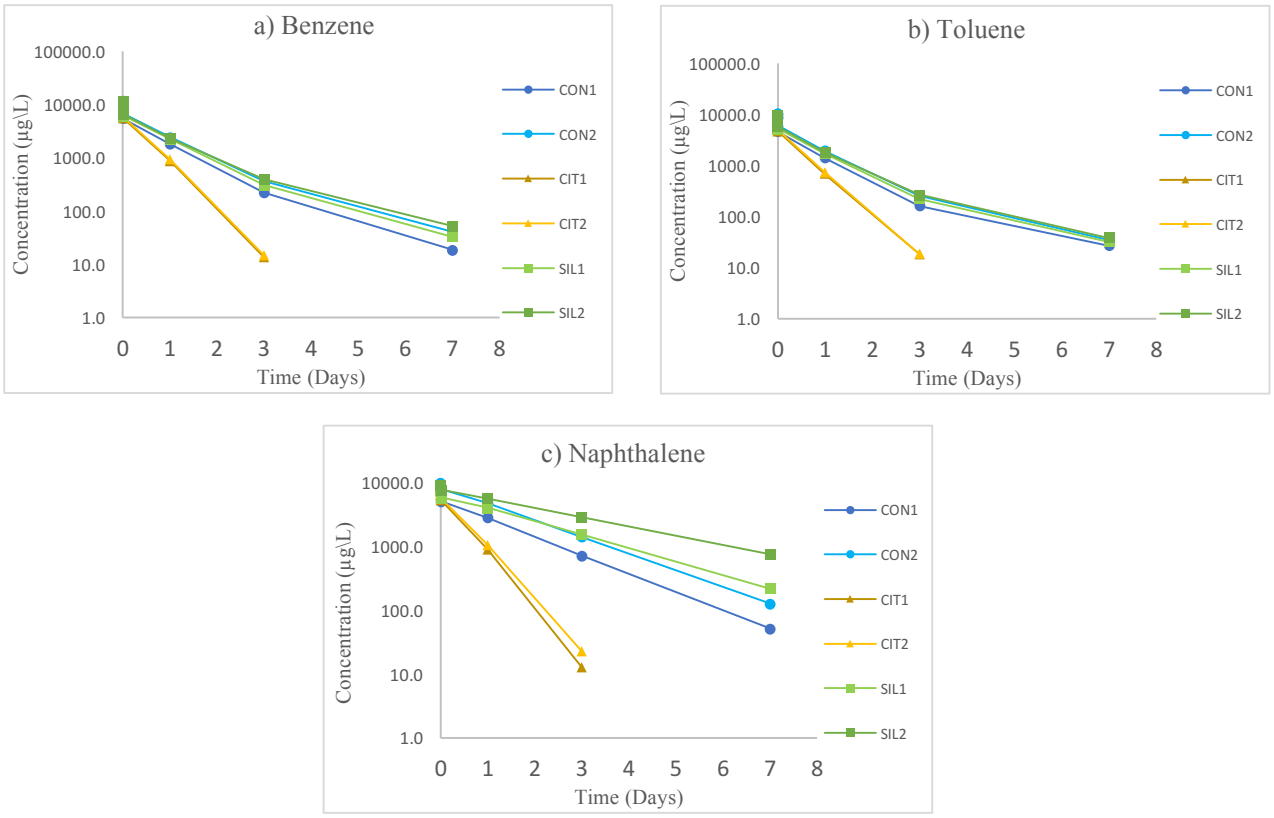

Figure 9: The concentration (µg/L) with time (days) of a) benzene, b) toluene, and c) naphthalene during the experiment of H_2O_2 stabilized by citrate and silica for site #2. CON = control samples (no stabilizers), Cit = citrate experiment, Sil = silica experiment.

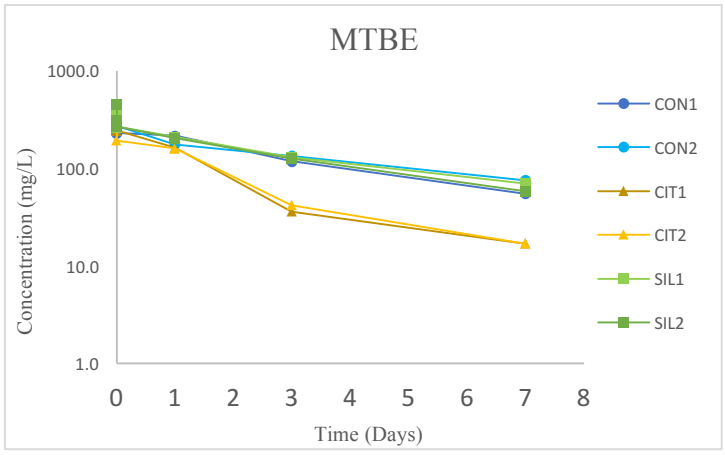

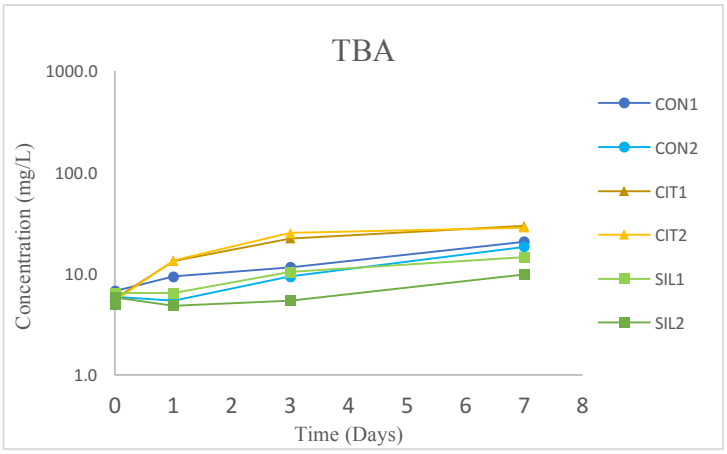

Figure 10: The concentration of MTBE (mg/L) versus TBA production (mg/L) with time (days) in the control, citrate, and silica experiments with H_2O_2 for site #2. CON = control samples (no stabilizers), Cit = citrate experiment, Sil = silica experiment.

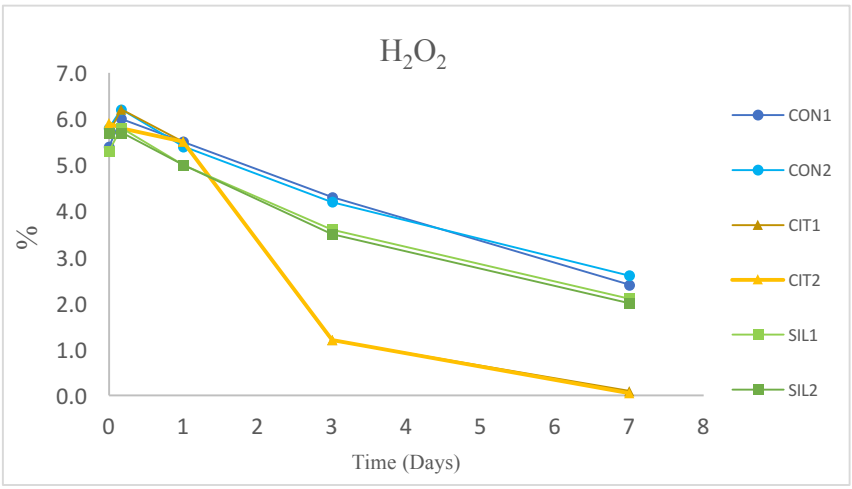

Figure 11: Persistence of H_2O_2 in the control, citrate, and silica experiments for site #2. CON = control samples (no stabilizers), Cit = citrate experiment, Sil = silica experiment.

Table 7: The initial and final concentration (mg/L) of anions and cations in the hydrogen peroxide stabilized by citrate and silica experiments along with the control (no stabilizer) experiment for site #2

Anions	Unit	Initial Values	Control final	Citrate final	Silica final	RDL
Chloride (Cl^-)	mg/L	8200	7300	7400	7300	50
Sulfate (SO_4^{2-})	mg/L	2900	2600	3200	2600	50
Nitrate (NO_3^-)	mg/L	57.6	55.9	55.3	55.9	2.0
Nitrite (NO_2^-)	mg/L	ND	0.071	0.045	0.071	0.010
Fluoride (F^-)	mg/L	0.96	0.85	1.1	0.78	0.10
Bromide (Br^-)	mg/L	ND	ND	ND	ND	50
Orthophosphate (PO_4^{3-})	mg/L	ND	ND	4.5	ND	0.010
Cations						
Sodium (Na^+)	mg/L	4700	4400	4300	4400	50
Calcium (Ca^{2+})	mg/L	1200	1100	2900	1100	0.5
Magnesium (Mg^{2+})	mg/L	390	360	380	350	0.5
Potassium (K^+)	mg/L	ND	28	30	27	10
Iron (Fe^{2+})	mg/L	ND	ND	0.3	ND	0.2
Manganese (Mn^{2+})	mg/L	ND	1.2	2.7	0.5	0.1

*ND: not detected

*RDL: reportable detection limit

3.2.0 The effect of pH on hydrocarbon contaminant remediation

3.2.1 Experiments with activated and unactivated persulfate for site #1

The initial pH at the start of all experiments with activated and unactivated persulfate was near neutral (7.7). The results obtained from the PSC 1 & 2 experiments showed a slight decrease (of about ~ 0.6) in pH to 7.1. In the CFEL 1 & 2 experiments, the pH dramatically dropped to around 2.7 because of the addition of sodium citrate ($Na_3C_6H_5O_7$). However, after one hour, the pH in the CFEL 1 & 2 experiments gradually increased to about 5.4 and 6.0, and then buffered at 6.7 and 6.6 at the end of day 14, respectively. Similarly, the pH in the CFEH

1 & 2 experiments dropped to 2.2 and 2.6, respectively, after the addition of sodium citrate. One hour later, the pH increased to ~5.6. The pH was buffered at ~6.4 by day 14 in the CFEH 1 & 2 experiments. Figure 12 demonstrates the pH pattern until the end of each experiment.

The reason for the initial decrease in pH when using activated persulfate was the addition of the chelating agent (citric acid), which maintained the availability of iron and allowed it to activate the persulfate. The persulfate had the ability to generate H^+ according to (Eq.3&4), therefore, the solution became more acidic. However, as discussed above, because of the generation of Caro's reagent that can produce H_2O_2, the solution starts increasing its pH until buffered at around 6 due to the reaction with iron to produce OH^-.

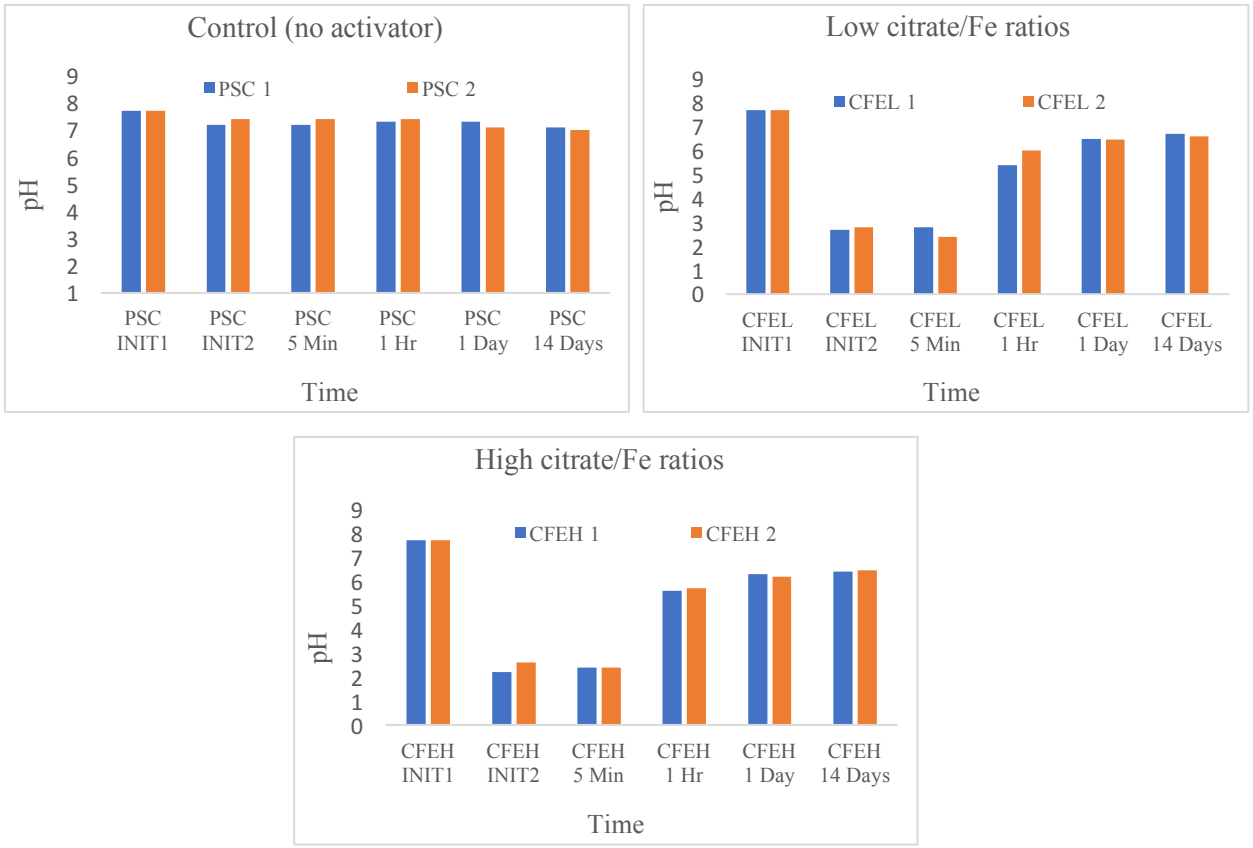

Figure 12: The initial and final pH in the unactivated persulfate (control without activator) and activated persulfate (CFEL = low citrate/Fe ratios; CFEH = high citrate/Fe ratios) experiments for site #1.

3.2.2 Experiments with H_2O_2 stabilized by citrate, phytate, and silica for site #1

Each set of duplicates for the experiments involving hydrogen peroxide stabilized by citrate, phytate, and silica yielded the same pH, therefore, the results stated below represent each experiment: control, low concentrations of the stabilizer (silica, citrate, and phytate), and high concentrations of the stabilizer (silica, citrate, and phytate).

The initial pH for the control experiment was 8 and then with addition of H_2O_2, the pH decreased to around 7.2. By day 2, the pH started to slowly decrease until buffered at 6.8 at the end of day 14. In the low silica concentration experiment, the pH started at 8 and was followed by a decrease to 7.3 after the addition of H_2O_2. The pH was constant over days 2-4, and then decreased afterwards, with a final pH value of 6.8 at the end of day 14. In the low citrate concentration experiment, initially, the pH decreased to 6 because of the addition of citric acid and did not change after the addition of H_2O_2. The pH in day 2 of the citrate experiment increased to 7.5 and was buffered at this value until day 14. In the phytate experiment, the pH dramatically dropped to 5 because of the addition of phytic acid, and did not change after H_2O_2 addition. By day 2, the pH had increased slightly to around 6 and remained at this value until the end of the experiment. Figure 13a shows the pH over time in the control experiment and the low silica, citrate, and phytate concentration experiments.

For the high silica concentration experiments, the initial pH was around 7.8 and then with the addition of H_2O_2, the pH decreased to 7.2 until day 2. At the beginning of day 4, the pH started to decrease, finishing with a slightly lower value of 6.8 at the end of the experiment (day 14). In the high citrate concentration experiment, the pH dropped to 5.0 because of the addition of citric acid and was buffered in this range after the H_2O_2 addition. By day 2, the pH increased to 7.2 and had a final value of 7.4 on day 14. In the high phytate concentration experiment, the pH remained at around 7 until the end of the experiment, with no change caused by the addition of phytic acid. Figure 13b shows the values of pH over time for the control experiment and the high silica, citrate, and phytate concentration experiments.

Overall, the initial pH was near-neutral (7.0 – 8.0), but it was observed that the pH decreased to around 5.0 – 6.0 in most cases due to the addition of acids, for example, the citrate experiment, and then increased to near-neutral values. By the end of all experiments, the pH was buffered between 6.0 and 7.4.

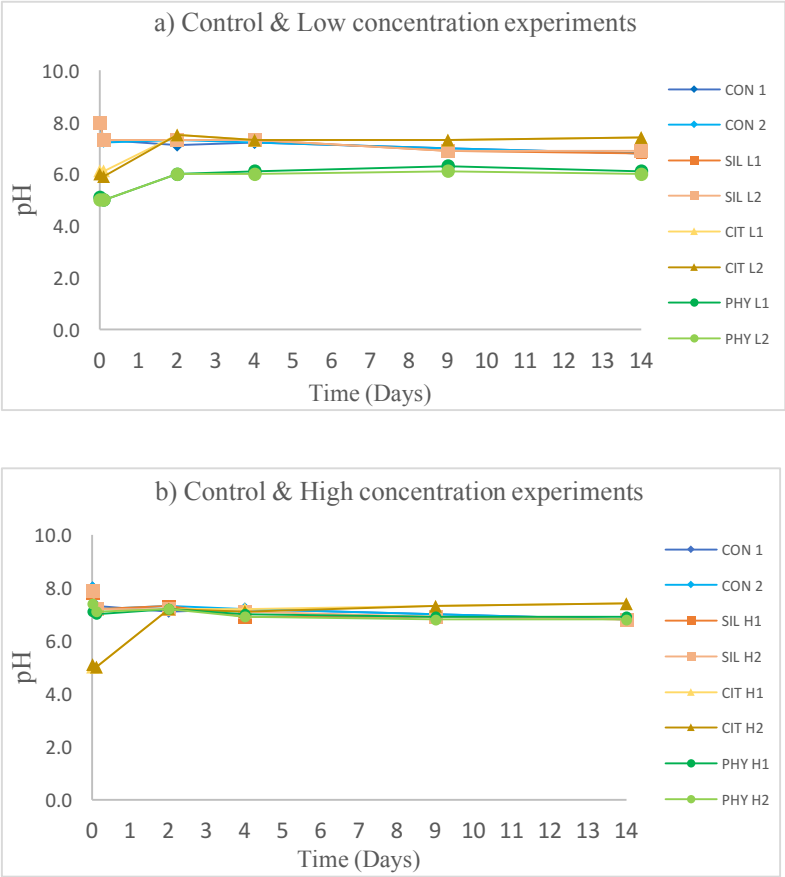

Figure 13: Variation in pH over time for the control and H_2O_2 stabilized by citrate, phytate, and silica experiments for site #1. a) control and the low silica, citrate and phytate concentration experiments, and b) control and the high silica, citrate and phytate concentration experiments. CON = control samples (no stabilizers), CIT = citrate experiments, SIL = silica experiments, PHY = phytate experiments.

3.2.3.0 Experiments with H_2O_2 stabilized by citrate and silica for site #1 and site #2

Like the experiments of H_2O_2 stabilized by citrate, phytate, and silica, each set of duplicates have almost the same pH from the beginning of the experiment until the end, therefore, the same procedure will be followed in terms of pH interpretation until the end of the experiment on day seven.

3.2.3.1 Site #1

The pH at the beginning of the control experiment was near neutral, and with addition of H_2O_2, the pH slightly decreased to 6.8. After four hours, the pH started to increase to around 7.0 and was buffered at this range until the end of day seven. Like the control experiment, the pH from the silica experiment decreased slightly, starting with the addition of H_2O_2, and then after 4 hours, the pH started to buffer around ~7.0 until day seven. In contrast, the pH from the citrate stabilized H_2O_2 experiment dropped to around 4.6 after the addition of citric acid and then, the pH started to increase at the four-hours sample to around 5.0 and reached 6.0 by the end of the first day. Thereafter, the pH became stable around 7.3 by the end of the experiment. Generally, all experiments that involved citrate experienced a decrease of pH after the addition of citrate. Figure 14 summarizes the variation in pH during the control, citrate, and silica experiments.

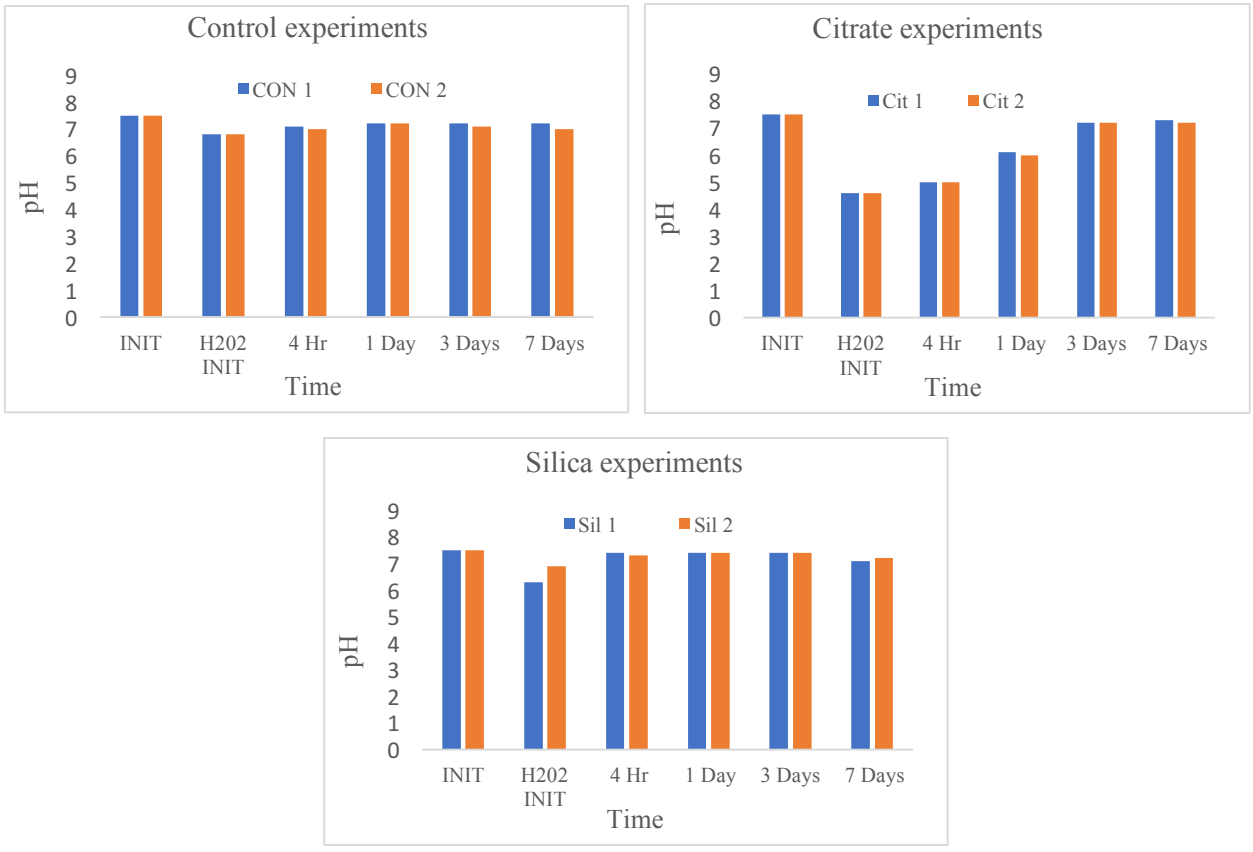

Figure 14: The initial and final pH in the control, citrate stabilized H_2O_2, and silica stabilized H_2O_2 experiments for site #1.

3.2.3.2 Site #2

The pH results from site #2 are similar to site #1 in all experiments. The pH in the control experiment started at 7.9 and then decreased to 6.4 following the addition of H_2O_2. Subsequently, the pH increased within four hours to 6.6, and at the end of the seventh day, the pH was buffered around 6.9. In the silica experiment, the pH began at 7.9 and decreased to 7.0 after the addition of H_2O_2. After that, the pH started to increase after four hours until becoming stable around 7.0 by day one until the end of the experiment. Unlike the control and silica experiments, the pH in the citrate experiment dropped to 4.5 following the addition of H_2O_2, and then started to increase after four hours to 5 and continued to increase until buffered around 7.4 by the end of the experiment. These pH trends are very similar to those observed in the experiment that was done on site #1 materials. Figure 15 shows the pH changes during the control, citrate, and silica experiments.

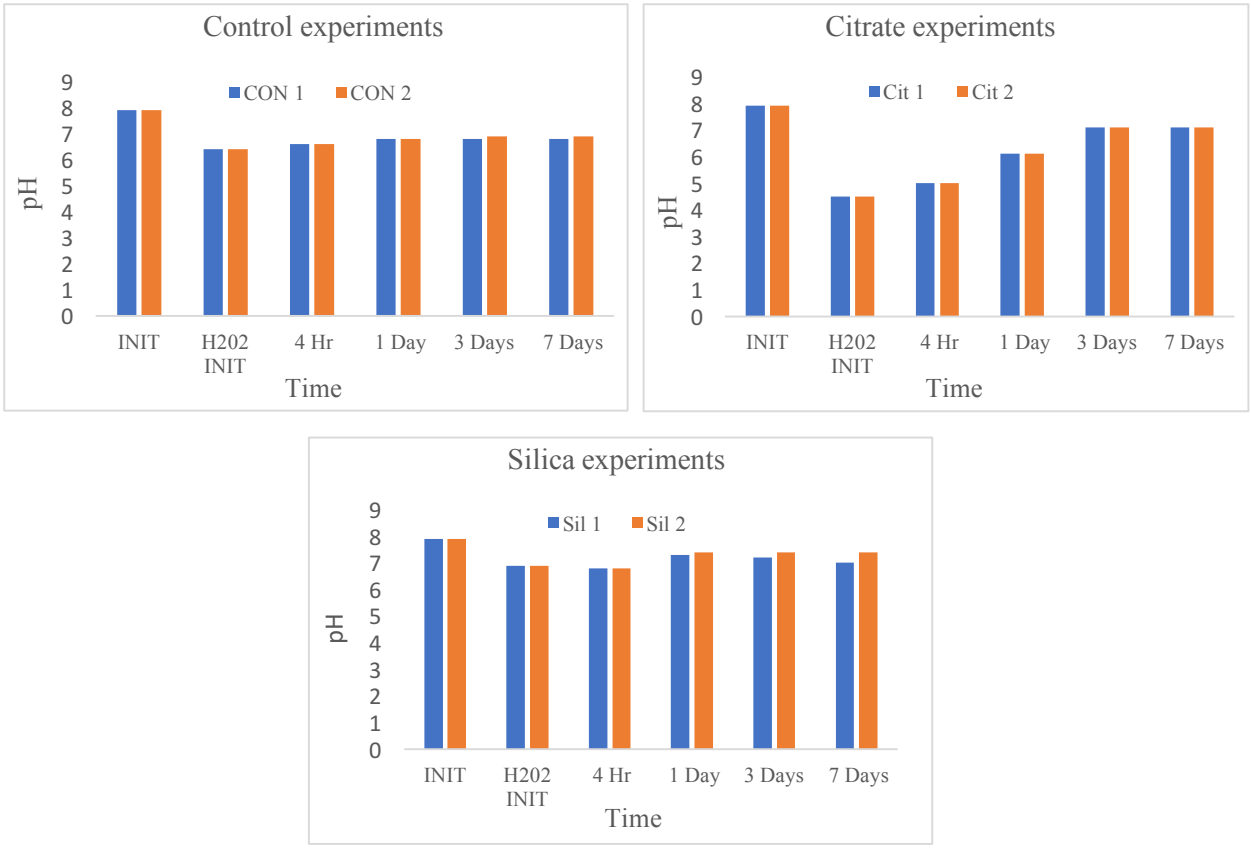

Figure 15: The initial and final pH in the control, citrate stabilized H_2O_2, and silica stabilized H_2O_2 experiments for site #2.

3.3.0 The carbon and hydrogen isotope analyses

3.3.1.0 Experiments with activated and unactivated persulfate for site #1

Only MTBE and benzene were measured for both C and H isotopes because the other compounds were almost fully oxidized by day 1. However, it is also worth mentioning the C isotope results for toluene because this compound had significantly enriched values (see Appendix F).

For the non-activated persulfate experiments (PSC 1&2), the $\delta^{13}C$ values of MTBE were enriched by 1.2‰ and ~3.0‰ by day 14, respectively. The $\delta^{13}C$ values for benzene had minimal change (0.2‰) for PSC 1 considering the analytical uncertainty of ±0.5‰ and was slightly enriched by 0.8‰ for PSC 2 by day 14 (Figure 16a, b). Toluene was slightly depleted by 0.4‰ for PSC 1 and was slightly enriched by 0.7‰ for PSC 2 (Figure 16c). Overall, the isotopic enrichments for the PSC experiments were small for MTBE and negligible for benzene and toluene.

The activated persulfate (CFEL & CFEH) experiments exhibited more C isotope enrichments than the unactivated persulfate experiments. In the CFEL 1&2 experiments, MTBE values were enriched by 2.1‰ for CFEL 1 and enriched by 2.3‰ for CFEL 2 (Figure 16a). For benzene, the isotopic changes were 0.4‰ for CFEL 1 and 0.7‰ for CFEL 2 (Figure 16b). These isotopic shifts are small or even negligible given the analytical uncertainty of ±0.5‰. However, the isotopic composition of toluene from both CFEL experiments showed a significant enrichment of 4.6‰ (Figure 16c). In the CFEH experiments, the carbon isotopic values of MTBE were enriched by 2.1‰ and 3.7‰ for CFEH 1 and CFEH 2, respectively. The carbon isotopic compositions of benzene became enriched by about 0.9‰ and 1.2‰ for CFEH 1 and CFEH 2, respectively. Once again and like the observations from the CFEL experiments, the toluene exhibited the most enrichment in carbon isotopic values, with a change of 7.8‰ for CFEH 1 and 9.2‰ for CFEH 2. In general, the CFEH 1&2 experiments showed more enriched values compared to the CFEL experiments for MTBE, benzene, and toluene. Furthermore, the CFEH experiments confirmed the large carbon isotopic enrichments observed in the CFEL experiments for toluene. Overall, the degree of C isotope enrichment in the CFEH 1&2 experiments reflected the use of a high citrate/Fe ratio which clearly achieved the higher enrichments (Figure 16a, b, c).

In the unactivated persulfate (PSC 1&2) experiments, the H isotope compositions of MTBE were enriched by 10.0‰ for PSC 1, and by 16.0‰ for PSC 2. In the case of benzene, the H isotopic values were enriched by 5.0‰ and 2.0‰ for PSC 1 and PSC 2, respectively. The isotopic changes are small compared to the analytical uncertainty for H isotopes, which is ± 5‰. The CFEL 1 experiments for MTBE showed some enrichment of H isotopes (19.0‰), however, the CFEL 2 experiments showed a negligible change (1.0‰). For benzene, the H isotope compositions became more enriched compared to the PSC experiments, with changes of 21.0‰ for CFEL 1 and 18.0‰ for CFEL 2. In the CFEH experiments for MTBE, a slight enrichment of 5.0‰ occurred for CFEH 1, and a significantly higher enrichment of 34.0‰ occurred for CFEH 2. The reason for the non-reproducibility of the CFEL and CFEH experiments for MTBE is not clear. Benzene showed enrichment of 18.0‰ and 9.0‰ for CFEH 1 and CFEH 2, respectively. Figure 17 shows changes in H isotope compositions of MTBE and benzene during the PSC, CFEL, and CFEH experiments.

The reason of having high isotope enrichment for some compounds than the others was because of less energy required to break the bond of lighter isotopes (e.g., ^{12}C) that caused the isotope fractionation. Overall, the CFEL and CFEH experiments yielded the most pronounced results in terms of the extent of enrichment in C and H isotopes. This finding will likely support the methodology of using iron as an activator along with citrate as a stabilizer.

To evaluate the changes in isotopic compositions during the experiments from a 2D-CSIA perspective, values of lambda (Λ) were calculated as the ratio of hydrogen to carbon isotopes ($\Lambda = \Delta \delta^{2}H / \Delta \delta^{13}C$). The resulting Λ values in the PSC 1 & 2 experiments for MTBE were 8.4 ± 5.5‰ and 5.7 ± 2.0‰, respectively, showing enriched values for both carbon and hydrogen isotopes with greater enrichment in hydrogen isotope compositions. Unlike MTBE, the Λ value of benzene for PSC 1 was 18.0 ± 32.3‰, in which changes in the carbon isotope composition were not appreciably different given analytical uncertainties (± 0.5‰). However, the benzene isotopic results from PSC 2, for which the C isotope enrichment was larger, yielded a Λ value of 2.2 ± 5.7‰ (Figure 18a, b). The MTBE Λ values produced from the CFEL 1 & 2 experiments were 8.8 ± 3.1‰ and 0.4 ± 2.1‰, respectively. The isotopic shifts during this experiment are small and they are only observed for the hydrogen isotopes (Figure 18c). The variation in the obtained Λ values from the duplicate experiments are due to the small isotopic shifts that are highly affected by the analytical

uncertainty and because of the non-reproducibility in isotope enrichments from some duplicate experiments. Benzene on the other hand, showed a large hydrogen isotope fractionation and a small carbon isotope fractionation in the CFEL 1 and 2 experiments, which had Λ values of 31.8 ± 32.1‰ and 7.1 ± 5.4‰, respectively (Figure 18d). For the CFEH 1 & 2 experiments, MTBE showed moderately positive results with carbon and hydrogen isotope fractionation exceeding the analytical uncertainties, resulting in Λ values of 2.4 ± 2.4‰ and 9.2 ± 1.8‰ for CFEH 1 & 2, respectively (Figure 18e). Once again, the reproducibility of the obtained Λ values was not great in the duplicate experiments because of the small isotopic shifts that are highly affected by the analytical uncertainty. Like MTBE, benzene showed a similar trend with enrichment values above the analytical uncertainty for both carbon and hydrogen isotopes, with Λ values of 19.5 ± 12.0‰ and 8.3 ± 5.8‰ for CFEH 1 & 2, respectively (Figure 18f). The variation in Λ values was mainly due to the large contribution of the analytical uncertainties.

In general, some experiments showed positive correlations between the carbon and hydrogen isotopic changes. Typically, 2D-CSIA has proved to be a useful tool in terms of determining contaminant sources and assessing the fate of contaminants (e.g., degradation processes of hydrocarbons). Systematic isotopic changes during chemical, physical and biological activities is a good indicator of the progress of a specific process and the intensity of the process. Therefore, pronounced isotopic shifts are necessary to utilize CSIA as an evaluation tool. Some of the results presented above showed isotopic shifts that are associated with hydrocarbon contaminant oxidation processes. However, not all experiments resulted in pronounced isotopic shifts. Some isotopic shifts were too small and were masked by the analytical uncertainty of the method (e.g., changes of isotopic values of benzene during the PSC and CFEL experiments).

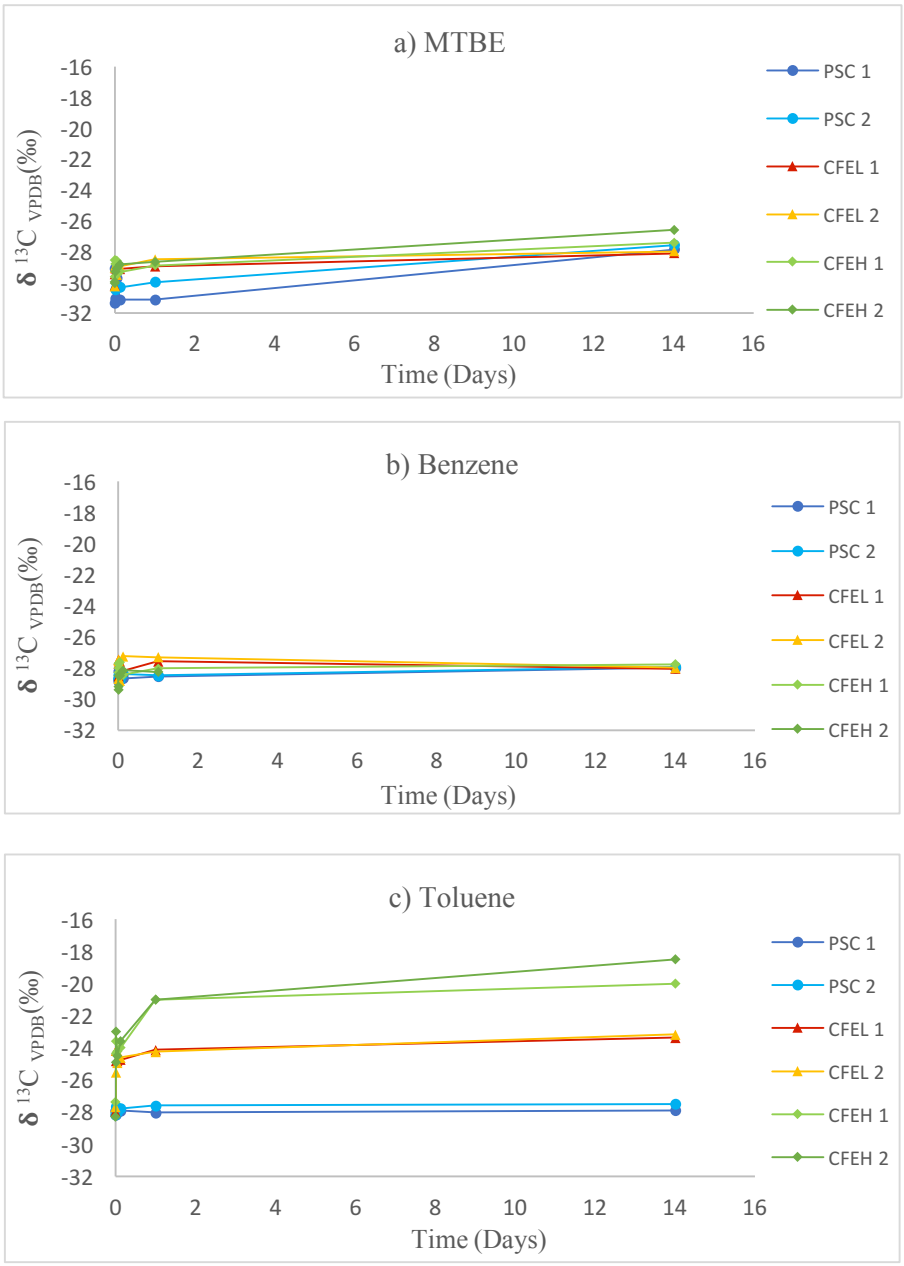

Figure 16: The variations of the $\delta^{13}C$ values with time for a) MTBE, b) benzene, and c) toluene during the activated and unactivated persulfate experiments for site #1. PSC = unactivated persulfate (Control), CFEL = persulfate activated by chelated iron with a lower citrate/Fe ratio, CFEH = persulfate activated by chelated iron with a higher citrate/Fe ratio.

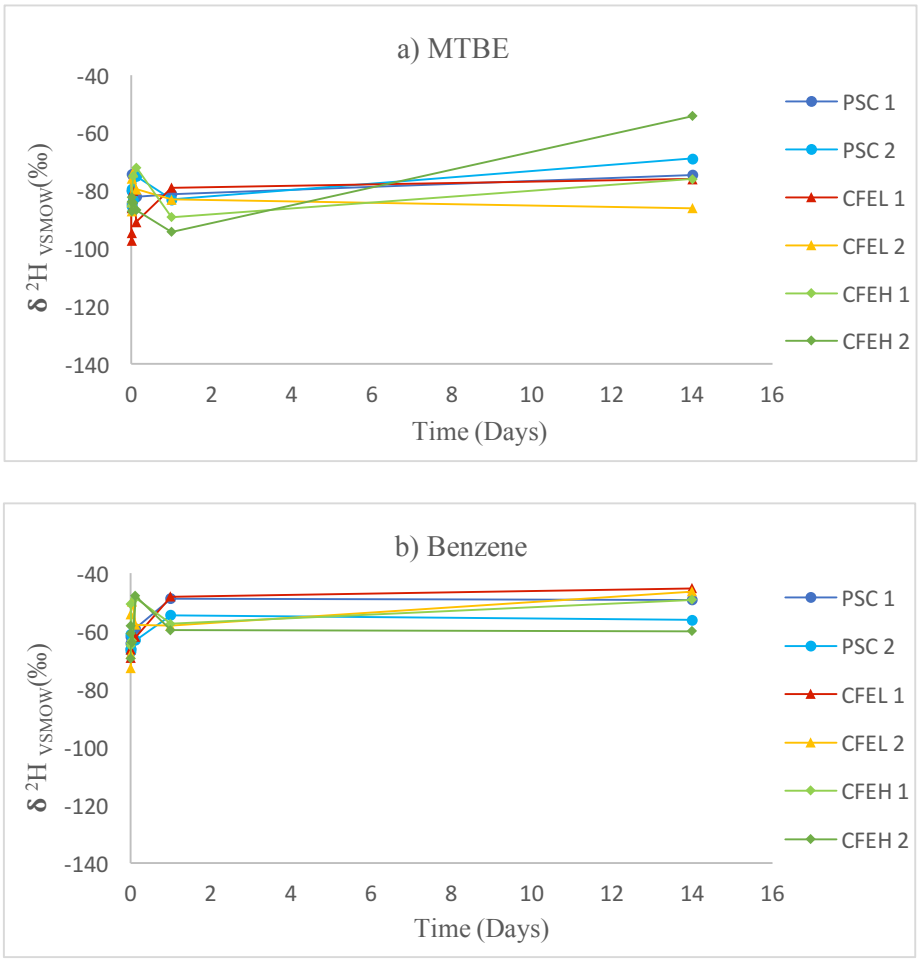

Figure 17: The variations of the δ^2H values with time for a) MTBE and b) benzene during the activated and unactivated persulfate experiments for site #1. PSC = unactivated persulfate (Control), CFEL = persulfate activated by chelated iron with a lower citrate/Fe ratio, CFEH = persulfate activated by chelated iron with a higher citrate/Fe ratio.

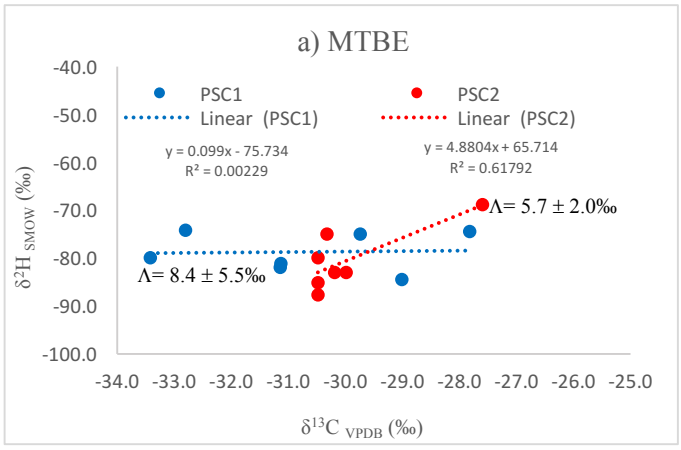

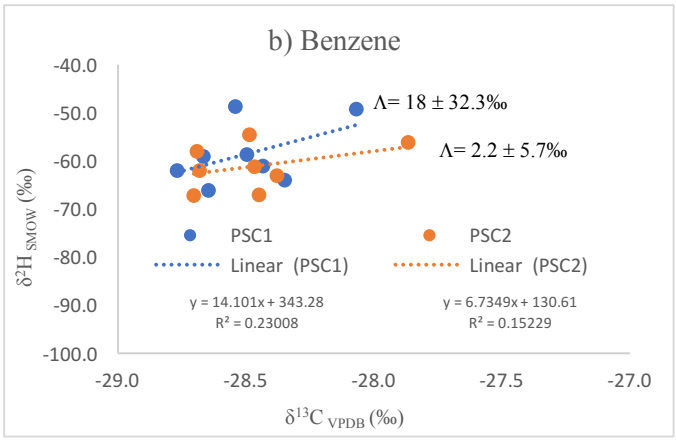
b) Benzene
Λ= 18 ± 32.3‰
Λ= 2.2 ± 5.7‰
PSC1
PSC2
Linear (PSC1)
Linear (PSC2)
y = 14.101x + 343.28
R² = 0.23008
y = 6.7349x + 130.61
R² = 0.15229
δ²H SMOW (‰)
δ¹³C VPDB (‰)

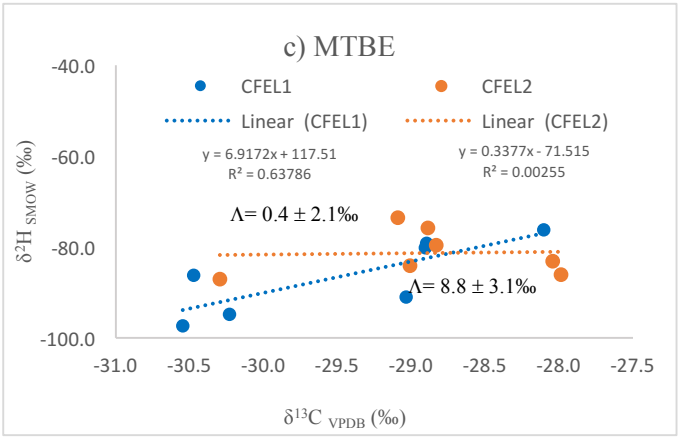
c) MTBE
CFEL1
CFEL2
Linear (CFEL1)
Linear (CFEL2)
y = 6.9172x + 117.51
R² = 0.63786
y = 0.3377x - 71.515
R² = 0.00255
Λ= 0.4 ± 2.1‰
Λ= 8.8 ± 3.1‰
δ²H SMOW (‰)
δ¹³C VPDB (‰)

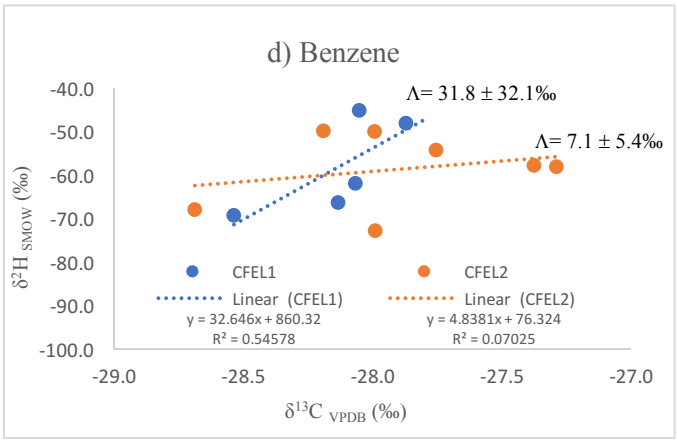
d) Benzene
Λ= 31.8 ± 32.1‰
Λ= 7.1 ± 5.4‰
CFEL1
CFEL2
Linear (CFEL1)
Linear (CFEL2)
y = 32.646x + 860.32
R² = 0.54578
y = 4.8381x + 76.324
R² = 0.07025
δ²H SMOW (‰)
δ¹³C VPDB (‰)

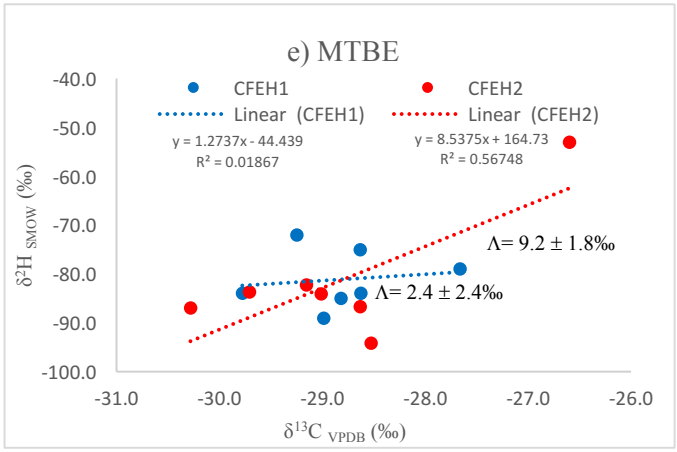

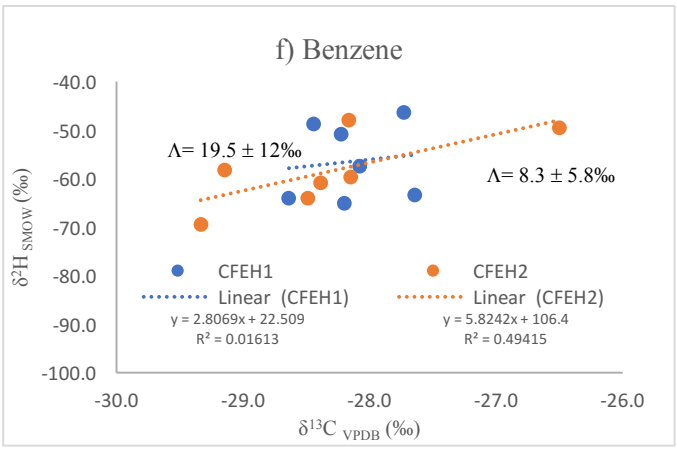

Figure 18: Dual δ^2H and $\delta^{13}C$ isotopes of a) MTBE and b) benzene in the PSC1&2 experiments, c) MTBE and d) benzene in the CFEL 1&2 experiments, e) MTBE and f) benzene in the CFEH 1&2 experiments involving unactivated and activated persulfate for site #1.

3.3.1.1 The enrichment factor

Changes in carbon and hydrogen isotope ratios with respect to changes in the concentrations of MTBE and benzene were calculated using the logarithmic form of the Rayleigh equation (Eq.12 &13) for the activated and unactivated persulfate experiments. However, only benzene yielded the largest number of results for C and H isotopes that were suitable to interpret the changes in concentration versus the changes in the isotopic composition. Only carbon isotopes were analyzed for toluene as hydrogen isotope analysis

was not possible to perform due to the low toluene concentration in most samples caused by rapid oxidation of this compound.

The enrichment factor calculated by the Rayleigh equation showed that the changes in concentration ($\ln (C_t / C_0)$), and in the isotopic composition ($\ln [(\delta_t + 1000) / (\delta_0 + 1000)]$), resulted in some positive correlation factors (R^2) in the activated and unactivated persulfate experiments, with a correlation factor between 0.3 and 0.8. The carbon enrichment factor (ε_C) of benzene in the PSC 1&2, CFEL 1&2, and CFEH 1&2 experiments were almost identical, with an ε_C of -0.5‰ & -0.7‰, -0.4‰ & -0.8‰, and -0.7‰ & -1.9‰, respectively (Figure 19a, b, c). Nearly the same average hydrogen enrichment factor (ε_H) was also observed for the PSC 1&2, CFEL 1&2, and CFEH 1&2 experiments, which yielded ε_H of -18.9‰ & -8.7‰, -28.0‰ & -18.9‰, and -12.3‰ & -17.5‰, respectively (Figure 19d, e, f). In the case of toluene, a small carbon enrichment factor was observed for the PSC experiments (ε_C = -0.04 ± 0.05‰), and high carbon enrichment factors of -1.4 ± 0.1‰ and -1.7 ± 0.1‰ were observed for the CFEL and CFEH experiments, respectively. Although toluene had a small carbon isotope enrichment factor in the PSC experiments, this enrichment factor reflected a rapid decrease in the concentration of toluene (Figure 20a). It was clear that the activated persulfate experiments (CFEL & CFEH) achieved better enrichment factors, as well as high degradation of toluene (Figure 20b, c).

Carbon and hydrogen enrichment factors of benzene and toluene have been extensively reported in the literature, for example, the ε_C and ε_H of benzene for alkaline-activated persulfate experiments were -2.0‰ and -10.6‰, respectively (Saeed, 2011), whereas ε_C and ε_H in the unactivated persulfate experiments ranged from -1.7 ± 0.1‰ to -2.0‰, and from ~0‰ to -10.9‰, respectively (Saeed, 2011; Solano et al., 2017). The reported ε_C and ε_H of benzene under aerobic conditions ranged from -1.4 ± 0.1‰ to -3.5 ± 0.3‰, and from -11.2 ± 1.8‰ to -12.8 ± 0.7‰, respectively (Hunkeler et al., 2001). Furthermore, different results were observed during sulfate-reducing conditions in which ε_C and ε_H range from -2.9 ± 0.5‰ to -3.0 ± 1.0‰, and from -69 ± 23‰ to -78 ± 12‰, respectively (Fischer et al., 2009). The reported carbon and hydrogen enrichment factors for toluene varied. For example, Herrmann et al. (2009) conducted a study using a pure sulfate-reducing culture (Desulfosarcina) and

found that the ε_C and ε_H values were -2.5 ± 0.5‰ and -107 ± 23‰, respectively. Another study using methanogenic and sulfate-reducing mixed cultures resulted in different ε_C values of -0.5 ‰ and -0.8 ‰, respectively (Ahad et al., 2000). Moreover, the carbon and hydrogen enrichment factors of toluene resulting from the chemical oxidation of unactivated persulfate ranged from -0.64 ± 0.10‰ to -1.6‰, and from -6.6‰ to -20 ± 3‰, respectively (Saeed, 2011; Solano et al., 2017). The data compiled in Table 8 shows different ε_C and ε_H values under different conditions from the literature as compared to those estimated in this study for the chemical oxidation of benzene and toluene using activated and unactivated persulfate.

Table 8: Carbon and hydrogen enrichment factors for chemical oxidation and biodegradation of benzene and toluene compiled from the literature.

Compound	System	ε_C	ε_H	Reference
Benzene	Unactivated persulfate	-0.6 ± 0.1‰	-13.8 ± 5.0‰	This study
	Iron-activated persulfate (high citrate/Fe ratio)	-0.6 ± 0.2‰	-23 ± 5‰	
	Iron-activated persulfate (low citrate/Fe ratio)	-1.3 ± 0.7‰	-14 ± 3‰	
Benzene	Pure culture (Acinetobacter sp)	-1.4 ± 0.06‰	-12.8 ± 0.7‰	Hunkeler et al. (2001)
	Pure culture (Burkholderia sp)	-3.5 ± 0.26‰	-11.2 ± 1.8‰	
Benzene	Enrichment culture Sulfate reducing	-2.9 ± 0.5‰	-78 ± 12‰	Fischer et al. (2009)
	Sulfate-reducing	-2.9 ± 1.1‰	-69 ± 23‰	
	Sulfate-reducing	-3.0 ± 1.0‰	-77 ± 26‰	
Benzene	Alkaline activate persulfate	-2.0‰	-10.6‰	Saeed (2011)
	Unactivated persulfate	-2.0‰	-10.9‰	
Benzene	Unactivated persulfate	-1.7 ± 0.1‰	No enrichment (±5‰)	Solano et al. (2017)
Toluene	Unactivated persulfate	-0.04 ± 0.05‰	NA*	This study
	Iron-activated persulfate (high citrate/Fe ratio)	-1.4 ± 0.1‰	NA*	
	Iron-activated persulfate (low citrate/Fe ratio)	-1.7 ± 0.1‰	NA*	
Toluene	Mixed culture (Methanogenic and sulfate-reducing)	-0.5‰ and -0.8‰, respectively	NA*	Ahad et al. (2000)
Toluene	Pure culture (Desulfosarcina) sulfate-reducing	-2.5 ± 0.5‰	-107 ± 23‰	Herrmann et al. (2009)
Toluene	Alkaline activate persulfate	-1.2‰	-6.4‰	Saeed (2011)
	Unactivated persulfate	-1.6‰	-6.6‰	
Toluene	Unactivated persulfate	-0.64 ± 0.1‰	-20 ± 3‰	Solano et al. (2017)

*NA = Not available.

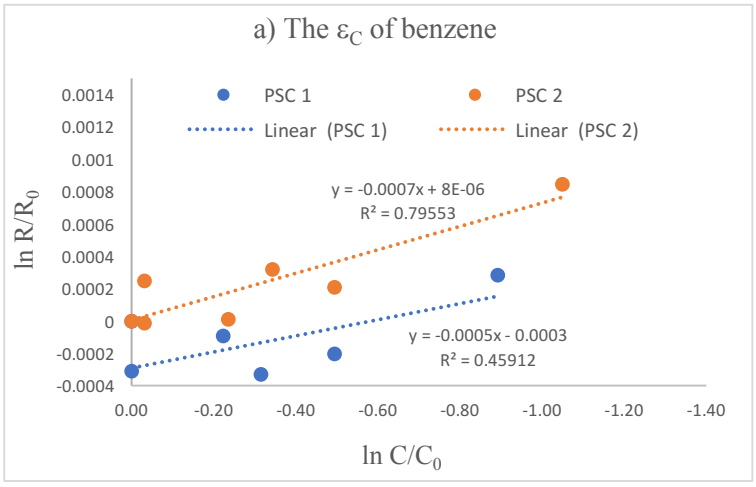
a) The ε_C of benzene
PSC 1
PSC 2
Linear (PSC 1)
Linear (PSC 2)
y = -0.0007x + 8E-06
R² = 0.79553
y = -0.0005x - 0.0003
R² = 0.45912
ln R/R0
ln C/C0
0.0014
0.0012
0.001
0.0008
0.0006
0.0004
0.0002
0
-0.0002
-0.0004
0.00
-0.20
-0.40
-0.60
-0.80
-1.00
-1.20
-1.40

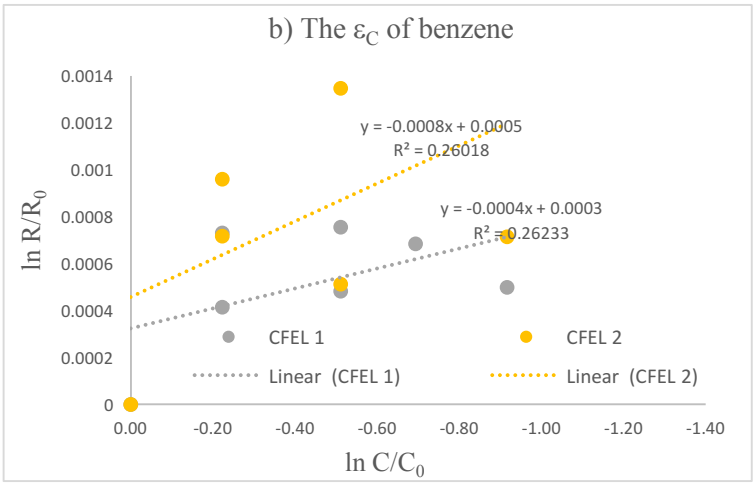
b) The ε_C of benzene
y = -0.0008x + 0.0005
R² = 0.26018
y = -0.0004x + 0.0003
R² = 0.26233
CFEL 1
CFEL 2
Linear (CFEL 1)
Linear (CFEL 2)
ln R/R0
ln C/C0
0.0014
0.0012
0.001
0.0008
0.0006
0.0004
0.0002
0
0.00
-0.20
-0.40
-0.60
-0.80
-1.00
-1.20
-1.40

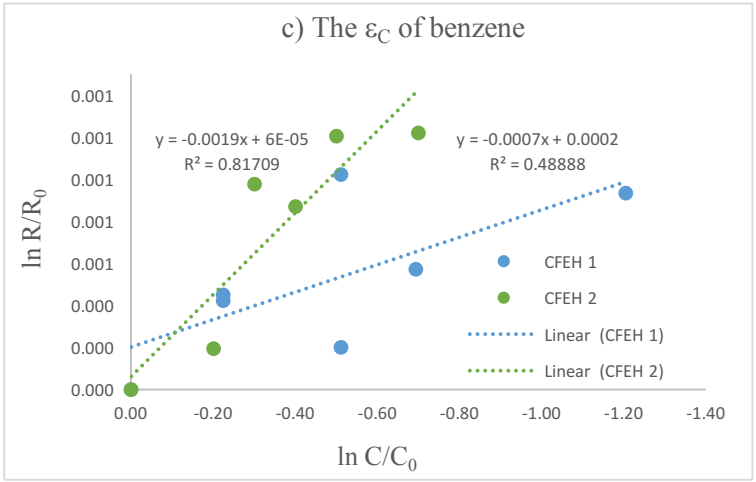
c) The ε_C of benzene
y = -0.0019x + 6E-05
R² = 0.81709
y = -0.0007x + 0.0002
R² = 0.48888
CFEH 1
CFEH 2
Linear (CFEH 1)
Linear (CFEH 2)
ln R/R0
ln C/C0
0.001
0.001
0.001
0.001
0.001
0.000
0.000
0.000
0.00
-0.20
-0.40
-0.60
-0.80
-1.00
-1.20
-1.40

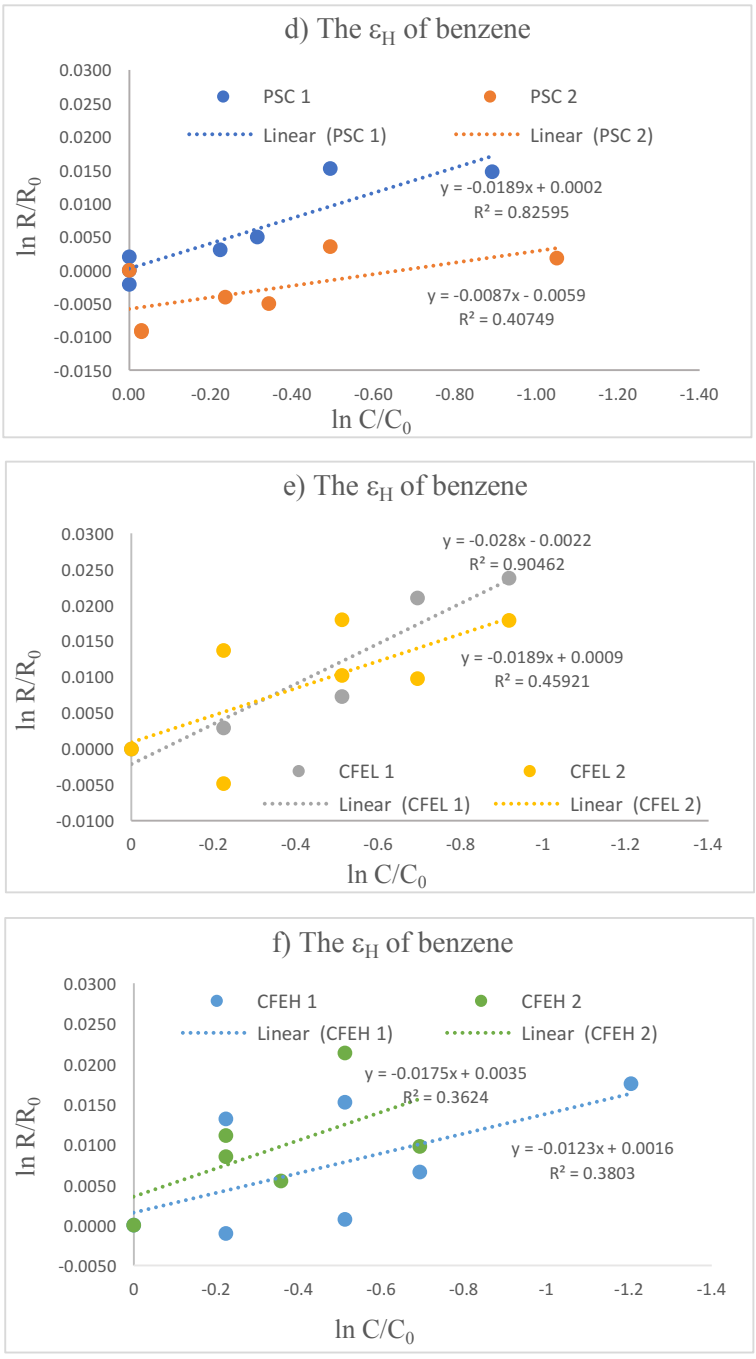

Figure 19: Double logarithmic plot according to the Rayleigh equation showing the changes in concentrations ($\ln(C/C_0)$) versus the changes in isotope ratios ($\ln[(\delta_t+1000) / (\delta_0+1000)]$) of benzene for persulfate experiments (site #1). The slope represents the calculated enrichment factor. Panels a, b, and c (carbon isotopes) and d, e, and f (hydrogen isotopes) show isotopic and concentration changes for the PSC 1&2, CFEL 1&2, and CFEH 1&2 experiments, respectively.

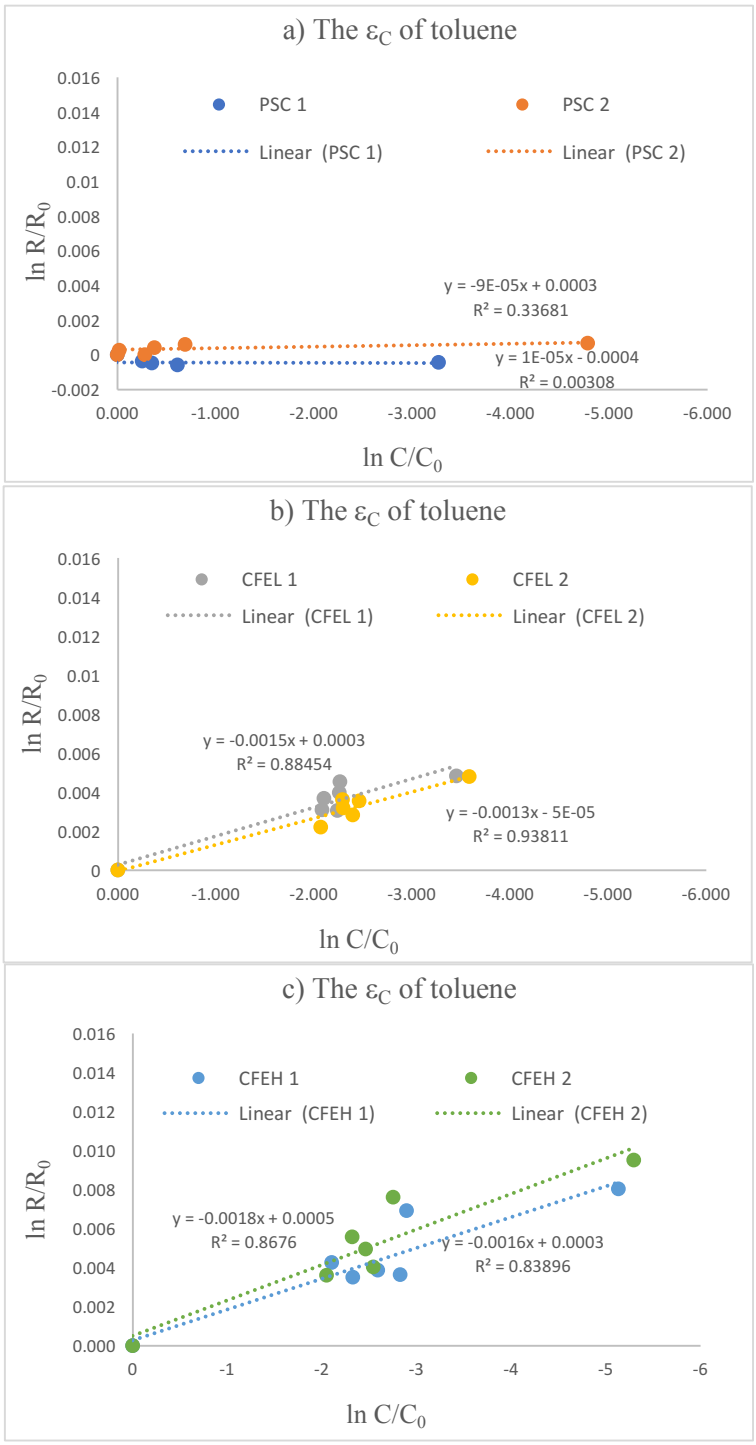

Figure 20: Double logarithmic plot according to the Rayleigh equation showing the changes in concentrations (ln(C/C$_0$)) versus the changes in isotope ratios (ln[(δ_t+1000) / (δ_0+1000)]) of toluene for the persulfate experiments (site #1). The slope represents the calculated enrichment factor. A, B, and C show carbon isotope and concentration changes for the PSC 1&2, CFEL 1&2, and CFEH 1&2 experiments, respectively.

3.3.2.0 Experiments with H_2O_2 stabilized by citrate and silica for site #1 and site #2

Some hydrocarbons (e.g., benzene, toluene, and o-xylene) in the citrate stabilized H_2O_2 experiments reached undetectable concentrations by the end of day 3, therefore, no isotopic results were determined after day 3. Hence, comparison between the three experiments (control (CON), citrate (CIT), and silica (SIL)) are only made for the first 3 days (see Appendix G for full description of the $\delta^{13}C$ values for MTBE, benzene, and toluene). Unfortunately, the H isotope data were not of adequate quality, and that is mainly due to the following reasons: 1) the initial contaminant concentration of the samples was low; 2) the reaction rate was very fast and the sampling interval was too long; and 3) the volume of each experiment was not enough to run the analysis of both isotopes (C and H) at these low concentrations. Therefore, data obtained from hydrogen isotope analysis from site #1 and site #2 were not consistent for all experiments. For example, in the CON 1 and CON 2 experiments at site #1, H isotope data for MTBE, benzene, and toluene are only available to the end of the fourth hour in the first day for CON 1, whereas H isotope data was obtained for CON 2 to the end of three days (Table 9), thus, no comparison can be made. Furthermore, the H isotope data collected for site #2 were different than data for site #1. For example, in the CON 1 experiment at site #2, H isotope data were obtained for MTBE, benzene, and toluene until the third day of the experiment, while in the CON 2 experiment, the initial H isotope composition was not available due to the low H concentration, thus, there is not enough data available to discuss the hydrogen isotopic results for this site (Table 10). The missing data were labeled as (BDL), which means below the detection limit.

The carbon isotope results, including a comparison between the three experiments, is presented below for MTBE, benzene, and toluene. Other hydrocarbon compounds acted in a similar fashion. Naphthalene at Site #2 was mentioned due to the unexpected behavior of the isotopic changes for this compound from the silica experiment.

Table 9: H isotope compositions (‰) of MTBE, benzene, and toluene for the control 1 and control 2 experiments at site #1

	MTBE	Benzene	Toluene
Control 1			
Initial	-84.0	-64.2	-56.4
H_2O_2 Initial	-73.5	-65.2	-40.8
4 Hours	-61.4	-48.2	-24.8
Day 1	BDL	BDL	BDL
Day 3	BDL	BDL	BDL
DAY 7	BDL	BDL	BDL
Control 2			
Initial	-87.0	-64.2	-109.1
H_2O_2 Initial	-55.9	-41.9	-87.6
4 Hours	-17.2	-7.5	-37.1
Day 1	-3.7	-4.9	-12.6
Day 3	8.2	-4.0	-11.1
DAY 7	BDL	BDL	BDL

*BDL: below detection limit

Table 10: H isotope compositions (‰) of MTBE, benzene, and toluene for the control 1 and control 2 experiments at site #2

	MTBE	Benzene	Toluene
Control 1			
Initial	-53.2	-47.0	-97.4
H_2O_2 Initial	-55.9	-50.0	-97.1
4 Hours	-47.4	-49.5	-90.6
Day 1	-27.6	-49.2	-97.4
Day 3	-18.8	-51.5	-102.4
DAY 7	BDL	BDL	BDL
Control 2			
Initial	BDL	BDL	BDL
H_2O_2 Initial	-54.4	-50.2	-90.0
4 Hours	-43.4	-44.6	-87.7
Day 1	-29.7	-51.7	-63.6
Day 3	-20.2	-54.5	-52.9
DAY 7	BDL	BDL	BDL

*BDL: below detection limit

3.3.2.1 Site #1

The C isotopic values of residual hydrocarbons after oxidation during the CON 1 & 2 experiments showed a minimal or slight increase (≤1.0‰), and the isotopic changes were within the analytical uncertainty (± 0.5‰) after three days for both experiments. MTBE shifted by about 0.9‰ and 0.6‰ for CON 1 & 2, respectively. The C isotopic composition of benzene had enriched by about 0.9‰ for CON 1 and by 0.2‰ for CON 2. Toluene showed similar results as MTBE and benzene, with C isotope values shifting by around 1.0‰ and 0.2‰ for CON 1 and CON 2, respectively. Figure 21a illustrates the C isotopic changes for MTBE, benzene, and toluene in the control experiments.

Like the control experiment, the silica-stabilized H_2O_2 experiment showed no significant C isotope changes for MTBE, benzene, and toluene, which had enrichments of ≤1.3‰. MTBE became enriched by 1.3‰ and 1.0‰ for SIL 1 and SIL 2, respectively. C isotope values of benzene for SIL 1 and SIL 2 were enriched by 0.3‰ and 0.7‰, respectively. There was negligible change in the C isotopic composition of toluene in the SIL 1 (0‰) and SIL 2 (0.3‰) experiments. Figure 21b shows the changes in C isotopic composition for MTBE, benzene, and toluene in the silica experiment.

In contrast, the citrate-stabilized H_2O_2 experiment resulted in a greater enrichment in the C isotopic values for all three compounds. The C isotope composition of MTBE was enriched by 2.4‰ and 4.0‰ for CIT 1 and CIT 2, respectively. Benzene was enriched by 1.6‰ and 2.1‰ for CIT 1 and CIT 2, respectively. Toluene showed the most enrichment, with a shift of 2.5‰ for CIT 1 and 4.4‰ for CIT 2. Figure 21c illustrates the changes in C isotopic composition for MTBE, benzene, and toluene in the citrate experiments.

The results showed that only the experiment where citrate was used as a stabilizer for H_2O_2 yielded pronounced isotopic changes (large C isotope enrichment) when compared with other experiments (control and silica stabilized H_2O_2). The control and silica stabilized H_2O_2 experiments did not demonstrate any significant C isotopic shifts and most isotopic changes were within or near the analytical uncertainty of the method (± 0.5‰).

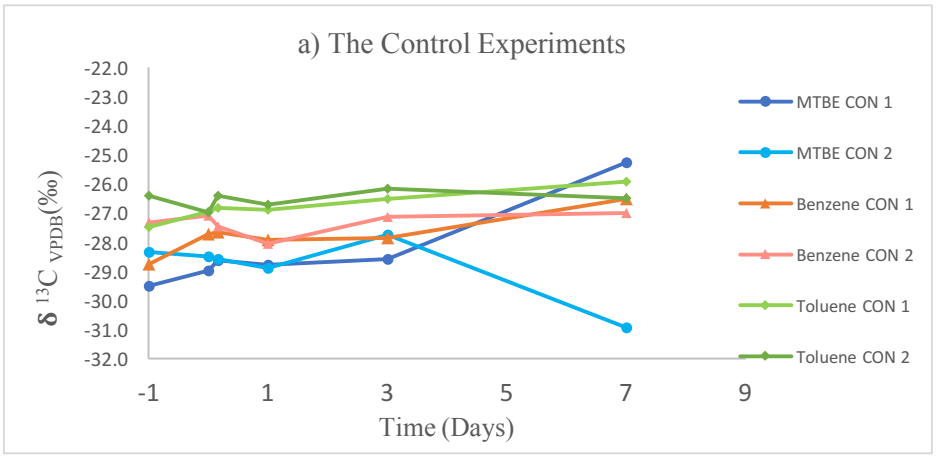

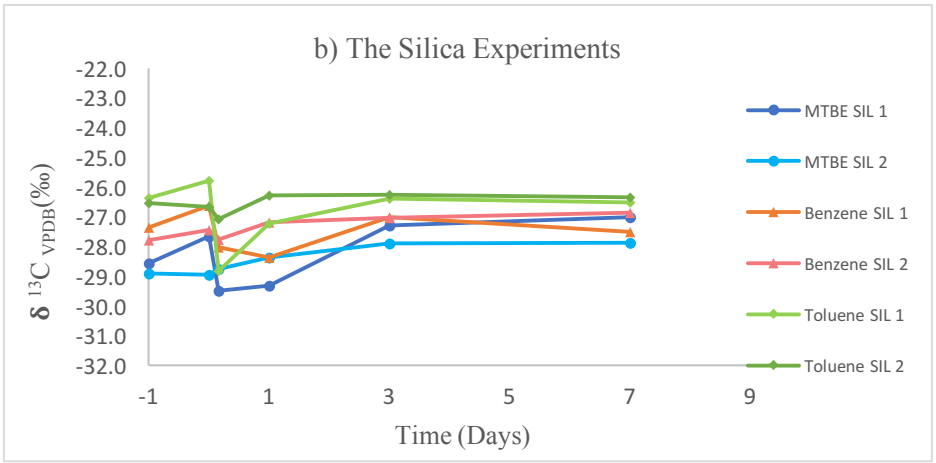

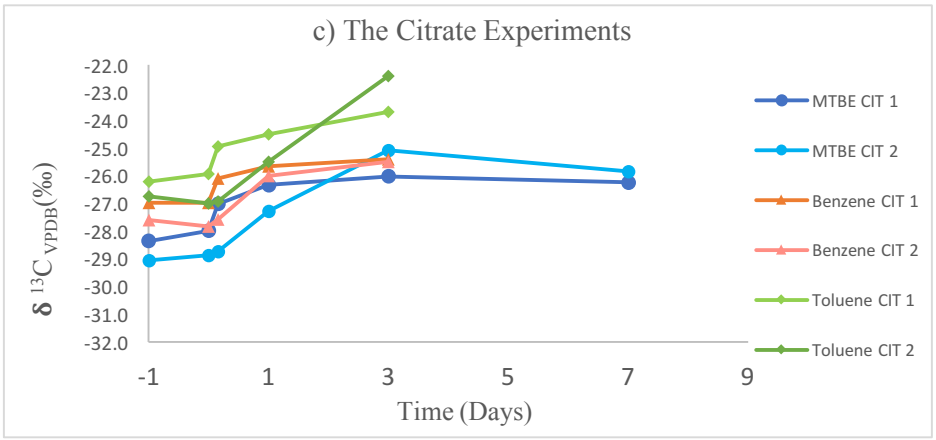

Figure 21: Changes in the $\delta^{13}C$ values with time for MTBE, benzene, and toluene during a) the controlled H_2O_2 (no stabilizer) experiment, b) the silica stabilized H_2O_2 experiment, and c) the citrate stabilized H_2O_2 experiment for site #1.

3.3.2.2 Site #2

In general, the C isotopic results from the Site #2 experiment were similar to the results obtained from the Site #1 experiment. The enrichment in C isotope values in the control experiments 1 and 2 were as follows: 1) MTBE = 1.9‰ and 1.0‰, benzene = 0.9‰ and 0.8‰, and toluene = 0.7‰ and 0.7‰ (Figure 22a). The silica-stabilized H_2O_2 experiments (SIL 1 and SIL 2) yielded no change or a slight increase in C isotope compositions (< 1‰) after three days. MTBE shifted by 0.8‰ and 0.5‰, whereas benzene and toluene showed no change in isotopic composition (Figure 22b). Only naphthalene showed a greater increase to higher carbon isotope values, ~2.3‰, in the silica-stabilized experiment by day 3 due to the rapid oxidation (Figure 23). In contrast, the carbon isotopic values of MTBE, benzene, and toluene compounds in the citrate-stabilized experiments (CIT 1 and CIT 2) showed significant enrichment in C isotope values. For example, MTBE shifted 2.0‰ and 3.1‰, and benzene shifted 2.8‰ and 2.6‰ after three days. Toluene was the most isotopically enriched compound with an increase of 3.8‰ and 4.2‰ (Figure 22c). However, naphthalene in the citrate experiments had a lower enrichment of 0.4‰ and 1.5‰ compared to the enrichment of 0.8‰ and 2.3‰ in the silica experiments.

Based on the results from Figure 22c, the citrate stabilized H_2O_2 experiments yielded the greatest enrichment in C isotope values, particularly for MTBE, benzene, and toluene. Other compounds had the same behavior with respect to changes in C isotopic compositions, except for naphthalene as mentioned above.

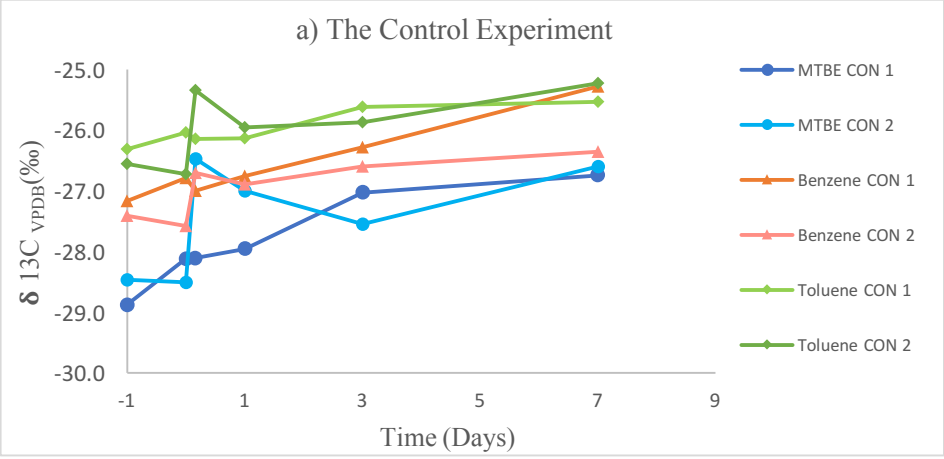

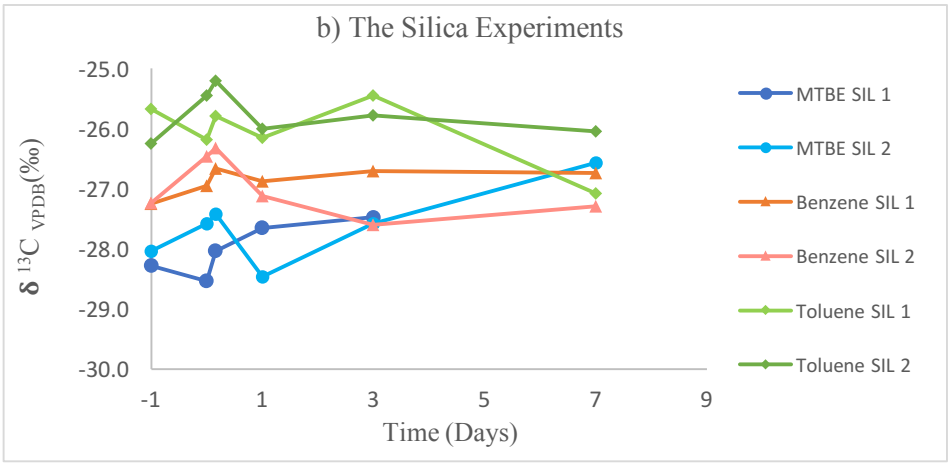

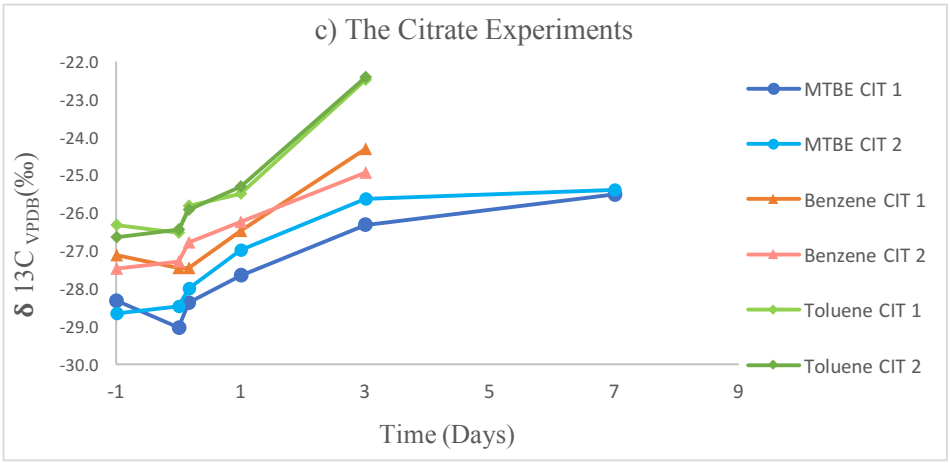

Figure 22: Variation in the $\delta^{13}C$ values with time for MTBE, benzene, and toluene during a) the controlled H_2O_2 (no stabilizer) experiment, b) the silica stabilized H_2O_2 experiment, and c) the citrate stabilized H_2O_2 experiment for site #2.

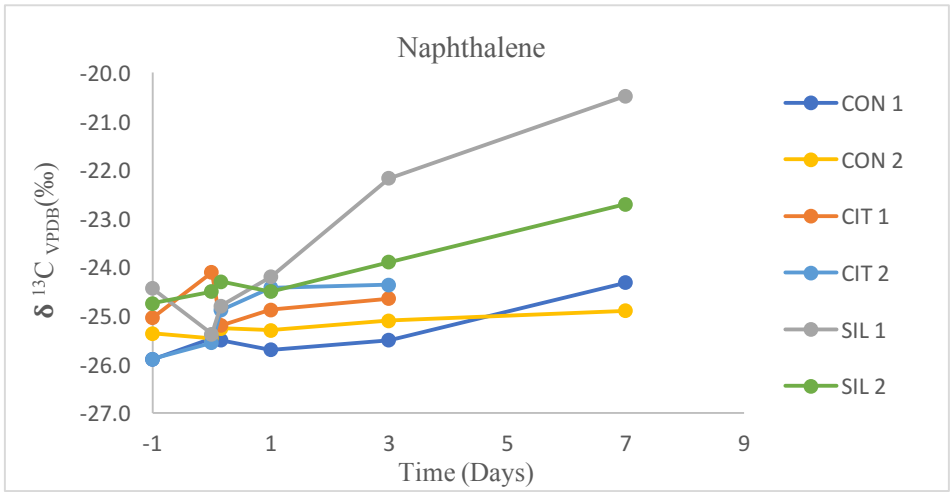

Figure 23: Changes in the $\delta^{13}C$ values of naphthalene with time during the controlled H_2O_2 (no stabilizer), silica stabilized H_2O_2, and citrate stabilized H_2O_2 experiments for site #2.

3.4.0 Synthesis

The chemical oxidation of petroleum hydrocarbons using persulfate and hydrogen peroxide as an oxidant is a promising tool for contaminant degradation. The results from this research were generally in agreement with previous studies that chemical oxidation of hydrocarbon contaminants using persulfate and hydrogen peroxide as oxidants would likely yield significant results (Bergendahl & Thies, 2004; Watts et al., 2007; Lemaire et al., 2013; Yen et al., 2013; Kashir et al., 2015).

In this study, chemical oxidation using persulfate achieved significant results with about 99% of removal for most of the target contaminants. However, benzene and MTBE had more resistance to degradation by persulfate than other compounds, with concentration decreases ranging from 59% - 65% and 4% - 13% for benzene and MTBE, respectively.

Unfortunately, the reason for the lower percent of destruction, especially for MTBE is due to the amount of persulfate that was used in this experiment (5 g/L), which was designed to be a suitable concentration along with the high temperature of the groundwater that might help enhance the oxidation process. This concentration of persulfate was not enough to oxidize a significant amount of MTBE and benzene. Moreover, it was found that significant destruction (99%) of BTEX occurred when the concentration of unactivated and chelated Fe(II)-activated persulfate was 20 g/L in comparison with no significant degradation of BTEX when the persulfate concentration was 1 g/L (Sra et al., 2013). Moreover, field and laboratory studies by Kashir & McGregor (2015) was also in agreement in which the 20 g/L of persulfate achieved better destruction of BTEX (65% and 99% of degradation for benzene and the other compounds (toluene, ethylbenzene, p, m, o-xylene), respectively) compared to 1 g/L of persulfate. Although this study used 5 g/L of persulfate, the degradation percentage is still in the range of 60 – 65% for benzene and 99% for the other compounds (toluene, ethylbenzene, p, m, o-xylene). It seemed that the benzene was more resistant than the other compounds,

thus, an appropriate concentration of persulfate should be carefully chosen, otherwise, contaminant oxidation may not be as effective.

The elevated temperature (30°C) used in the experiments of this study likely enhanced chemical oxidation and, therefore, more degradation of the target hydrocarbons is expected. Huang et al. (2005) determined that 80% of benzene was removed when the temperature was 30°C compared to 34% at 20°C in a thermally activated persulfate experiment.

In this study, hydrogen peroxide achieved better results for MTBE and benzene removal than persulfate. In the hydrogen peroxide experiments, MTBE degraded by 80% - 95% compared to 4% - 13% in the persulfate experiments. Moreover, similar results were observed for benzene which degraded by > 95% in the hydrogen peroxide experiments compared to 59% - 65% of benzene removal in the persulfate experiments. This observation agrees with the results from a study by Ray et al. (2002) in which H_2O_2 accompanied with iron as a catalyst was used for contaminant destruction (>90% of MTBE). Ferrarese et al. (2008) conducted a study in fresh water sediments that used hydrogen peroxide and persulfate as oxidants and both were catalyzed by ferrous ions and used catechol as a chelating agent. That study found that the experiment with H_2O_2 yielded better results (about 97% of PAHs removed) compared with the persulfate experiment (about 82% of PAHs were removed).

It is well known that decreasing the pH would likely enhance the chemical oxidation of hydrocarbon contaminants (Ferrarese et al., 2008; Sra et al., 20013; Li et al., 2017). This study ran several experiments that used citrate (citric acid) as a stabilizer, which ultimately affects the pH. In details, the experiment where H_2O_2 was stabilized by citrate caused the pH to decrease to ~4.6, and that improved the oxidation process and therefore achieved the best results for BTEX and MTBE oxidation compared with the control and silica experiments. For example, benzene reached > 99% of removal when citrate was used to stabilize H_2O_2 compared to ~ 95% of removal from the control and silica experiments in which the maximum drop of pH was around 6.5. Similarly, Ray et al. (2002) found that the oxidation of MTBE by Fenton's reagent with a 1:1 ratio of H_2O_2:Fe was 98% when the pH was 5.0 and no significant change occurred when the pH was 7. In addition, Bergendahl & Thies (2004) conducted a study of MTBE degradation by Fenton's reagent with Fe^0 as a source of Fe^{2+} and found that the extent of MTBE degradation at pH 7 was about 96% compared to 99% when the pH was 4.

In general, most experiments of persulfate and hydrogen peroxide that were performed during this study resulted in enriched values for both C and H isotopes. The isotopic enrichments varied from one experiment to another and from one compound to another as the isotopic changes are typically specific to processes and reaction mechanisms.

The enrichments in C isotope values observed from the persulfate and hydrogen peroxide experiments were quite different. In details, MTBE in the PSC, CFEL, and CFEH persulfate experiments for site #1 had enriched values shifted by 1.2‰ to 3.0‰, 2.1‰ to 2.3‰, and 2.1‰ to 3.7‰, respectively. On the other hand, the enriched values of MTBE in the hydrogen peroxide experiments at site #1 shifted by 0.6‰ to 0.9‰ and 1.0‰ to 1.3‰ for the CON and SIL experiments, respectively. Furthermore, almost the same C isotope enrichments were observed for MTBE at site #2 for the CON and SIL experiments, which had enrichments of 0.9‰ to 1.9‰ and 0.5‰ to 0.8‰, respectively. However, in the experiment where hydrogen peroxide was stabilized by citrate (CIT), the MTBE had higher C isotope enrichments of 2.0‰ to 4.0‰ at Site #1 and Site #2, respectively. All MTBE degradation experiments resulted in enriched values for C isotopes in the persulfate and hydrogen peroxide experiments and for H isotopes in the persulfate experiments, however, the H isotopic fractionation was always higher than that for carbon. The same carbon and hydrogen isotopic changes were found in previous studies in which the hydrogen isotopic shift is higher than the carbon isotopic shift, for example, aerobic biodegradation of MTBE (Zwank et al., 2005).

For benzene and toluene, almost the same C isotope enrichment patterns as MTBE were observed for both the persulfate and hydrogen peroxide experiments. The higher enrichments were achieved from the citrate stabilized H_2O_2 (CIT) experiments for benzene and toluene in which the C isotope enrichments ranged from 1.6‰ to 2.8‰ and 2.5‰ to 4.4‰, respectively.

Generally, hydrogen isotopes showed larger fractionation than carbon isotopes, which is expected given that the two hydrogen isotopes are characterized by a relatively larger mass difference between the two isotopes (mass 1 to mass 2 for hydrogen isotopes which is double the mass between the two isotopes of hydrogen (i.e., 100 percent increase of mass) versus mass 12 to mass 13 for carbon isotopes (~8.3 percent increase of mass). Although 1D-CSIA can aid in identifying and assessing degradation processes, the utilization of 2D-CSIA is a much better tool as the isotopic trends formed by plotting the δ^2H and $\delta^{13}C$ values can provide a higher resolution and help the interpretation of contaminant degradation.

For discussion purposes, enrichment factors calculated in this study will be compared to some but not all studies from the literature. Complete description of the enrichment factors reported in the literature can be seen in Table 8. The higher carbon enrichment factor of contaminants (e.g., benzene) observed in the activated persulfate experiment (ε_C = -1.3 ± 0.7‰) was close to the carbon enrichment factor reported by previous studies (e.g. Saeed, 2011) for alkaline-activated persulfate experiments at 30°C (ε_C = 2.0‰), and also similar to those observed by Solano et al. (2017) (ε_C = -1.7 ± 0.2‰) in an unactivated persulfate experiment. Moreover, the higher hydrogen enrichment factor was in the activated persulfate experiments with a range of -14 ± 3‰ to -23 ± 5‰ in this study versus -10.9‰ reported by Saeed (2011). The differences in the enrichment factors of hydrogen isotopes between the result obtained from this study and the study by Saeed (2011) were most likely due to the different oxidation mechanism involving activated persulfate by iron versus alkaline-activated persulfate. Another example of different observations of carbon and hydrogen enrichment factors for benzene was reported by Fischer et al. (2009). In that study, biodegradation of benzene was monitored under sulfate reducing conditions and yielded higher carbon and hydrogen enrichment factors (ε_C = -2.9 ±0.5‰; ε_H = -78 ±12‰) compared to those obtained by this study. A small carbon enrichment factor for toluene was observed in the PSC experiments (ε_C = -0.04 ± 0.04‰), and a high carbon enrichment factor of 1.4 ± 0.1‰ and 1.7 ± 0.1‰ was observed in the CFEL and CFEH experiments of this study, respectively. The carbon enrichment factors of toluene in this study are in good agreement with those observed in a study by Saeed (2011), in which the carbon enrichment factor of toluene was 1.2‰ and 1.6‰ under experimental conditions of alkaline-activated and unactivated persulfate at 30°C, respectively. In contrast, the carbon enrichment factors of toluene reported by this study and Saeed (2011) were different than those observed in Solano et al. (2017) under the condition of unactivated persulfate and Herrmann et al. (2009) in a sulfate-reducing condition in which the carbon enrichment factors of toluene were -0.64 ± 0.1‰ and -2.5 ±0.5‰, respectively.

Based on the observed enrichment factors from this study and other studies, it can be concluded that the calculated enrichment factors can reflect a specific degradation pathway, for example, higher ε_C observed from biodegradation (ε_C = -2.9 ± 0.5‰; ε_H = -78 ± 12‰)

(Fischer et al., 2008), and lower ε_C observed by this study which involved the chemical oxidation by iron-activated and unactivated persulfate (-0.6 ± 0.1‰ to -1.3 ± 0.7‰).

Overall, based on the results observed from using persulfate and hydrogen peroxide as oxidants, the hydrogen peroxide stabilized by citrate achieved significant degradation of hydrocarbons in comparison with the other stabilizers (silica and phytate). Hydrogen peroxide stabilized by citrate caused a large fractionation in the isotopic composition of C and H which helped the interpretation of hydrocarbon degradation. In addition, CSIA can be utilized to distinguish between two different transformation mechanisms such as biodegradation and chemical oxidation by using the calculated enrichment factors.

Chapter 4

Conclusions

Persulfate and hydrogen peroxide are most desirable oxidants because of their efficiency and rapid reaction with contaminants in groundwater. The experiments in this study explored the application of these oxidants to saline groundwater that had an elevated temperature (30°C). However, there were some limitations faced in this study and it will be explained later in this chapter.

Using persulfate as an oxidant and without the addition of any activator for hydrocarbon oxidation resulted in a small percentage of contaminant removal. However, persulfate activated by chelated iron caused significant degradation of hydrocarbons, resulting in undetectable concentrations for most compounds. Using 5 g/L of persulfate (activated and unactivated) resulted in insignificant degradation of MTBE accompanied by high production of TBA. Increasing the concentration of persulfate would likely enhance the degradation of MTBE as demonstrated by previous studies (Sra et al., 2013). Compared with persulfate, hydrogen peroxide stabilized by citrate oxidized BTEX and MTBE to a greater extent, with almost complete degradation of MTBE because the citrate stabilizer was capable of maintaining the hydrogen peroxide oxidation until the complete removal of MTBE.

The C and H isotopic compositions of hydrocarbon contaminants in the activated persulfate experiment became more enriched compared to the unactivated persulfate experiment. These enriched values reflect the rapid oxidation of hydrocarbons and MTBE by the iron-activated persulfate, which produced the sulfate radicals that were capable of enhancing the oxidation process and therefore caused greater isotopic fractionation. The isotopic results from H_2O_2 stabilized by citrate showed higher isotopic enrichments compared to the control and silica experiments.

The enrichment factors of carbon and hydrogen isotopes observed by this study were different from previous literature studies that were conducted under different conditions (e.g., alkaline activated persulfate, and sulfate reducing conditions). Therefore, it can be concluded

that the calculated enrichment factor (ε) of the two isotopes can discriminate between the different degradation patterns and help to understand the reaction mechanism and whether it involves one pathway or multiple pathways.

4.1 Limitations

The limitations that were faced in this study were as follows: 1) the low concentration of some samples, especially those from the persulfate experiments, have limited the number of samples to be analyzed. Consequently, data on the extent of hydrocarbon degradation could not be collected for later days in the experiments (e.g., day 3, 7, 10) and also caused some non-reproducibility of the results from duplicate experiments. 2) The small volume of samples, where the sample was collected from some of the experiment, was not enough to run the analysis of both carbon and hydrogen isotopes. Reliable hydrogen isotope data could not be obtained for the hydrogen peroxide experiments. Future work should overcome the limitations that occurred in this study, for example, increase the amount and concentration of samples and decrease the sample collection time interval during the experiments.

4.2 Recommendations and suggestions

The oil and gas industry is very large and dynamic with serious potential for incidents that might cause environmental contamination, such as oil spills and leakage of hydrocarbons into drinking water supplies. Such contamination is a serious issue that requires immediate attention and hence research dealing with chemical oxidation to treat contaminated sites is important. Limited studies have been conducted for groundwater that is saline and has high temperature (30°C). Hence, the results obtained in this study are important and should be considered for current and future work.

Based on the findings of this research, my recommendation is to use the hydrogen peroxide stabilized by citrate in remediation projects where groundwater is similar or close to the conditions of saline and elevated temperature (30°C) in this study. This remediation approach can result in significant removal of hydrocarbons and cause large isotopic fractionation that can help to identify the degradation pathways.

References

Ahad, J., B. Lollar, E. Edwards, G. Slater, and B. Sleep. (2000). Carbon isotope fractionation during anaerobic biodegradation of toluene: Implications for intrinsic bioremediation. *Environmental Science & Technology* 34, no. 5: 892– 896.

Audí-Miró, C., Cretnik, S., Torrentó, C., Rosell, M., Shouakar-Stash, O., Otero, N., . . . Soler, A. (2015). C, cl and H compound-specific isotope analysis to assess natural versus fe (0) barrier-induced degradation of chlorinated ethenes at a contaminated site. *Journal of Hazardous Materials, 299*, 747-754. doi: 10.1016/j.jhazmat.2015.06.052

Bendouz, M., Tran, L. H., Coudert, L., Mercier, G., & Blais, J. (2017). Degradation of polycyclic aromatic hydrocarbons in different synthetic solutions by fenton's oxidation. *Environmental Technology, 38*(1), 116. doi:10.1080/09593330.2016.1188161

Bennedsen, L. R. (2014). In Søgaard E. G. Editor., *Chapter 2 - in situ chemical oxidation: The mechanisms and applications of Chemical oxidants for Remediation Purposes*. Amsterdam: Elsevier. 13-74. doi: https://doi.org/10.1016/B978-0-444-53178-0.00002-X

Bergendahl, J. A., & Thies, T. P. (2004). Fenton's oxidation of MTBE with zero- valent iron. *Water Research, 38*(2), 327-334. doi:10.1016/j.watres.2003.10.003

Bouchard, D., Hunkeler, D., Gaganis, P., Aravena, R., Hoehener, P., Broholm, M., & Kjeldsen, P. (2008). Carbon isotope fractionation during diffusion and biodegradation of petroleum hydrocarbons in the unsaturated zone: Field experiment at vaerloese airbase, denmark, and modeling. *Environmental Science & Technology, 42*(2), 596-601. doi:10.1021/es070718f

Boyd, T. J., Osburn, C. L., Johnson, K. J., Birgl, K. B., & Coffin, R. B. (2006). Compound-specific isotope analysis coupled with multivariate statistics to source- apportion hydrocarbon mixtures. *Environmental Science & Technology, 40*(6), 1916-1924.

Braeckevelt, M., Fischer, A., & Kastner, M. (2012). Field applicability of compound- specific isotope analysis (CSIA) for characterization and quantification of in situ contaminant degradation in aquifers. *Applied Microbiology and Biotechnology, 94*(6), 1401-1421. doi:10.1007/s00253-012-4077-1

Cai, XD., Du, WT., Wu, JY., Li, RF., Guo, Y., Yang ZJ. (2012) Effective treatment of trichloroethylene-contaminated soil by hydrogen peroxide in soil slurries. *Pedosphere* 22(4):572–579. doi.org/10.1016/S1002-0160(12)60042-3

Cassidy, D. P., Srivastava, V. J., Dombrowski, F. J., & Lingle, J. W. (2015). Combining in situ chemical oxidation, stabilization, and anaerobic bioremediation in a single application to reduce contaminant mass and leachability in soil. *Journal of Hazardous Materials, 297*, 347-355. doi: 10.1016/j.jhazmat.2015.05.030

Chan, C., Mundle, S., Eckert, T., Liang, X., Tang, S., Lacrampe-Couloume, G., Edwards, E., Lollar, B. S. (2012). Large carbon isotope fractionation during biodegradation of chloroform by dehalobacter cultures. *Environmental Science & Technology, 46*(18), 10154-10160. doi:10.1021/es3010317

Chikaraishi, Y., Kashiyama, Y., Ogawa, N. O., Kitazato, H., Satoh, M., Nomoto, S., & Ohkouchi, N. (2008). A compound- specific isotope method for measuring the stable

nitrogen isotopic composition of tetrapyrroles. *Organic Geochemistry, 39*(5), 510-520. doi: 10.1016/j.orggeochem.2007.08.010

Cincinelli, A., Pieri, F., Zhang, Y., Seed, M., & Jones, K. C. (2012). Compound specific isotope analysis (CSIA) for chlorine and bromine: A review of techniques and applications to elucidate environmental sources and processes. *Environmental Pollution, 169*, 112-127. doi: 10.1016/j.envpol.2012.05.006

Das, N., & Chandran, P. (2011). Microbial degradation of petroleum hydrocarbon contaminants: An overview. *Biotechnology Research International, 2011*, 941810. 10.4061/2011/941810

Deng, D., Peng, L., Guan, M., & Kang, Y. (2014). Impact of activation methods on persulfate oxidation of methyl tert-butyl ether. *Journal of Hazardous Materials, 264*, 521-528. doi: 10.1016/j.jhazmat.2013.10.042

Devi, P., Das, U., & Dalai, A. K. (2016). In- situ chemical oxidation: Principle and applications of peroxide and persulfate treatments in wastewater systems. *Science of the Total Environment, 571*, 643-657. doi:10.1016/j.scitotenv.2016.07.032

Dorer, C., Vogt, C., Kleinsteuber, S., Stams, A. J. M., & Richnow, H. (2014). Compound-specific isotope analysis as a tool to characterize biodegradation of ethylbenzene. *Environmental Science & Technology, 48*(16), 9122-9132. doi:10.1021/es500282t

Elsayed, O., Maillard, E., Vuilleumier, S., Nijenhuis, I., Richnow, H., & Imfeld, G. (2014). Using compound-specific isotope analysis to assess the degradation of chloroacetanilide

herbicides in lab-scale wetlands. *Chemosphere, 99*, 89-95. doi: 10.1016/j.chemosphere.2013.10.027

Ferrarese, E., Andreottola, G., & Oprea, I. A. (2008). Remediation of PAH-contaminated sediments by chemical oxidation. *Journal of Hazardous Materials, 152*(1), 128-139. doi: 10.1016/j.jhazmat.2007.06.080

Ferreira, I., Prieto, T., Freitas, J., Thomson, N., Nantes, I., & Bechara, E. (2017). Natural persulfate activation for anthracene remediation in tropical environments. *Water, Air, & Soil Pollution, 228*(4), 1-10. doi:10.1007/s11270-017-3322-8

Fischer, A., Herklotz, I., Herrmann, S., Thullner, M., Weelink, S. A. B., Stams, A. J. M., Schlomann, M., Richnow, H., & Vogt, C. (2008). Combined carbon and hydrogen isotope fractionation investigations for elucidating benzene biodegradation pathways. *Environmental Science & Technology, 42*(12), 4356-4363. doi:10.1021/es702468f

Fischer, A., Gehre, M., Breitfeld, J., Richnow, H., & Vogt, C. (2009). Carbon and hydrogen isotope fractionation of benzene during biodegradation under sulfate- reducing conditions: A laboratory to field site approach. *Rapid Communications in Mass Spectrometry, 23*(16), 2439-2447. 10.1002/rcm.4049

Grebel, J. E., Pignatello, J. J., & Mitch, W. A. (2010). Effect of halide ions and carbonates on organic contaminant degradation by hydroxyl radical- based advanced oxidation processes in saline waters. *Environmental Science & Technology, 44*(17), 6822-6828. doi:10.1021/es1010225

Han, D., Wan, J., Ma, Y., Wang, Y., Li, Y., Li, D., & Guan, Z. (2015). New insights into the role of organic chelating agents in Fe(II) activated persulfate processes. *Chemical Engineering Journal*, *269*, 425-433. doi:10.1016/j.cej.2015.01.106

Herrmann, S., Vogt, C., Fischer, A., Kuppardt, A., & Richnow, H. (2009). Characterization of anaerobic xylene biodegradation by two- dimensional isotope fractionation analysis. *Environmental Microbiology Reports, 1*(6), 535-544. doi:10.1111/j.1758-2229.2009.00076.x

House, D. A. (1962). Kinetics and mechanism of oxidations by peroxydisulfate. *Chemical Reviews, 62*(3), 185-203. doi:10.1021/cr60217a001

Huang, K., Zhao, Z., Hoag, G. E., Dahmani, A., & Block, P. A. (2005). Degradation of volatile organic compounds with thermally activated persulfate oxidation. *Chemosphere, 61*(4), 551-560. doi:10.1016/j.chemosphere.2005.02.032

Hunkeler, D., N. Anderson, R. Aravena, S. Bernasconi, and B. Butler. (2001). Hydrogen and carbon isotope fractionation during aerobic biodegradation of benzene. *Environmental Science & Technology* 35, no. 17: 3462– 3467.

ITRC (Interstate Technology & Regulatory Council). (2005). Technical and Regulatory Guidance for In Situ Chemical Oxidation of Contaminated Soil and Groundwater, 2nd ed. ISCO-2. Washington, D.C.: Interstate Technology & Regulatory Council, In Situ Chemical Oxidation Team. Available on the Internet at http://www.itrcweb.org.

Karpenko, O., Lubenets, V., Karpenko, E., & Novikov, V. (2009). Chemical oxidants for remediation of contaminated soil and water. A review. *Chemistry & Chemical Technology*, *3*(1), 41-45. Retrieved from http://ena.lp.edu.ua:8080/handle/ntb/1524

Kashir, M., & McGregor, R. (2015). Chemical oxidation performance in high temperature, saline groundwater impacted with hydrocarbons. *Remediation Journal, 25*(2), 55-70. doi:10.1002/rem.21424

Kashir, M., McGregor, R., Gusti, W., & Shouakar-Stash, O. (2017). Chemical oxidation using stabilized hydrogen peroxide in high temperature, saline groundwater impacted with hydrocarbons and MTBE. *Remediation Journal, 27*(4), 19-28. doi:10.1002/rem.21526

Kolthoff, I. M., & Miller, I. K. (1951). The chemistry of persulfate. I. the kinetics and mechanism of the decomposition of the persulfate ion in aqueous medium 1. *Journal of the American Chemical Society, 73*(7), 3055-3059. doi:10.1021/ja01151a024

Lemaire, J., Croze, V., Maier, J., & Simonnot, M. (2011). Is it possible to remediate a BTEX contaminated chalky aquifer by in situ chemical oxidation? *Chemosphere, 84*, 1181-1187. doi: 10.1016/j.chemosphere.2011.06.052

Lemaire, J., Buès, M., Kabeche, T., Hanna, K., & Simonnot, M. (2013). Oxidant selection to treat an aged PAH contaminated soil by in situ chemical oxidation. *Journal of Environmental Chemical Engineering, 1*(4), 1261-1268. doi: 10.1016/j.jece.2013.09.018

Levchuk, I., Bhatnagar, A., & Sillanpää, M. (2014). Overview of technologies for removal of methyltert-butyl ether (MTBE) from water. *Science of the Total Environment, 476-477*, 415-433. doi:10.1016/j.scitotenv.2014.01.037

Li, W., Orozco, R., Camargos, N., & Liu, H. (2017). Mechanisms on the impacts of alkalinity, pH, and chloride on persulfate- based groundwater remediation. *Environmental Science & Technology, 51*(7), 3948-3959. doi:10.1021/acs.est.6b04849

Liang, C., & Bruell, C., Marley, M., Sperry, K. (2003). Thermally activated persulfate oxidation of trichloroethylene (TCE) and 1,1,1- trichloroethane (TCA) in aqueous systems and soil slurries. *Soil & Sediment Contamination, 12*(2), 207-228.

Liang, C., Huang, C., & Chen, Y. (2008). Potential for activated persulfate degradation of BTEX contamination. *Water Research, 42*(15), 4091-4100. doi:10.1016/j.watres.2008.06.022

Liang, S. H., & K. (2011). In situ oxidation of petroleum- hydrocarbon contaminated groundwater using passive ISCO system. *Water Research, 45*(8), 2496-2506. doi: 10.1016/j.watres.2011.02.005

Luca, M., Balan, R., & Manescu, A. (2011). Monitoring the pollution of groundwater in the area of industrial waste. *Aerul Şi Apa: Componente Ale Mediului, 2011*, 30-37.

Lutz, S., & Van Breukelen, B. (2014). Combined source apportionment and degradation quantification of organic pollutants with CSIA: 2. model validation and application. *Environmental Science & Technology, 48*(11), 6229-6236. doi:10.1021/es405400w

Ma, X., Zhao, L., Dong, Y., Chen, H., & Zhong, M. (2018). Enhanced Fenton degradation of polychlorinated biphenyls in capacitor-oil-contaminated soil by chelating agents. *Chemical Engineering Journal*, *333*, 370-379. doi:10.1016/j.cej.2017.09.167

Manoli, E., & Samara, C. (2008). The removal of polycyclic aromatic hydrocarbons in the wastewater treatment process: Experimental calculations and model predictions. *Environmental Pollution, 151*(3), 477-485. doi:10.1016/j.envpol.2007.04.009

Marchesi, M., Thomson, N. R., Aravena, R., Sra, K. S., Otero, N., & Soler, A. (2013). Carbon isotope fractionation of 1,1,1- trichloroethane during base- catalyzed persulfate treatment. *Journal of Hazardous Materials, 260*, 61-66. doi: 10.1016/j.jhazmat.2013.05.011

Monteagudo, J. M., & Duran, A., Gonzales, R., Exposito, A.J. (2015). In situ chemical oxidation of carbamazepine solutions using persulfate simultaneously activated by heat energy, UV light, Fe^{2+} ions, and H_2O_2. *Applied Catalysis B: Environmental, 176-177*, 120-129. doi:10.1016/j.apcatb.2015.03.055

Palau, J., Shouakar-Stash, O., & Hunkeler, D. (2014). Carbon and chlorine isotope analysis to identify abiotic degradation pathways of 1,1,1-trichloroethane. *Environmental Science & Technology, 48*(24), 14400-14408. doi:10.1021/es504252z

Peluffo, M., & P. (2016). Use of different kinds of persulfate activation with iron for the remediation of a PAH- contaminated soil. *Science of the Total Environment, 563-564*, 649-656. doi:10.1016/j.scitotenv.2015.09.034

Peyton, G. R. (1993). The free- radical chemistry of persulfate- based total organic carbon analyzers. *Marine Chemistry, 41*(1), 91-103. doi:10.1016/0304-4203(93)90108-Z

Ranc, B., Faure, P., Croze, V., & Simonnot, M.O. (2016). Selection of oxidant doses for in situ chemical oxidation of soils contaminated by polycyclic aromatic hydrocarbons (PAHs): A review. *Journal of Hazardous Materials, 312*, 280-297. doi: 10.1016/j.jhazmat.2016.03.068

Ray, A. B., Selvakumar, A., & Tafuri, A. N. (2002). Treatment of MTBE- contaminated waters with fenton's reagent. *Remediation Journal, 12*(3), 81-93. doi:10.1002/rem.10035

Roy, J. W., & Bickerton, G. (2012). Toxic groundwater contaminants: An overlooked contributor to urban stream syndrome? *Environmental Science & Technology, 46*(2), 729-736. doi:10.1021/es2034137

Saeed, W. (2011). *The effectiveness of persulfate in the oxidation of petroleum contaminants in saline environment at elevated groundwater temperature.* Retrieved from University of Waterloo's institutional repository. *http://hdl.handle.net.proxy.lib.uwaterloo.ca/10012/6396*

Schmidt, T., Zwank, L., Elsner, M., Berg, M., Meckenstock, R., & Haderlein, S. (2004). Compound- specific stable isotope analysis of organic contaminants in natural environments: A critical review of the state of the art, prospects, and future challenges. *Analytical and Bioanalytical Chemistry, 378*(2), 283-300. doi:10.1007/s00216-003-2350-y

Schmidt, J. T., Ahmad, M., Teel, A. L., & Watts, R. J. (2011). Hydrogen peroxide stabilization in one- dimensional flow columns. *Journal of Contaminant Hydrology, 126*(1), 1-7. doi:10.1016/j.jconhyd.2011.05.008.

Shin, W., & Lee, K. (2010). Carbon isotope fractionation of benzene and toluene by progressive evaporation. *Rapid Communications in Mass Spectrometry, 24*(11), 1636-1640. doi:10.1002/rcm.4562

Siegrist, R. L., Crimi, M., Thomson, N. R., Clayton, W. S., & Marley, M. (2014). In situ Chemical Oxidation. In *Chlorinated Solvent Source Zone Remediation* (pp. 253-305). Retrieved from https://doi.org/10.1007/978-1-4614-6922-3_9

Smith, M. A., & North Atlantic Treaty Organization. (1985). *Contaminated land: Reclamation and treatment*. New York, NY: Plenum Press.

Solano, F. M., Massimo, M., Thomson, N. R., Daniel, B., & Ramon, A. (2017). Carbon and hydrogen isotope fractionation of benzene, toluene, and o-Xylene during chemical oxidation by persulfate. *Groundwater Monitoring & Remediation,* 1-11. doi:10.1111/gwmr.12228

Sra, K. S., Thomson, N. R., & Barker, J. F. (2013). Persulfate treatment of dissolved gasoline compounds. *Journal of Hazardous, Toxic, and Radioactive Waste, 17*(1), 9-15. doi:10.1061/(ASCE)HZ.2153-5515.0000143

Stroo, H. F., Leeson, A., Marqusee, J. A., Johnson, P. C., Ward, C. H., Kavanaugh, M. C., Sale, T. C., Newell, C. J., Pennell, K. D., Lebron, C. A., Unger, M. (2012). Chlorinated ethene source remediation: Lessons learned. *Environmental Science & Technology, 46*(12), 6438-6447. doi:10.1021/es204714w

Tsitonaki, A., Petri, B., Crimi, M., Mosbæk, H., Siegrist, R. L., & Bjerg, P. L. (2010). In situ chemical oxidation of contaminated soil and groundwater using persulfate: A review.

Critical Reviews in Environmental Science and Technology, 40(1), 55-91. doi:10.1080/10643380802039303

Tyagi, V. P. (2009). *Essential Chemistry*. Delhi, India: Ratna Sagar P. Ltd.

Usman, M., Faure, P., Ruby, C., and Hanna, K. (2012). Application of magnetite- activated persulfate oxidation for the degradation of PAHs in contaminated soils. *Chemosphere, 87*(3), 234-240. doi: 10.1016/j.chemosphere.2012.01.001

Venny, S., Gan, H. K., & Ng, H. K. (2011). Inorganic chelated modified-fenton treatment of polycyclic aromatic hydrocarbon (PAH)-contaminated soils. *Chemical Engineering Journal, 180,* 1-8. doi:10.1016/j.cej.2011.10.082

Viisimaa, M., & Goi, A. (2014). Use of hydrogen peroxide and percarbonate to treat chlorinated aromatic hydrocarbon-contaminated soil. *Journal of Environmental Engineering and Landscape Management, 22*(1), 30-39. doi:10.3846/16486897.2013.804827

Watts, R. J., Haller, D. R., Jones, A. P., & Teel, A. L. (2000). A foundation for the risk- based treatment of gasoline- contaminated soils using modified fenton's reactions. *Journal of Hazardous Materials, 76*(1), 73-89. doi:10.1016/S0304-3894(00)00173-4.

Watts, R. J., Finn, D. D., Cutler, L. M., Schmidt, J. T., & Teel, A. L. (2007). Enhanced stability of hydrogen peroxide in the presence of subsurface solids. *Journal of Contaminant Hydrology, 91*(3), 312-326. doi: 10.1016/j.jconhyd.2006.11.004.

Wu, L., Kümmel, S., & Richnow, H. (2017). Validation of GC– IRMS techniques for $\delta^{13}C$ and $\delta^{2}H$ CSIA of organophosphorus compounds and their potential for studying the mode of

hydrolysis in the environment. *Analytical and Bioanalytical Chemistry, 409*(10), 2581-2590. doi:10.1007/s00216-017-0203-3

Wu, X., Gu, X., Lu, S., Xu, M., Zang, X., Miao, Z., Qiu, Z., Sui, Q. (2014). Degradation of trichloroethylene in aqueous solution by persulfate activated with citric acid chelated ferrous ion. *Chemical Engineering Journal, 255*, 585-592. doi: 10.1016/j.cej.2014.06.085

Yan, J., Zhu, L., Luo, Z., Huang, Y., Tang, H., & Chen, M. (2013). Oxidative decomposition of organic pollutants by using persulfate with ferrous hydroxide colloids as efficient heterogeneous activator. *Separation and Purification Technology, 106*, 8-14. doi: 10.1016/j.seppur.2012.12.012

Yen, C., Chen, K., Kao, C., Liang, S., & Chen, T. (2011). Application of persulfate to remediate petroleum hydrocarbon- contaminated soil: Feasibility and comparison with common oxidants. *Journal of Hazardous Materials, 186*(2-3), 2097-2102. doi: 10.1016/j.jhazmat.2010.12.129

Zhao, D., Yan, X. L., Liao, X. Y., Tu, S. X., & Shi, Q. W. (2011). Chemical oxidants for remediation of BTEX-contaminated soils at coking sites. *Huanjing Kexue*, *32*(2), 849-856.

Zingaretti, D., Verginelli, I., & Baciocchi, R. (2016). Catalyzed hydrogen peroxide combined with CO2 sparging for the treatment of contaminated groundwater. *Chemical Engineering Journal, 300*, 119-126. doi: 10.1016/j.cej.2016.04.056.

Zwank, L., Berg, M., Elsner, M., Schmidt, T. C., Schwarzenbach, R. P., & Haderlein, S. B. (2005). New evaluation scheme for two- dimensional isotope analysis to decipher

biodegradation processes: Application to groundwater contamination by MTBE. *Environmental Science & Technology, 39*(4), 1018-1029.

Appendix A: The concentration of hydrocarbons, pH, TIC, and persulfate from the experiments of activated and unactivated persulfate at site #1.

Sample	Benzene	Toluene	Ethylbe -nzene	M, P-Xylene	O-Xylene	135 TMB	124 TMB	123 TMB	Naphth -alene	Total	MTBE	TBA	pH	TIC	Persulf -ate
						µg/L									mg/L
PSC1 INIT1	3989.2	3833.7	3412.2	3265.5	3884.1	2292.0	2674.4	2822.1	4851.2	31024	54.1	ND	7.7	52.0	
PSC1 INIT2	3989.9	3867.2	3462.5	3314.1	3929.0	2335.6	2718.4	2860.3	4878.0	31355	68.3	ND	7.2	48.1	6.6
PSC1 5MIN	3999.0	3862.3	3457.9	3314.1	3941.0	2347.1	2734.5	2889.7	4974.5	31520	NA	NA	7.2	50.4	5.7
PSC1 1HR	3209.2	2979.4	2543.5	2448.5	3016.9	1616.2	1941.6	2153.8	4116.5	24025	NA	NA	7.3	44.7	5.3
PSC1 3HR	2920.0	2698.3	2288.0	2204.4	2819.7	1432.8	1774.0	2062.0	4080.2	22279	58.6	ND	NA	NA	NA
PSC1 1DY	2440.7	2080.4	1632.9	1380.0	2059.8	650.9	709.5	1169.1	1512.3	13635	81.9	ND	7.3	42.1	5.5
PSC1 3DY	NA	NA	NA	NA	NA	NA	NA	NA	NA	NA	89.6	ND	NA	NA	NA
PSC1 7DY	NA	NA	NA	NA	NA	NA	NA	NA	NA	NA	78.1	3.2	NA	NA	NA
PSC1 10DY	NA	NA	NA	NA	NA	NA	NA	NA	NA	NA	76.5	6.0	NA	NA	NA
PSC1 14DY	1634.3	146.4	0.0	0.0	0.0	0.0	0.0	0.0	0.0	1780	73.6	11.6	7.1	52.0	4.7
PSC2 INIT1	4511.1	4307.6	3852.1	3674.9	4275.5	2600.6	2991.1	3088.9	4898.9	34200	92.9	ND	7.7	47.2	
PSC2 INIT2	4356.0	4230.5	3770.2	3634.2	4261.6	2548.2	2958.8	3082.7	4971.9	33813	88.2	ND	7.4	46.3	6.2
PSC2 5MIN	4388.7	4318.4	3879.9	3762.0	4416.0	2661.6	3087.3	3220.2	5209.4	34943	NA	NA	7.4	45.7	5.6
PSC2 1HR	3551.3	3262.1	2748.7	2649.8	3295.4	1720.0	2098.7	2365.0	4433.7	26124	NA	NA	7.4		5.5
PSC2 3HR	3213.0	2944.4	2475.9	2338.9	3045.2	1430.7	1795.8	2157.7	3999.4	23401	83.6	ND	NA	NA	NA
PSC2 1DY	2770.2	2155.9	1660.7	676.2	1803.3	222.4	77.5	334.4	90.2	9790	93.1	ND	7.1	39.3	5.4
PSC2 3DY	NA	NA	NA	NA	NA	NA	NA	NA	NA	NA	92.0	ND	NA	NA	NA
PSC2 7DY	NA	NA	NA	NA	NA	NA	NA	NA	NA	NA	79.6	5.6	NA	NA	NA
PSC2 10DY	NA	NA	NA	NA	NA	NA	NA	NA	NA	NA	74.4	9	NA	NA	NA
PSC2 14DY	1584.6	36.1	0.0	0.0	0.0	0.0	0.0	0.0	0.0	1620	67.1	16.3	7.0	56.5	4.4
CFEL1 INIT	3748.7	3631.3	3244.4	3109.5	3742.2	2223.3	2601.8	2783.3	5006.5	30091	81.9	ND	7.7		
CFEL1 INIT2	2909.1	452.6	279.9	128.0	149.5	26.6	54.9	42.2	3756.9	7799	86.0	0.9	2.7	76.2	3.2
CFEL1 5MIN	2845.6	376.3	211.3	78.4	92.3	16.2	31.3	24.1	3365.9	7041	NA	NA	2.8	72.4	3.5
CFEL1 1HR	2176.6	387.3	272.2	159.7	217.4	108.2	113.8	139.8	1396.9	4971	NA	NA	5.4	70.8	2.9
CFEL1 3HR	2139.2	443.8	328.0	217.1	280.3	135.1	145.6	174.1	1388.7	5252	78.8	1.1	NA	NA	NA
CFEL1 1DY	1943.4	380.1	266.1	107.8	202.7	50.1	22.7	60.2	63.3	3096	81.3	1.2	6.5	107	3.5
CFEL1 3DY	NA	NA	NA	NA	NA	NA	NA	NA	NA	NA	77.7	0.8	NA	NA	NA
CFEL1 7DY	NA	NA	NA	NA	NA	NA	NA	NA	NA	NA	85.6	2.3	NA	NA	NA

CFEL1 10DY	NA	NA	NA	NA	NA	NA	NA	NA	NA	NA	85.3	3.2	NA	NA	NA
CFEL1 14DY	1546.7	114.7	58.4	0.0	11.8	0.0	0.0	0.0	0.0	1731	81.4	3.8	6.7	100	3.1
CFEL2 INIT	3975.0	3912.7	3559.7	3407.5	4048.5	2466.7	2862.5	3015.2	5328.9	32576	92.2	ND	7.7		
CFEL2 INIT2	3164.0	493.3	312.0	143.1	168.0	27.1	57.3	43.3	3905.4	8313	86.1	0.9	2.8	67.1	3.5
CFEL2 5MIN	3054.0	395.5	219.9	75.3	86.9	12.2	22.1	14.4	3336.0	7216	NA	NA	2.4	71.3	2.3
CFEL2 1HR	2268.6	355.1	220.7	104.2	152.7	41.6	47.6	68.2	1492.5	4751	NA	NA	6.0	72.3	3.4
CFEL2 3HR	2248.4	393.1	259.1	142.3	196.8	66.4	71.4	96.9	1304.2	4778	76.1	1.1	NA	NA	NA
CFEL2 1DAY	1954.7	333.2	216.7	79.6	159.7	30.0	9.8	38.5	58.8	2881	84.9	1.0	6.5	96.9	3.5
CFEL2 3DY	NA	NA	NA	NA	NA	NA	NA	NA	NA	NA	86.9	1.2	NA	NA	NA
CFEL2 7DY	NA	NA	NA	NA	NA	NA	NA	NA	NA	NA	82.5	2.1	NA	NA	NA
CFEL2 10DY	NA	NA	NA	NA	NA	NA	NA	NA	NA	NA	80.3	2.7	NA	NA	NA
CFEL2 14DY	1581.7	108.9	55.8	0.0	14.1	0.0	0.0	0.0	0.0	1760	81.2	3.7	6.6	112	3.1
CFEH1 INIT1	3628.8	3498.9	3142.2	2998.6	3563.3	2116.7	2463.4	2609.3	4790.6	28811	78.6	ND	7.7		
CFEH1 INIT2	2998.8	426.0	255.4	118.1	120.6	27.1	71.2	40.7	4170.0	8227	67.6	0.7	2.2	111	2.9
CFEH1 5MIN	2959.2	341.2	178.0	61.6	62.9	12.6	34.7	20.7	4058.5	7729	NA	NA	2.4	116	3.4
CFEH1 1HR	2233.0	207.5	129.0	57.6	72.7	32.3	47.3	55.7	2884.1	5719	NA	NA	5.6	93.8	3.5
CFEH1 3HR	2063.1	263.4	194.9	101.6	141.2	31.9	44.2	65.2	1228.9	4134	60.1	0.6	NA	NA	NA
CFEH1 1DAY	1797.6	193.9	137.3	37.1	83.4	12.5	0.0	18.4	48.5	2328	75.4	1.4	6.3	111	3.4
CFEH1 3DAY	NA	NA	NA	NA	NA	NA	NA	NA	NA	NA	72.1	2.3	NA	NA	NA
CFEH1 7DAY	NA	NA	NA	NA	NA	NA	NA	NA	NA	NA	70.1	2.6	NA	NA	NA
CFEH1 10DAY	NA	NA	NA	NA	NA	NA	NA	NA	NA	NA	76.7	3.8	NA	NA	NA
CFEH1 14DAY	1269.7	20.7	17.0	0.0	0.0	0.0	0.0	0.0	0.0	1307	75.1	4.5	6.4	110	2.2
CFEH2 INIT	3624.9	3504.8	3152.7	3014.6	3550.8	2151.5	2486.4	2606.7	4613.2	28705	87.9	ND	7.7		
CFEH2 INIT2	3017.6	451.1	261.5	118.7	118.9	19.5	72.7	28.9	4190.3	8279	85.6	1.3	2.6	124	3.7
CFEH2 5MIN	2820.7	344.2	182.4	65.9	66.4	10.1	36.2	20.2	3949.3	7495	NA	NA	2.4	129	3.5
CFEH2 1HR	2381.8	275.7	174.1	85.9	110.1	38.6	55.4	60.4	2935.3	6117	NA	NA	5.7	101	3.2
CFEH2 3HR	2183.1	299.2	217.8	116.8	150.3	35.1	51.2	63.5	1447.8	4564	78.1	1.5	NA	NA	NA
CFEH2 1DAY	1784.9	222.9	165.7	47.8	95.3	13.8	0.0	17.7	53.0	2401	74.1	1.3	6.2	99.1	3.9
CFEH2 3DAY	NA	NA	NA	NA	NA	NA	NA	NA	NA	NA	76.5	1.6	NA	NA	NA
CFEH2 7DAY	NA	NA	NA	NA	NA	NA	NA	NA	NA	NA	79.7	3.1	NA	NA	NA
CFEH2 10DAY	NA	NA	NA	NA	NA	NA	NA	NA	NA	NA	74.6	3.7	NA	NA	NA
CFEH2 14DAY	1256.5	17.6	16.5	0.0	0.0	0.0	0.0	0.0	0.0	1290	70.2	4.8	6.5	105	2.2

*NA: not analyzed

Appendix B: MTBE and TBA concentrations versus time in the experiments for H_2O_2 stabilized by silica, citrate, and phytate plus the controlled experiment (no stabilizer) at site #1.

Days	0	0.1	2	4	9	14
MTBE						
Microcosm	mg/L					
CON 1	287.0	198.0	118.0	66.0	24.4	13.1
CON 2	307.0	195.0	164.0	92.0	38.5	21.0
Sil L1	271.0	191.0	124.0	84.0	36.7	21.0
Sil L2	295.0	181.0	142.0	83.0	35.8	24.0
Sil H1	300.0	194.0	146.0	114.0	46.5	26.3
Sil H2	302.0	190.0	174.0	132.0	58.9	30.4
Cit L1	314.0	193.0	69.0	33.0	12.9	11.8
Cit L2	321.0	216.0	113.0	46.0	16.0	14.4
Cit H1	276.0	170.0	50.0	27.0	17.5	18.0
Cit H2	288.0	156.0	65.0	32.0	19.5	19.5
Phy L1	322.0	190.0	202.0	205.0	125.0	76.4
Phy L2	337.0	246.0	243.0	160.0	141.0	88.3
Phy H1	394.0	250.0	174.0	137.0	63.5	37.3
Phy H2	422.0	258.0	194.0	120.0	45.5	21.2
TBA						
Microcosm	mg/L					
CON 1	0	2.3	11.6	19.1	21.9	25.7
CON 2	0	3.3	11.2	16.8	21.4	25.4
Sil L1	0	3.6	8.1	13.3	17.3	21.4
Sil L2	0	3.1	9.0	13.3	15.9	22.0
Sil H1	0	2.2	6.4	11.0	14.3	19.2
Sil H2	0	3.5	8.3	13.0	16.8	22.0
Cit L1	0	3.1	15.5	21.8	25.8	34.3
Cit L2	0	5.5	25.0	29.6	32.4	41.8
Cit H1	0	3.0	16.3	23.5	31.0	40.8
Cit H2	0	3.9	20.7	27.8	31.1	40.8
Phy L1	0	4.4	6.7	7.2	10.5	16.8
Phy L2	0	6.0	6.7	6.4	10.9	18.4
Phy H1	0	3.9	10.9	17.3	24.3	31.6
Phy H2	0	6.1	19.1	30.6	35.2	40.0

Appendix C**:** The initial and final concentration of leachable iron from sediments at site #1.

	Initial				**Final (after 14 days)**			
	Fe (II)		Fe total		Fe (II)		Fe total	
	mg/g	mg/g	mg/g	mg/g	mg/g	mg/g	mg/g	mg/g
Experiment	Set 1	Set 2	Set 1	Set 2	Set 1	Set 2	Set 1	Set 2
CON1	0.03	0.03	0.35	0.39	0.03	0.03	0.39	0.36
CON2	0.03	0.03	0.35	0.39	0.03	0.03	0.32	0.39
Sil L1	0.03	0.03	0.35	0.39	0.04	0.03	0.43	0.36
Sil L2	0.03	0.03	0.35	0.39	0.03	0.03	0.39	0.38
Sil H1	0.03	0.03	0.35	0.39	0.03	0.03	0.34	0.34
Sil H2	0.03	0.03	0.35	0.39	0.03	0.03	0.38	0.39
Cit L1	0.03	0.03	0.35	0.39	0.05	0.05	0.41	0.37
Cit L2	0.03	0.03	0.35	0.39	0.04	0.05	0.36	0.36
Cit H1	0.03	0.03	0.35	0.39	0.06	0.07	0.43	0.45
Cit H2	0.03	0.03	0.35	0.39	0.05	0.05	0.39	0.39
Phy L1	0.03	0.03	0.35	0.39	0.08	0.07	0.20	0.20
Phy L2	0.03	0.03	0.35	0.39	0.08	0.10	0.21	0.22
Phy H1	0.03	0.03	0.35	0.39	0.03	0.05	0.39	0.39
Phy H2	0.03	0.03	0.35	0.39	0.07	0.04	0.43	0.37

Appendix D: Hydrocarbon concentrations versus time in the experiment of H_2O_2 stabilized by citrate, and silica plus the control (no stabilizer) experiment for site #1 and site #2.

	Benzene	Toluene	EthylBenzene	M Xylene	O Xylene	135 TMB	124 TMB	123 TMB	Naphthalene	Total
Site #1	µg/L									
CON1INIT	11642.2	10426.7	8261.2	7819.6	8910.2	5682.9	6543.6	6960.5	10857.7	77104.7
CON1H_2O_2INIT	10255.0	9048.9	6923.7	6530.0	7490.0	4404.6	5138.0	5518.9	8822.0	64131.0
CON1 4HR	7740.7	6708.4	4931.4	4713.8	5964.6	3116.0	3910.9	4579.4	8538.6	50203.7
CON 1 1DY	2388.9	1893.8	1194.3	1205.4	2046.3	888.3	1303.8	1893.8	4655.1	17469.7
CON 1 3DY	470.1	344.7	204.5	220.4	501.3	262.0	385.3	653.4	1945.8	4987.6
CON 1 7DY	36.4	42.1	15.6	23.7	39.8	27.7	56.3	80.7	175.9	498.2
CON2INIT	11381.8	10117.0	8021.4	7607.2	8726.8	5580.7	6480.1	6987.2	11550.8	76453.0
CON2H_2O_2INIT	10706.8	9497.0	7447.5	7039.7	8135.8	4895.0	5744.8	6234.8	10508.1	70209.4
CON2 4HR	7059.0	6022.1	4291.5	4134.7	5470.6	2711.3	3529.2	4320.5	8780.9	46319.8
CON 2 1DY	1848.1	1465.1	962.7	980.1	1706.2	822.4	1172.3	1712.5	4378.2	15047.6
CON 2 3DY	314.4	244.1	145.5	159.3	361.4	215.9	316.8	511.5	1442.4	3711.2
CON 2 7DY	25.0	27.1	13.4	22.4	30.8	26.4	45.6	61.3	117.2	369.2
CIT1INIT	10179.4	9150.8	6810.6	6485.9	7884.3	4070.9	5046.0	5761.1	10085.1	65473.9
CIT1H_2O_2INIT	8324.9	7429.2	5491.8	5239.6	6408.7	3308.1	4103.8	4722.7	8340.3	53369.0
CIT14HR	5506.0	4598.3	3162.5	3087.8	4305.2	2001.4	2701.8	3450.1	7233.6	36046.6
CIT1 1DY	1144.4	889.8	603.1	614.8	1001.1	550.9	715.5	970.5	1401.1	7891.1
CIT1 3DY	15.0	25.4	ND	22.7	12.0	10.8	26.1	27.8	11.9	151.6
CIT1 7DY	ND	ND	30.8	22.2	ND	ND	ND	ND	ND	53.0
CIT2INIT	10930.7	9484.3	6908.4	6563.9	7934.5	4067.4	5019.5	5716.1	10008.5	66633.2
CIT2H_2O_2INIT	8599.6	7539.4	5499.4	5243.1	6428.7	3268.5	4068.2	4683.6	8396.3	53726.8
CIT2 4HR	5958.2	4999.4	3430.3	3346.6	4682.6	2111.5	2882.4	3702.4	7706.5	38819.9
CIT2 1DY	1203.7	933.9	639.6	646.6	1042.0	577.9	739.0	994.7	1416.8	8194.1
CIT2 3DY	12.1	23.0	ND	23.5	11.6	10.7	22.9	25.0	18.9	147.7
CIT2 7DY	ND	ND	26.5	19.1	ND	ND	ND	ND	ND	45.5
	large peak just before Ethylbenzene, cannot detect Ethylbenzene, it is not seen in day 7 samples and is smaller in earlier samples									
SIL1INIT	11327.2	10168.5	8071.4	7603.6	8862.7	5449.5	6367.0	6931.8	11668.5	76450.1
SIL1H_2O_2INIT	9832.5	8831.4	6806.2	6427.9	7443.8	4306.9	5073.5	5505.1	9077.1	63304.4
SIL1 4HR	6434.6	5529.2	4022.3	3867.3	5085.6	2591.1	3308.1	4002.8	7697.8	42538.8
SIL1 1DY	2206.7	1726.7	1082.4	1103.7	1961.3	834.9	1268.9	1904.5	5103.2	17192.3
SIL1 3DY	479.2	350.0	196.3	214.3	514.8	254.7	396.6	704.6	2314.4	5425.0
SIL1 7DY	44.6	35.1	18.1	25.8	53.3	36.4	67.3	117.6	318.7	716.8
SIL2INIT	11653.1	10367.4	8091.1	7655.8	8807.5	5383.0	6277.2	6786.1	11013.1	76034.2
SIL2H_2O_2INIT	10506.4	9261.1	7111.4	6709.4	7760.7	4451.5	5248.5	5709.0	9499.6	66257.5
SIL2 4HR	7682.0	6685.0	4847.8	4665.5	6079.8	3062.1	3954.8	4729.6	9192.2	50899.0
SIL2 1DY	2191.5	1683.0	1042.8	1073.2	1984.5	800.9	1273.2	1968.1	5667.3	17684.6
SIL2 3DY	541.9	394.6	219.3	240.9	598.1	275.1	458.7	829.9	2947.7	6506.2
SIL2 7DY	50.0	37.9	20.8	28.0	70.4	44.9	81.5	152.6	515.5	1001.7

	Benzene	Toluene	Ethylbenzene	M Xylene	O Xylene	135 TMB	124 TMB	123 TMB	Naphthalene	Total
Site #2					µg/L					
CON1INIT	11912.3	9813.3	6980.5	6547.9	7631.4	3548.8	4275.5	4720.4	7862.3	63292.3
CON1H_20_2INIT	9977.8	8388.1	5976.3	5603.7	6531.5	3017.9	3633.3	4028.4	6716.9	53873.9
CON1 4HR	5543.1	4551.1	3085.2	2941.4	3881.8	1624.6	2104.3	2583.0	5102.3	31416.7
CON1 1DY	1822.8	1389.0	851.7	854.3	1452.4	577.2	805.6	1154.8	2834.4	11742.2
CON1 DY3	223.4	160.8	89.6	99.3	219.7	123.3	174.9	276.7	716.9	2084.6
CON1 DY7	18.8	26.7	9.0	ND	19.0	ND	36.3	36.7	51.5	197.9
CON2INIT	11761.9	10184.7	7805.3	7380.6	8494.8	4761.4	5611.3	6078.0	9837.1	71915.2
CON2H_20_2INIT	9784.0	8671.1	6690.0	6332.2	7319.4	4086.3	4824.8	5245.3	8656.5	61609.7
CON2 4HR	6948.0	5980.7	4367.0	4197.2	5409.5	2648.2	3411.3	4079.0	7976.5	45017.4
CON2 1DY	2455.6	1920.1	1168.5	1170.2	2000.7	748.3	1159.4	1780.2	4827.5	17230.4
CON2 3DY	359.8	250.7	119.4	128.5	315.8	117.2	179.0	358.8	1408.9	3238.0
CON2 7DY	40.6	34.1	11.7	ND	25.0	ND	23.1	32.7	126.4	293.5
CIT1INIT	10030.8	8303.4	5698.7	5386.5	6618.2	2729.7	3457.7	4040.4	7282.3	53547.7
CIT1H_2O_2INIT	8466.6	7073.0	4818.8	4571.4	5702.3	2320.7	2980.4	3518.1	6390.7	45842.0
CIT1 4HR	5629.9	4623.0	3069.4	2958.7	4042.1	1560.0	2094.0	2646.9	5319.4	31943.4
CIT1 1DY	872.9	677.5	437.6	449.4	725.0	345.4	439.7	595.8	898.2	5441.7
CIT1 DY3	13.6	18.2	ND	ND	ND	ND	22.2	15.7	12.9	82.7
CIT1 DY7	ND	ND	ND	ND	ND	ND	12.8	0.0	0.0	12.8
CIT2INIT	10106.2	8541.5	5901.8	5579.5	6836.3	2860.6	3613.4	4200.1	7410.0	55049.4
CIT2H_2O_2INIT	8407.7	7147.6	4954.0	4698.0	5819.4	2436.1	3103.6	3630.1	6590.7	46787.1
CIT2 4HR	5996.0	4932.3	3281.8	3166.4	4305.8	1665.3	2247.2	2828.7	5689.4	34112.9
CIT2 1DY	941.1	724.5	465.7	480.3	790.2	370.7	487.5	676.9	1064.7	6001.7
CIT2 DY3	14.8	18.4	ND	ND	ND	ND	20.0	15.3	22.9	91.4
CIT2 DY7	ND	ND	ND	ND	ND	ND	ND	ND	ND	0.0
SIL1INIT	11163.8	9525.3	6952.0	6541.5	7620.1	3662.2	4401.6	4842.5	8010.9	62719.9
SIL1H_2O_2INIT	10196.7	8761.6	6374.3	5984.8	6985.8	3272.3	3963.0	4397.9	7458.6	57394.8
SIL1 4HR	6232.1	5205.2	3531.5	3383.2	4522.9	1782.6	2383.4	2933.2	5847.2	35821.3
SIL1 1DY	2258.5	1706.8	992.0	1003.4	1798.6	611.4	952.5	1458.5	4057.6	14839.3
SIL1 DY3	308.4	218.7	116.9	128.3	328.6	141.0	223.2	421.3	1550.6	3437.0
SIL1 DY7	33.0	31.9	14.0	24.6	39.4	ND	52.4	82.7	219.0	497.2
SIL2INIT	11394.4	9833.3	7477.1	7065.4	8157.9	4435.9	5220.7	5652.4	9139.3	68376.5
SIL2H_2O_2INIT	9810.8	8833.6	6890.4	6529.6	7603.8	4143.9	4921.1	5352.9	9000.3	63086.4
SIL24 HR	6684.6	5693.5	4048.6	3910.3	5188.8	2377.0	3149.9	3843.9	7724.4	42621.1
SIL2 1DY	2343.6	1777.6	1032.8	1048.5	1934.0	616.3	1054.7	1751.2	5626.2	17184.9
SIL2 DY3	397.5	263.7	111.1	122.7	368.6	94.8	183.3	465.2	2879.6	4886.4
SIL2 DY7	52.9	37.7	12.5	18.4	55.0	ND	30.7	81.1	746.5	1034.8

*ND: not detected

Appendix E: Concentrations of MTBE, TBA, pH, dissolved oxygen, and hydrogen peroxide versus time during the analysis of H_2O_2 stabilized by citrate, and silica plus the control (no stabilizer) experiment for site #1 and site #2.

	MTBE	TBA	pH	DO	H_2O_2
Site #1	mg/L			mg/L	%
CON 1 INIT	406	ND*	ND	ND	ND
CON 1 H_2O_2 INIT	368	3.2	6.8	48.5	5.6
CON 1 4 Hr	318	5.1	7.1	49.6	6.0
CON 1 1 DY	224	8.5	7.2	44.5	5.0
CON 1 3 DY	177	11.4	7.2	34.9	3.4
CON 1 7 DY	86	24.2	7.2	37.3	2.0
CON 2 INIT	429	ND	ND	ND	ND
CON 2 H_20_2 INIT	357	4.8	6.8	41.7	5.8
CON2 4 Hr	302	6.1	7.0	42.6	6.4
CON 2 1 DY	242	8.8	7.2	45.1	5.0
CON 2 3 DY	173	14.0	7.1	38.6	3.7
CON 2 7 DY	65	11.7	7.0	27.5	1.9
CIT 1 INIT	445	ND	ND	ND	ND
CIT 1 H_2O_2 INIT	355	4.8	4.6	20.5	6.1
CIT 1 4 Hr	304	6.9	5.0	33.2	6.1
CIT 1 1 DY	179	18.9	6.1	83.0	5.5
CIT 1 3 DY	75	27.2	7.2	43.6	1.6
CIT 1 7 DY	27	37.8	7.3	18.2	0.1
CIT 2 INIT	430	ND	ND	ND	ND
CIT 2 H_2O_2 INIT	330	6.1	4.6	20.9	6.1
CIT 2 4 Hr	267	8.6	5.0	42.2	6.5
CIT 2 1 DY	179	21.0	6.0	89.0	6.1
CIT 2 3 DY	68	26.4	7.2	56.0	1.5
CIT 2 7 DY	28	37.5	7.2	20.5	0.1

SIL 1 INIT	435	ND	ND	ND	ND
SIL 1 H_2O_2 INIT	328	5.3	6.3	39.0	5.9
SIL 1 4 Hr	333	5.6	7.4	35.6	6.4
SIL 1 1 DY	277	7.2	7.4	34.3	5.1
SIL 1 3 DY	202	13.1	7.4	36.4	3.6
SIL 1 7 DY	100	19.0	7.1	29.3	2.0
SIL 2 INIT	438	ND	ND	ND	ND
SIL 2 H_2O_2 INIT	374	5.1	6.9	30.1	6.1
SIL 2 4 Hr	302	5.4	7.3	34.5	5.7
SIL 2 1 DY	245	5.9	7.4	32.5	5.0
SIL 2 3 DY	186	8.3	7.4	34.3	3.4
SIL 2 7 DY	73	23.2	7.2	31.0	1.9
	MTBE	**TBA**	**pH**	**DO**	**H_2O_2**
Site #2	mg/L			mg/L	%
CON 1 INIT	437	ND	7.9	9.6	ND
CON 1 H_20_2 INIT	305	5.4	6.4	35	5.4
CON 1 4 Hr	230	6.7	6.6	38	6.0
CON 1 1 DY	216	9.3	6.8	46	5.5
CON 1 3 DY	118.2	11.5	6.8	38	4.3
CON 1 7 DY	55	20.6	6.8	30	2.4
CON 2 INIT	454	ND	ND	ND	ND
CON2 H_20_2 INIT	306	5.4	6.4	42	5.8
CON 2 4 Hr	272	5.9	6.6	42	6.2
CON 2 1 DY	177	5.4	6.8	45	5.4
CON 2 3 DY	135	9.3	6.9	51	4.2
CON 2 7 DY	76	18.4	6.9	34	2.6
CIT 1 INIT	426	ND			
CIT 1 H_2O_2 INIT	336	5.6	4.5	16	5.7

CIT 1 4 Hr	245	5.6	5	29	6.2
CIT 1 1 DY	162	13.3	6.1	69	5.5
CIT 1 3 DY	36	22.2	7.1	39	1.2
CIT 1 7 DY	17	29.5	7.1	20	0.1
CIT 2 INIT	409	ND	ND	ND	ND
CIT2 H_2O_2 INIT	306	5.3	4.5	15	5.9
CIT 2 4 Hr	194	5.4	5	30	5.8
CIT 2 1 DY	160	13.4	6.1	67	5.5
CIT 2 3 DY	42	25	7.1	47	1.2
CIT 2 7 DY	17	28.3	7.1	21	0.05
SIL 1 INIT	418	ND	ND	ND	ND
SIL 1 H_2O_2 INIT	342	5.3	6.9	29	5.3
SIL 1 4 HR	267	6.4	6.8	33	5.8
SIL 1 1 DY	210	6.4	7.3	37	5.0
SIL 1 3 DY	131	10.3	7.2	40	3.6
SIL 1 7 DY	70	14.4	7	28	2.1
SIL 2 INIT	450	ND	ND	ND	ND
SIL 2 H_2O_2 INIT	315	5	6.9	25	5.7
SIL 2 4 Hr	270	5.8	6.8	32	5.7
SIL 2 1 DY	204	4.8	7.4	43	5.0
SIL 2 3 DY	127	5.4	7.4	42	3.5
SIL 2 7 DY	58	9.8	7.4	28	2.0

* ND: not detected

Appendix F: Isotopic compositions of $\delta^{13}C$ (‰) for MTBE, benzene, and toluene, and $\delta^{2}H$ (‰) for MTBE and benzene on the activated and unactivated persulfate experiments for site #1.

	MTBE	Benzene	Toluene	MTBE	Benzene
	$\delta^{13}C$			$\delta^{2}H$	
PSC 1 INIT 1	-29.0	-28.3	-27.5	-85	-64
PSC 1 INIT 2	-32.8	-28.6	-27.9	-74	-66
PSC 1 5 Min	-33.4	-28.8	-28.2	-80	-62
PSC 1 1 Hr	-29.7	-28.4	-27.8	-75	-61
PSC 1 3 Hr	-31.2	-28.7	-27.9	-82	-59
PSC 1 1DY	-31.1	-28.5	-28.0	-81	-49
PSC 1 14DY	-27.8	-28.1	-27.9	-75	-49
PSC 2 INIT 1		-28.7	-28.2	-85	-58
PSC 2 INIT 2		-28.7	-27.9	-88	-67
PSC 2 5 Min	-30.5	-28.5	-27.7	-80	-67
PSC 2 1 Hr	-30.2	-28.7	-28.1	-83	-62
PSC 2 3 Hr	-30.3	-28.4	-27.8	-75	-63
PSC 2 1DY	-30.0	-28.5	-27.6	-83	-54
PSC 2 14DY	-27.6	-27.9	-27.5	-69	-56
CFEL 1 INIT 1	-30.2	-28.5	-28.0	-95	-69
CFEL 1 INIT 2	-30.5	-28.1	-25.0	-97	-66
CFEL 1 5 Min	-30.5	-27.8	-23.6	-86	
CFEL 1 1 Hr	-28.9	-27.8	-25.0	-80	
CFEL 1 3 Hr	-29.0	-28.1	-24.4	-91	-62
CFEL 1 1 DY	-28.9	-27.9	-24.1	-79	-48
CFEL 1 14 DY	-28.1	-28.1	-23.3	-76	-45

CFEL 2 INIT 1	-30.3	-28.7	-27.7	-87	-68
CFEL INIT 2	-29.0	-28.0	-25.5	-84	-73
CFEL 2 5 Min	-28.9	-27.8	-24.2	-76	-54
CFEL 2 1 Hr	-29.1	-28.2	-24.9	-74	-50
CFEL 2 3 Hr	-28.8	-27.4	-24.6	-80	-58
CFEL 2 1 DY	-28.0	-27.3	-24.2	-83	-58
CFEL 2 14 DY	-28.0	-28.0	-23.0	-86	-50
CFEH 1 INIT 1	-29.8	-28.6	-27.7	-84	-64
CFEH1 INIT 2	-28.6	-28.2	-23.6	-84	-65
CFEH 1 5 Min	-28.8	-28.2	-24.3	-85	-51
CFEH 1 1 Hr	-28.6	-27.6	-24.2	-75	-63
CFEH 1 3 Hr	-29.3	-28.4	-24.0	-72	-49
CFEH 1 1 DY	-29.0	-28.1	-21.0	-89	-57
CFEH 1 14 DY	-27.7	-27.7	-19.9	-79	-46
CFEH 2 INIT 1	-30.3	-29.3	-28.4	-87	-69
CFEH 2 INIT 2	-29.7	-29.1	-24.9	-84	-58
CFEH 2 5 Min	-29.2	-28.4	-23.0	-82	-61
CFEH 2 1 Hr	-29.0	-28.5	-24.5	-84	-64
CFEH 2 3 Hr	-28.6	-28.2	-23.6	-87	-48
CFEH 2 1 DY	-28.5	-28.1	-21.0	-94	-60
CFEH 2 14 DY	-26.6		-19.1	-53	

Appendix G: Isotopic compositions of $\delta^{13}C$ (‰) for MTBE, benzene, and toluene on H_2O_2 stabilized by citrate and silica plus the control (no stabilizer) experiment at site #1 and site #2.

	MTBE	Benzene	Toluene
	$\delta^{13}C$		
	Site #1		
CON 1 INIT	-29.5	-28.8	-27.5
CON 1 H_20_2 INIT	-29.0	-27.7	-27.0
CON 1 4 Hr	-28.6	-27.7	-26.8
CON 1 1 DY	-28.8	-27.9	-26.9
CON 1 3 DY	-28.6	-27.9	-26.5
CON 1 7 DY	-25.3	-26.5	-25.9
CON 2 INIT	-28.3	-27.3	-26.4
CON 2 H_20_2 INIT	-28.5	-27.1	-27.0
CON 2 4 Hr	-28.6	-27.5	-26.4
CON 2 1 DY	-28.9	-28.0	-26.7
CON 2 3 DY	-27.7	-27.1	-26.2
CON 2 7 DY	-30.9	-27.0	-26.5
CIT 1 INIT	-28.4	-27.0	-26.2
CIT 1 H_2O_2 INIT	-28.0	-27.0	-25.9
CIT 1 4 Hr	-27.0	-26.1	-24.9
CIT 1 1 DY	-26.3	-25.7	-24.5
CIT 1 3 DY	-26.0	-25.4	-23.7
CIT 1 7 DY	-26.2	ND	ND
CIT 2 INIT	-29.0	-27.6	-26.7
CIT 2 H_2O_2 INIT	-28.9	-27.8	-27.0
CIT 2 4 Hr	-28.7	-27.6	-26.9
CIT 2 1 DY	-27.3	-26.0	-25.5
CIT 2 3 DY	-25.1	-25.5	-22.4
CIT 2 7 DY	-25.8	ND	ND

SIL 1 INIT	-28.6	-27.3	-26.4
SIL 1 H_2O_2 INIT	-27.6	-26.6	-25.8
SIL 1 4 Hr	-29.5	-28.0	-28.8
SIL 1 1 DY	-29.3	-28.4	-27.2
SIL 1 3 DY	-27.3	-27.0	-26.4
SIL 1 7 DY	ND	-27.5	-26.5
SIL 2 INIT	-28.9	-28.0	-26.5
SIL 2 H_2O_2 INIT	-28.9	-27.4	-26.7
SIL 2 4 Hr	-28.8	-27.8	-27.1
SIL 2 1 DY	-28.4	-27.2	-26.3
SIL 2 3 DY	-27.9	-27.0	-26.3
SIL 2 7 DY	-27.4	-26.9	-26.3
	Site #2		
CON 1 INIT	-28.9	-27.2	-26.3
CON 1 H_20_2 INIT	-28.1	-26.8	-26.0
CON 1 4 Hr	-28.1	-27.0	-26.2
CON 1 1 DY	-28.0	-26.8	-26.1
CON 1 3 DY	-27.0	-26.3	-25.6
CON 1 7 DY	-26.7	-25.3	-25.5
CON 2 INIT	-28.5	-27.4	-26.6
CON 2 H_20_2 INIT	-28.5	-27.6	-26.7
CON 2 4 Hr	-26.5	-26.7	-25.3
CON 2 1 DY	-27.0	-26.9	-26.0
CON 2 3 DY	-27.5	-26.6	-25.9
CON 2 7 DY	-26.6	-26.4	-25.2
CIT 1 INIT	-28.3	-27.1	-26.3
CIT 1 H_2O_2 INIT	-29.0	-27.5	-26.5

CIT 1 4 Hr	-28.4	-27.5	-25.8
CIT 1 1 DY	-27.7	-26.5	-25.5
CIT 1 3 DY	-26.3	-24.3	-22.5
CIT 1 7 DY	-25.5	ND	ND
CIT 2 INIT	-28.7	-27.5	-26.6
CIT 2 H_2O_2 INIT	-28.5	-27.3	-26.4
CIT 2 4 Hr	-28.0	-26.8	-25.9
CIT 2 1 DY	-27.0	-26.2	-25.3
CIT 2 3 DY	-25.6	-24.9	-22.4
CIT 2 7 DY	-25.4	ND	ND
SIL 1 INIT	-28.3	-27.3	-25.7
SIL 1 H_2O_2 INIT	-28.5	-26.9	-26.2
SIL 1 4 Hr	-28.0	-26.7	-25.8
SIL 1 1 DY	-27.7	-26.9	-26.1
SIL 1 3 DY	-27.5	-26.7	-25.4
SIL 1 7 DY	ND	-26.7	-27.1
SIL 2 INIT	-28.0	-27.2	-26.3
SIL 2 H_2O_2 INIT	-27.6	-26.5	-25.5
SIL 2 4 Hr	-27.4	-26.3	-25.2
SIL 2 1 DY	-28.5	-27.1	-26.0
SIL 2 3 DY	-27.6	-27.6	-25.8
SIL 2 7 DY	-26.6	-27.3	-26.0

*ND: not detected